

NAVAL POSTGRADUATE SCHOOL

Monterey, California



19980414 125

THESIS

DTIC QUALITY INSPECTED &

TESTING AND ANALYSIS
OF A
TRANSONIC AXIAL COMPRESSOR

by

Bart L. Grossman

September, 1997

Thesis Advisor:
Second Reader:

Raymond P. Shreeve
Garth V. Hobson

Approved for public release; distribution is unlimited.

REPORT DOCUMENTATION PAGE

Form Approved
OMB No. 0704-0188

Public reporting burden for this collection of information is estimated to average 1 hour per response, including the time for reviewing instruction, searching existing data sources, gathering and maintaining the data needed, and completing and reviewing the collection of information. Send comments regarding this burden estimate or any other aspect of this collection of information, including suggestions for reducing this burden, to Washington headquarters Services, Directorate for Information Operations and Reports, 1215 Jefferson Davis Highway, Suite 1204, Arlington, VA 22202-4302, and to the Office of Management and Budget, Paperwork Reduction Project (0704-0188) Washington DC 20503.

1. AGENCY USE ONLY (Leave blank)

2. REPORT DATE

September 1997

3. REPORT TYPE AND DATES COVERED

Master's Thesis

4. TITLE AND SUBTITLE

TESTING AND ANALYSIS OF A TRANSONIC AXIAL COMPRESSOR

5. FUNDING NUMBERS

6. AUTHOR(S)

Grossman, Bart L.

7. PERFORMING ORGANIZATION NAME(S) AND ADDRESS(ES)

Naval Postgraduate School
Monterey, CA 93943-5000

8. PERFORMING
ORGANIZATION REPORT
NUMBER

9. SPONSORING / MONITORING AGENCY NAME(S) AND ADDRESS(ES)

10. SPONSORING /
MONITORING
AGENCY REPORT NUMBER

11. SUPPLEMENTARY NOTES

The views expressed in this thesis are those of the author and do not reflect the official policy or position of the Department of Defense or the U.S. Government.

12a. DISTRIBUTION / AVAILABILITY STATEMENT

Approved for public release; distribution unlimited.

12b. DISTRIBUTION CODE

13. ABSTRACT (maximum 200 words)

A test program to evaluate a new transonic axial compressor stage was conducted. The stage was designed (by Nelson Sanger of NASA Lewis) relying heavily on CFD techniques while minimizing conventional empirical design methods. The stage was installed in the NPS Transonic Compressor Test Rig and instrumented with fixed temperature and pressure probes. A new PC-based data acquisition system was commissioned and programmed for stage performance measurements. These were obtained at 50, 60, 65, 70, and 80% of the design speed before failure of the spinner retaining bolt led to the loss of the stage. The flow through the rotor was analyzed and the rotor performance predicted using a 3-dimensional viscous code (RVC3D). The predicted rotor performance agreed qualitatively and was numerically consistent with the measured stage performance.

14. SUBJECT TERMS

Compressor, Transonic, CFD, Turbomachinery, RVC3D

15. NUMBER OF
PAGES

119

16. PRICE CODE

17. SECURITY CLASSIFICATION OF
REPORT

Unclassified

18. SECURITY CLASSIFICATION OF
THIS PAGE

Unclassified

19. SECURITY CLASSIFI- CATION
OF ABSTRACT

Unclassified

20. LIMITATION
OF ABSTRACT

UL

NSN 7540-01-280-5500

Standard Form 298 (Rev. 2-89)
Prescribed by ANSI Std. Z39-18

Approved for public release; distribution is unlimited

**TESTING AND ANALYSIS OF A TRANSONIC AXIAL
COMPRESSOR**

Bart L. Grossman
Lieutenant, United States Navy
BSEE, University of Texas, Austin, May 1987

Submitted in partial fulfillment of the requirements
for the degree of

MASTER OF SCIENCE IN AERONAUTICAL ENGINEERING

from the

**NAVAL POSTGRADUATE SCHOOL
September 1997**

Author: Bart L. Grossman
Bart L. Grossman

Approved by: Raymond P. Shreeve
Raymond P. Shreeve, Thesis Advisor

Garth V. Hobson
Garth V. Hobson, Second Reader

Gerald Lindsey
Gerald Lindsey, Chairman
Department of Aeronautics
And Astronautics

ABSTRACT

A test program to evaluate a new transonic axial compressor stage was conducted. The stage was designed (by Nelson Sanger of NASA Lewis) relying heavily on CFD techniques while minimizing conventional empirical design methods. The stage was installed in the NPS Transonic Compressor Test Rig and instrumented with fixed temperature and pressure probes. A new PC-based data acquisition system was commissioned and programmed for stage performance measurements. These were obtained at 50, 60, 65, 70, and 80% of the design speed before failure of the spinner retaining bolt led to the loss of the stage. The flow through the rotor was analyzed and the rotor performance predicted using a 3-dimensional viscous code (RVC3D). The predicted rotor performance agreed qualitatively and was numerically consistent with the measured stage performance.

TABLE OF CONTENTS

I.	INTRODUCTION	1
II.	TRANSONIC COMPRESSOR RIG AND INSTRUMENTATION.....	7
A.	COMPRESSOR INSTALLATION.....	7
B.	INSTRUMENTATION.....	8
1.	Measurement Devices.....	8
2.	Instrument Placement.....	13
C.	TEST PROCEDURE.....	14
III.	DATA ACQUISITION AND REDUCTION.....	17
A.	OVERVIEW.....	17
B.	HARDWARE.....	17
1.	Scanivalve Control.....	19
2.	Scanning Digital Voltmeter.....	22
3.	Counter/Totalizer.....	26
C.	SOFTWARE.....	26
D.	DATA REDUCTION.....	27
IV.	RESULTS OF THE TEST PROGRAM.....	31
A.	INTRODUCTION.....	31
B.	STAGE PERFORMANCE MAPS.....	31
C.	PRESSURE PROFILES.....	33
V.	RESULTS OF CFD ANALYSIS.....	47
A.	INTRODUCTION.....	47
B.	GRID GENERATION.....	47
C.	COMPUTATION.....	49
D.	RESULTS.....	50
VI.	CONCLUSIONS AND RECOMMENDATIONS.....	55
	LIST OF REFERENCES.....	57

APPENDIX A	ANALYSIS OF THE SPINNER BOLT FAILURE.....	59
A.	OVERVIEW.....	59
B.	CONSTRUCTION.....	59
C.	ANALYSIS.....	60
APPENDIX B	RESULTS.....	67
APPENDIX C	SOFTWARE USER'S GUIDE.....	71
A.	HPVEE.....	71
B.	RVC3D.....	98
INITIAL DISTRIBUTION LIST.....		105

LIST OF FIGURES

1. Schematic of the Transonic Compressor Test Rig.....	3
2. View of the Assembled Stage.....	4
3. View of the Instrumented Assembly With Lucite Case Wall.....	5
4. Schematic of the Flow Path Showing Measurement Stations.....	10
5. Torque Calibration Curve.....	12
6. Schematic of the Data Acquisition System.....	18
7. Schematic of Switchbox Connections to HG78.....	20
8. Schematic of Differential Temperature Measurement.....	25
9. Pressure Ratio (T-T) vs Referred Mass Flow Rate.....	35
10. Adiabatic Efficiency (η_3) vs Referred Mass Flow Rate.....	36
11. Adiabatic Efficiency (η_1) vs Referred Mass Flow Rate.....	37
12. Adiabatic Efficiency (η_2) vs Referred Mass Flow Rate.....	38
13. Referred Torque vs Referred Mass Flow Rate.....	39
14. Stage Temperature Rise vs Referred Mass Flow Rate.....	40
15. Referred Horsepower vs Referred Mass Flow Rate.....	41
16. Exit Pressure Distribution at 70% Speed.....	42
17. Exit Pressure Distribution at 80% Speed.....	43
18. Axial Static Pressure Distribution at 70% Speed.....	44
19. Axial Static Pressure Profile at 80% Speed.....	45
20. Computational Grid for RVC3D Calculations.....	48
21. Rotor Total Pressure Ratio vs Corrected (Referred) Flow Rate Computed Using RVC3D.....	52
22. Rotor Adiabatic Efficiency vs Corrected (Referred) Flow Rate Computed Using RVC3D.....	53

LIST OF TABLES

1.	Design Parameters for the Sanger Stage.....	2
2.	Location of Probes at the Stage Exit.....	13
3.	Scanivalve Port Assignments.....	21
4.	Scanning Multiplexer Channel Assignments.....	23

ACKNOWLEDGEMENT

The author would like to acknowledge the financial support of NAWCAD, Propulsion and Power Engineering, Code 4.4.7.1, for the experimental study reported here. The work was performed under Contract N004219WR01221.

I. INTRODUCTION

A new transonic axial compressor stage designed specifically for the Naval Postgraduate School (NPS) Transonic Compressor Rig (TCR) was completed at NASA Lewis in 1994, by Nelson L. Sanger [Ref. 1]. A schematic of the TCR is shown in Fig. 1. The new stage design was developed to serve as a vehicle for instructional purposes, and to provide a test bed for research. With the emergence of Computational Fluid Dynamics (CFD) as a reliable tool, the design of the stage developed into, as Sanger described it, "...the ultimate CFD validation experiment". The design parameters produced from this process are presented in Table 1.

The manufactured stage, after assembly in the TCR, is shown in Fig. 2. The stage was installed in the same manner as previously operated stages and as documented in Ref. 2. However, a Lucite case wall was installed, as seen in Fig. 3, and a new data acquisition system was employed. The data acquisition system used a Personal Computer (PC) running Hewlett-Packard HPVEE software to control various instruments in a HP75000 VXI-bus mainframe. The stage was tested and measurements taken at 50, 60, 65, 70 and 80 percent of design speed. Testing was unavoidably halted during the test at 80% speed due to the failure of the

spinner retaining bolt, which resulted in the loss of the stage.

The present report documents the first test program of the Sanger stage. The report contains three main sections. The first section details the rig and the newly developed data acquisition system. The second section focuses on the results. The final section gives the results of a CFD analysis of the rotor using the "Rotor Viscous Code 3 Dimensional" (RVC3D) code developed by R. Chima [Ref. 3].

Parameter	Final Selection
Rotor Pressure Ratio	1.61
Stage Pressure Ratio	1.56
Tip Speed	1300 ft/sec
Design Mass Flow	17.09 lbm/sec
Specific Mass Flow	35 lbm/sec-ft ²
Specific Head Rise	0.246
Tip Inlet Relative Mach Number	1.28
Hub/Tip Radius Ratio	0.51
Rotor Inlet Ramp Angle	28.2 degrees
Power Required	457 HP

Table 1. Design Parameters for the Sanger Stage.

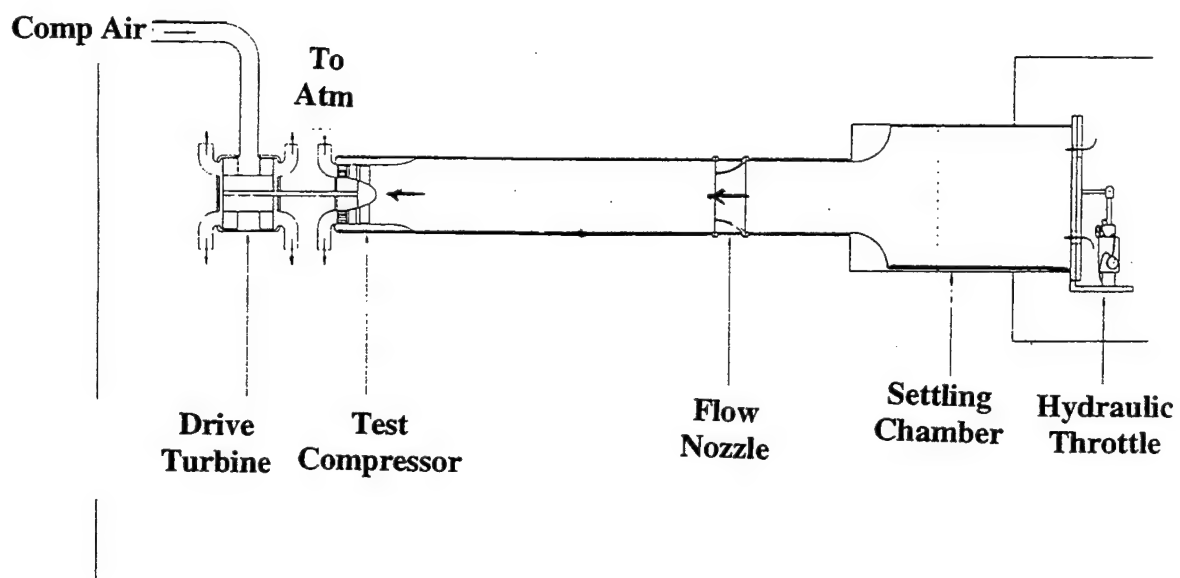


Fig. 1 Schematic of the Transonic Compressor Test Rig.

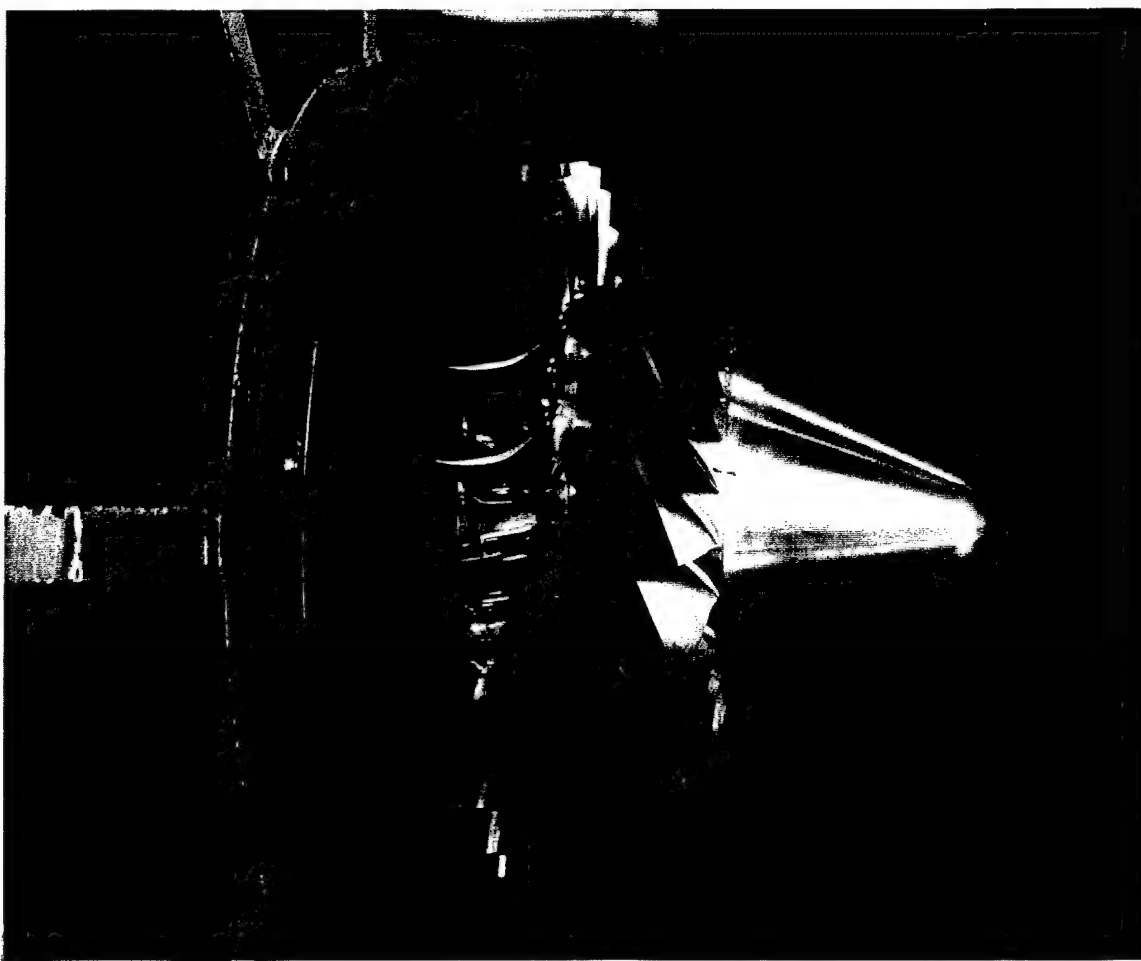


Fig. 2 View of the Assembled Stage.

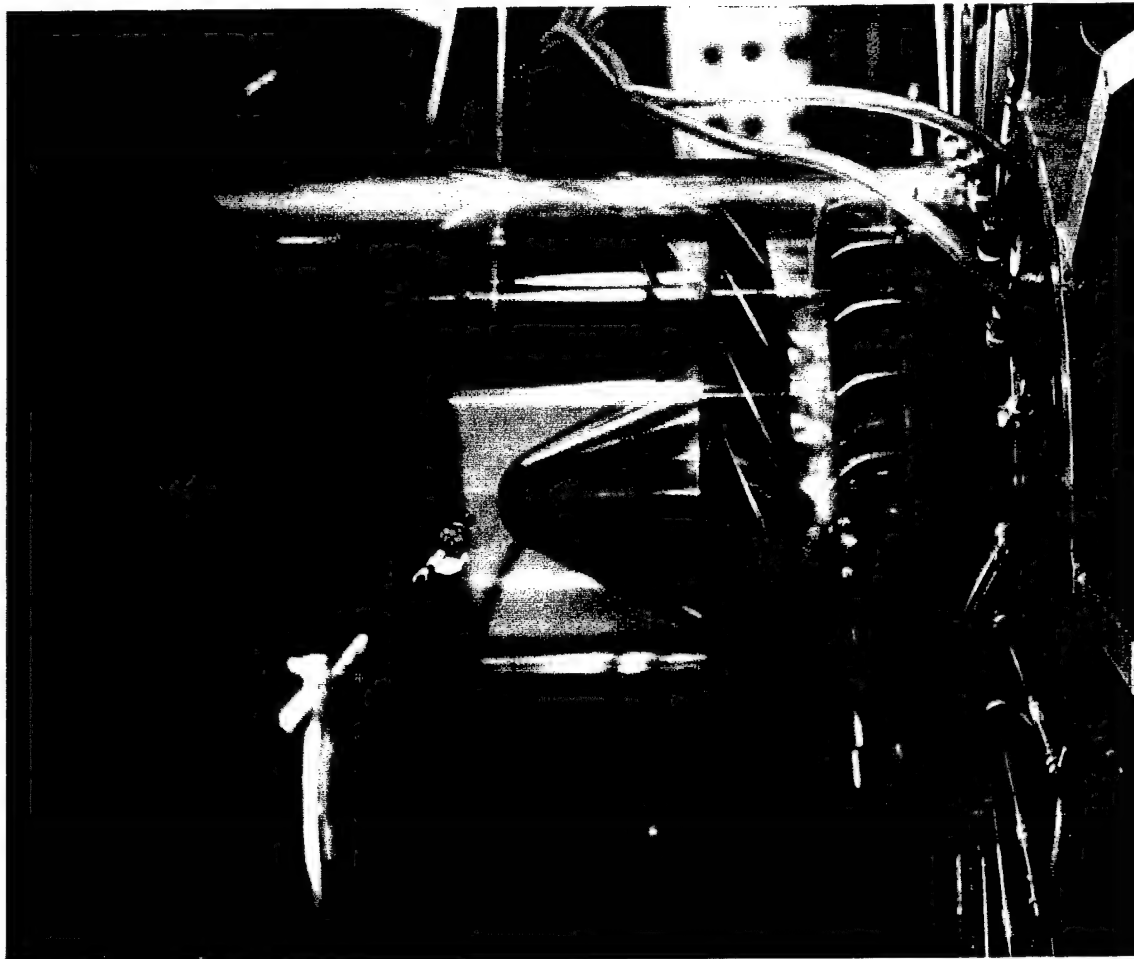


Fig. 3 View of the Instrumented Assembly With Lucite Case Wall.

II. TRANSONIC COMPRESSOR RIG AND INSTRUMENTATION

A. COMPRESSOR INSTALLATION

The general layout of the TCR is shown in Fig. 1. The manner in which the stage was mounted on the rig was unchanged from the previously installed Vavra stage documented in Ref. 2. The flow entered the rotor axially. A honeycomb section ensured that the flow left the compressor with zero circumferential velocity. In this manner the torque supplied to the rotor was equal to the torque experienced by the blading and honeycomb of the stator section. The stator section was mounted on ball races and was free to rotate against a flexure instrumented with strain gauges. The strain gauge reading was then a measure of the torque supplied to the rotor.

The tip clearance between the rotor and the steel casing that had been used previously was a concern. The decision was made to use a similar clear plastic (Lucite) casing until the steel casing could be modified to have an abradable material where the rotor might rub. The Lucite casing proved to function extremely well. The static tip gap clearance was 0.010-0.012 inches which was larger than the 0.004 inches the design called for; however, this ensured that no rub would occur during the first test of this unique stage. Additionally, the transparent case provided an

opportunity to see transonic turbomachinery in operation. One interesting observation was that excess oil from the bearing lubrication system indicated a flow pattern and was seen to collect between the casing and the rotor tip.

B. INSTRUMENTATION

1. Measurement Devices

Fig. 4 shows the location of measurement stations relative to the stage. The instrumentation for stage performance measurements included Kiel pressure probes, Kiel/thermocouple combination probes, static pressure taps, torque flexure, flow nozzle, and a magnetic pick up. Total pressure was measured using United Sensor Kiel Probes. Two types were used, a 1/16 inch "Miniature Head" Kiel Probe (United Sensor KAA-8, Ref. 4) and 1/8 inch "Standard Head" combination Kiel/thermocouple Probe (United Sensor KT-8-J-12-C, Ref. 4). The 1/16 inch mini probe had a yaw range of 52° and pitch range of 40° . Range was defined by the manufacturer as the point at which error was equal to 1% of dynamic pressure. The 1/8 inch standard probe had a yaw range of 48° and a pitch range 45° . The static pressure ports were 1/32 inch taps located in the wall along the length of the casing, and in the hub of the stator at stations 2 and 3.

Thermocouples were J type (iron-constantan) in a probe combined with a Kiel type impact probe. The thermocouple had an exposed junction and bleed slot.

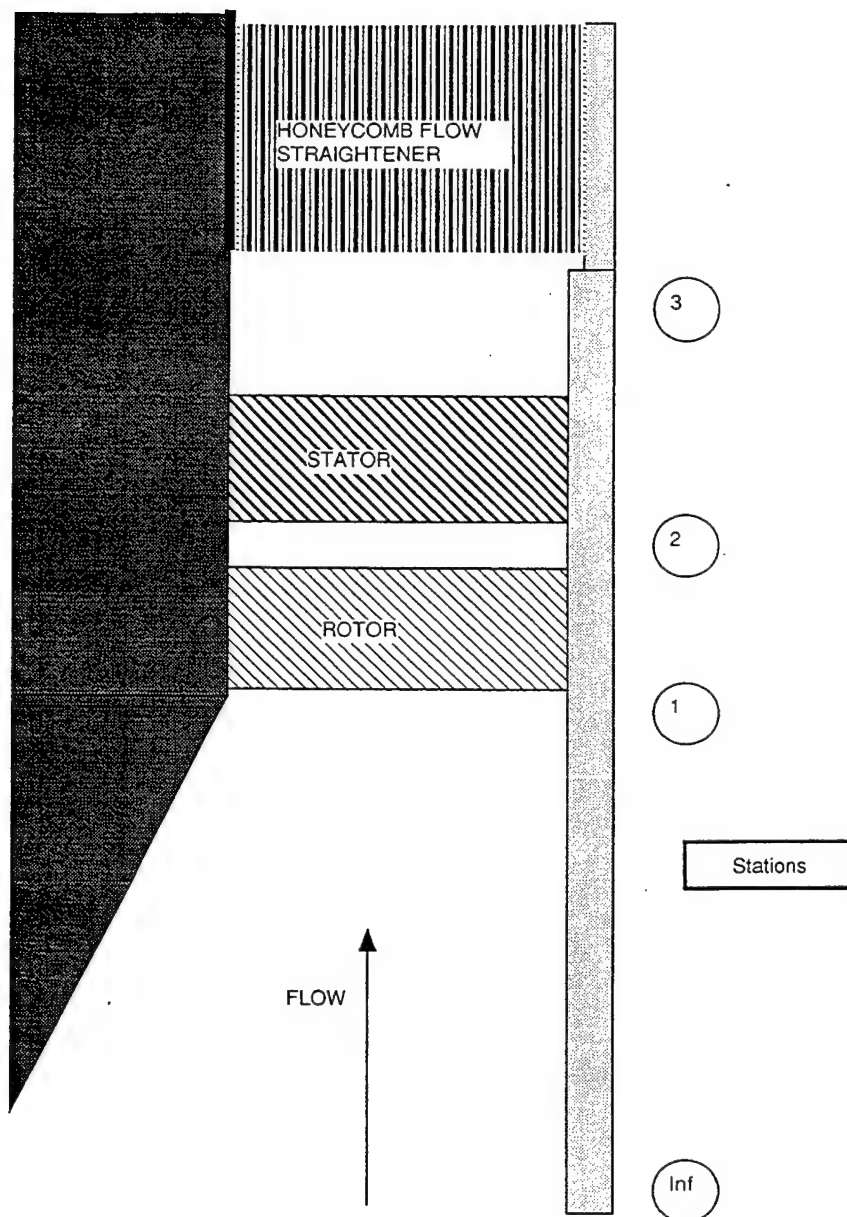


Fig. 4 Schematic of the Flow Path Showing Measurement Stations.

The torque acting on the stator and exit-honeycomb section (equal to the rotor torque) was measured by the deflection of a cantilevered flexure. The cantilever arm was instrumented with four strain gauges providing a near linear response to bending. The arrangement and calibration method of the torque measurement system is extensively documented in Ref. 2. Calibration of the torque measuring system was necessary each time the rig was rebuilt. The calibration curve obtained in the present study and resulting equation used in the data reduction program are shown in Fig. 5.

Rotational speed was measured using a magnetic flux cutter and a disk with six holes mounted on the shaft of the drive turbine (Fig. 1). This device produced six pulses per revolution making the frequency (in Hz) from the pickup multiplied by 10 equal to the revolutions per minute (RPM) of the stage.

Mass flow rate was measured using a flow nozzle located upstream of the stage as shown in Fig. 1. Mass flow rate was calculated using the pressure difference of the total pressure (p_t) and static pressure (p_s) at the flow nozzle and the total temperature of the flow. The differential pressure between p_t and p_s was displayed on a water manometer in the control room to allow precise control of mass flow rate settings during the throttling process.

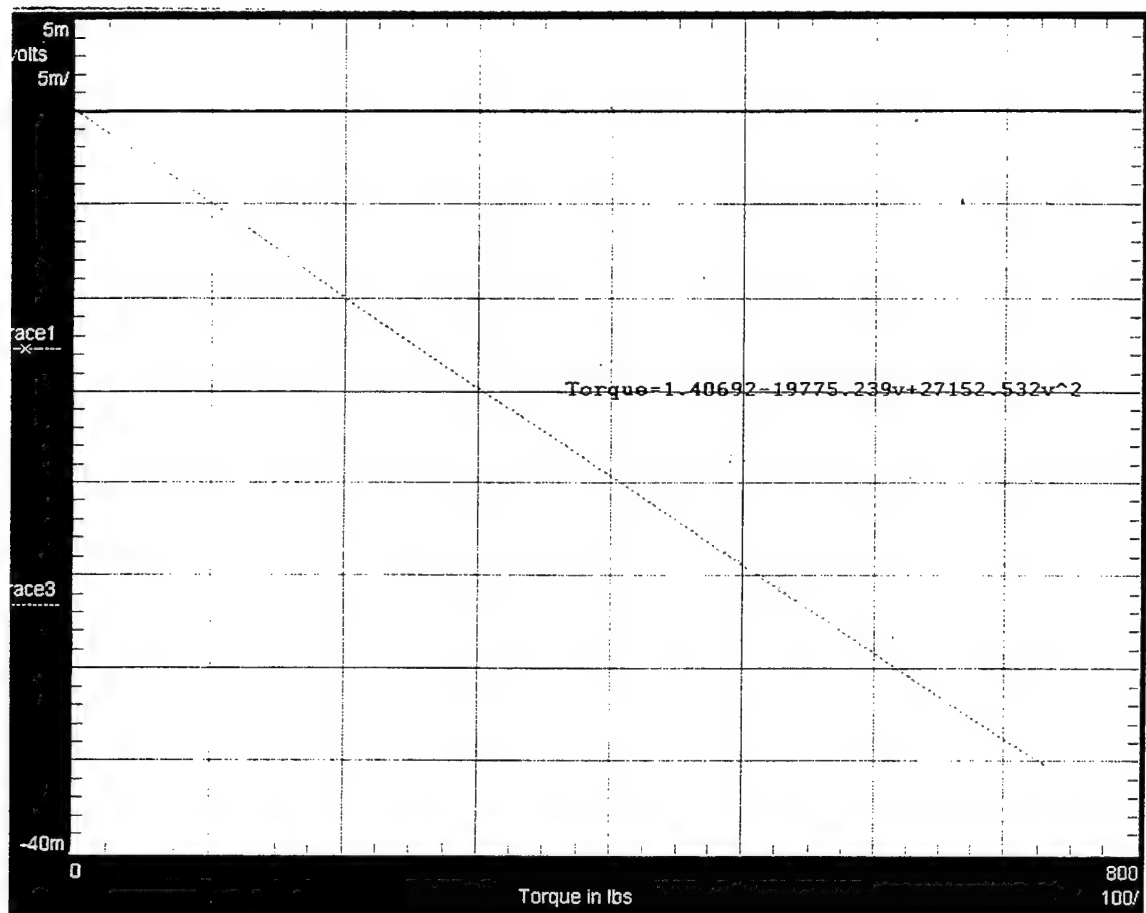
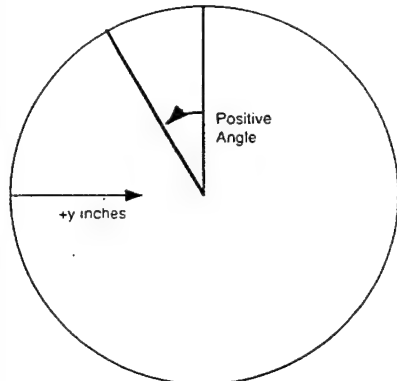


Fig. 5 Torque Calibration Curve.

2. Instrument Placement

Two combination probes were placed upstream of the rotor, each two inches from the wall of the casing to measure inlet total pressure and temperature. At station 3, 17 Kiel probes and three Kiel/thermocouple combination probes were placed as shown in Table 2.

Probe #	Probe Type	Radial Distance (y)	Angle
18	Kiel	0.7	15
15	Kiel	0.4	30
12	Kiel	0.1	45
41	Static Port	n/a	60
11	Kiel	0.05	75
29	Kiel	1.8	90
26	Kiel	1.5	105
23	Combo	1.2	120
20	Kiel	0.9	135
17	Kiel	0.6	150
14	Kiel	0.3	165
42	Static Port	n/a	180
plug	n/a	n/a	195
28	Kiel	1.7	210
25	Kiel	1.4	225
22	Combo	1.1	240
19	Kiel	0.8	255
16	Kiel	0.5	270
13	Kiel	0.2	285
43	Static Port	n/a	300
30	Kiel	1.85	315
27	Kiel	1.6	330
24	Kiel	1.3	345
21	Combo	1	360



View Looking Downstream

Table 2. Location of Probes at the Stage Exit.

The pressures acquired from the impact probes at station 3 (probe numbers 11-30 in Table 2) were mass averaged to obtain the total pressure at the exit of the stage.

Static pressure ports were placed at stations Inf, 1, 2 and 3 along the Lucite casing (Fig. 4). Additionally, static taps were drilled in the stator to measure hub static pressure at station 2. The exit spacer between the stator and honeycomb also had four static taps to measure exit static pressure on the hub at station 3.

C. TEST PROCEDURE

The test compressor was driven by two opposed-rotor air turbine stages (on a common shaft) supplied from the laboratory compressed-air power supply. The laboratory compressed-air power supply was a 12-stage Allis-Chalmers axial compressor supplying up to 11 pounds per second at up to two atmospheres gauge pressure. The test compressor was connected by a splined shaft to the rotor of the turbine drive unit. The speed of the drive unit was controlled using an electrically actuated butterfly valve. Air was drawn into the test compressor through a rotating plate throttle followed by a settling chamber containing perforated plates (Fig. 1). A flow nozzle was positioned upstream of the rotor. The calibration of the flow nozzle was documented in Ref. 5.

Preparation for a run consisted of bringing the Allis-Chalmers compressor up to stable speed, verifying that compressed air was available to the balance piston (which maintained low axial loading on the compressor bearings), and setting the lubrication system. The bearing lubrication system was an oil-mist system. The operating temperature of the bearings was found to be directly related to the supply pressure of the air driving the oil mist. Increasing the pressure of the oil mist supply air had the observed effect of lowering the bearing operating temperature. Adjusting the oil droplet rate down to 2-3 drops-per-minute was essential. According to the bearing manufacturer, wetting the bearing well before a run was of extreme importance. Allowing the oil mist to operate for fifteen minutes before operating was the procedure adopted.

During a compressor test, operating data were monitored by the operator at the control console. Records were kept of oil drop rate and pressure to the bearing lubrication system, of the temperatures of the turbine and compressor bearings, and of vibration levels from four accelerometers on the turbine drive unit. The axial force was constantly monitored and the balance-piston air adjusted to keep the axial force constant at a level approximately equal to the force produced at 5000 RPM. These data were mainly of interest for the safety and operation of the unit and will not be reported.

A typical test would be conducted at a constant speed. The run started with the compressor throttle wide open. After the speed had settled to the desired level, a measurement recording cycle was started. Then the throttle would be closed fractionally until the flow was reduced to the desired amount. Then the drive turbine speed was adjusted until it was steady again and at the desired level. This procedure was repeated until stall occurred. After the stall point was reached (up to 70% speed only) the process was progressively reversed to obtain intermediate settings until the throttle was fully open.

III. DATA ACQUISITION AND REDUCTION

A. OVERVIEW

In order to standardize equipment for data acquisition in the three buildings at the NPS Turbopropulsion Laboratory the decision was made to use the HP75000 Series B VXI-Bus Mainframe controlled by HPVEE software running on a personal computer (PC). This allowed the Hewlett-Packard (HP) instruments with the HP-IB interface that had been used previously to remain viable while incorporating a new state-of-the-art data acquisition system. In the present work the mainframe with an internal digital voltmeter (DVM), two scanning multiplexers, a switchbox multiplexer, a counter, and a Quad 8-bit Digital I/O Module were used exclusively. The system, shown in Fig. 6, proved to be flexible, easy to interrogate when connecting new sensors, and provided real time feedback when acquiring data.

B. HARDWARE

The use of the HP75000 Mainframe allowed a variety of instruments to be grouped together and addressed directly. Communication between the PC (with a HP 82341C Controller Card installed) and the mainframe was via a HP-IB (IEEE-488) interface cable. The functions performed with the instruments in the mainframe were Scanivalve control, measurement of Scanivalve transducer output, thermocouple

measurement, strain gauge measurement and frequency counting.

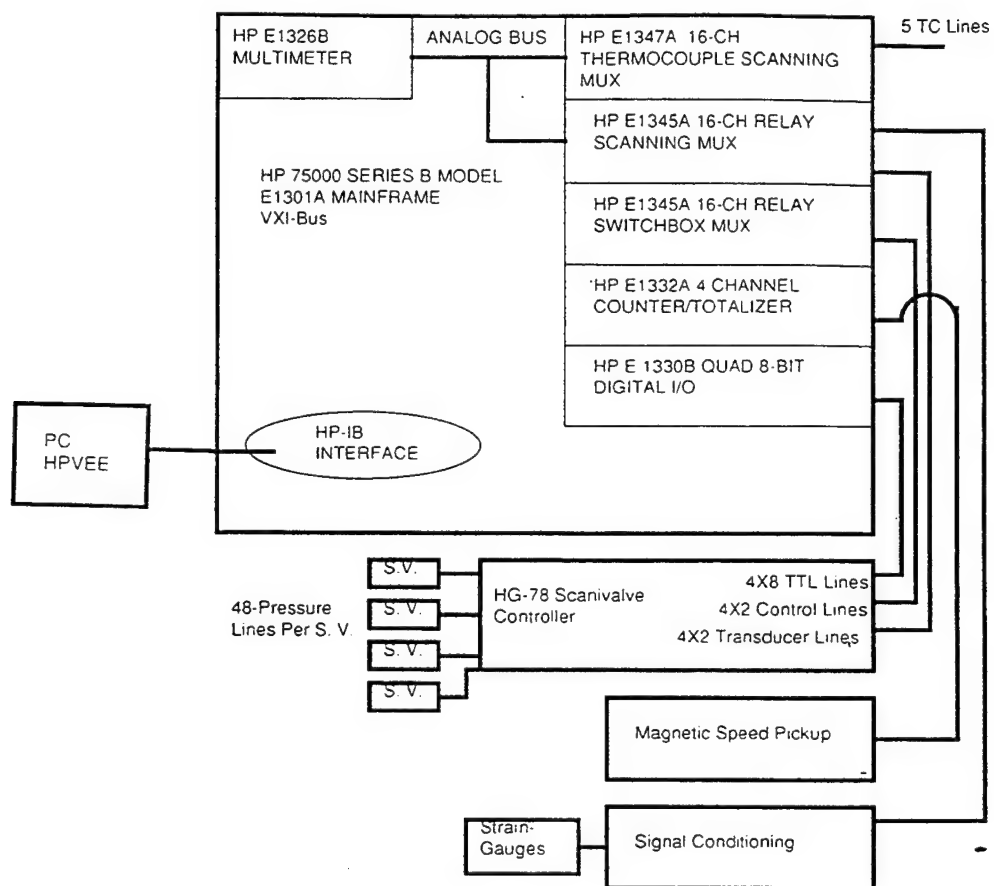


Fig. 6 Schematic of the Data Acquisition System.

1. Scanivalve Control

The Scanivalve and Scanivalve control (HG-78) system that the present system was designed to replace, are described in Ref. 6. Scanivalve control involved stepping and homing the 48-port pneumatic valve and ensuring that the correct port was selected and measured. One HP E1345A 16-channel multiplexer was configured as a switchbox as shown in Fig. 7. This configuration allowed the control of four different Scanivalves with one switchbox. The measurements required for the test program required the control of only one Scanivalve at position 1. To reset the Scanivalve, channel 12 was closed, sending the signal to the HG-78 to reset the Scanivalve connected to position 1. To step to the next port, channel 8 was closed, sending the signal to advance one port. The position of the Scanivalve was obtained from the HG-78, which contained LED displays of the port setting, manual step and home controls (in parallel), and signal conditioning for the Scanivalve transducers. From the HG-78, eight TTL lines (from each Scanivalve) were connected to one of four addressable sections of the HP E1330B Quad 8-bit Digital I/O card. The port which the Scanivalve was currently set at was then read (using negative logic) and converted to a decimal number using Binary Convert Decimal (BCD) logic. The assignment of the 48 Scanivalve ports is shown in Table 3.

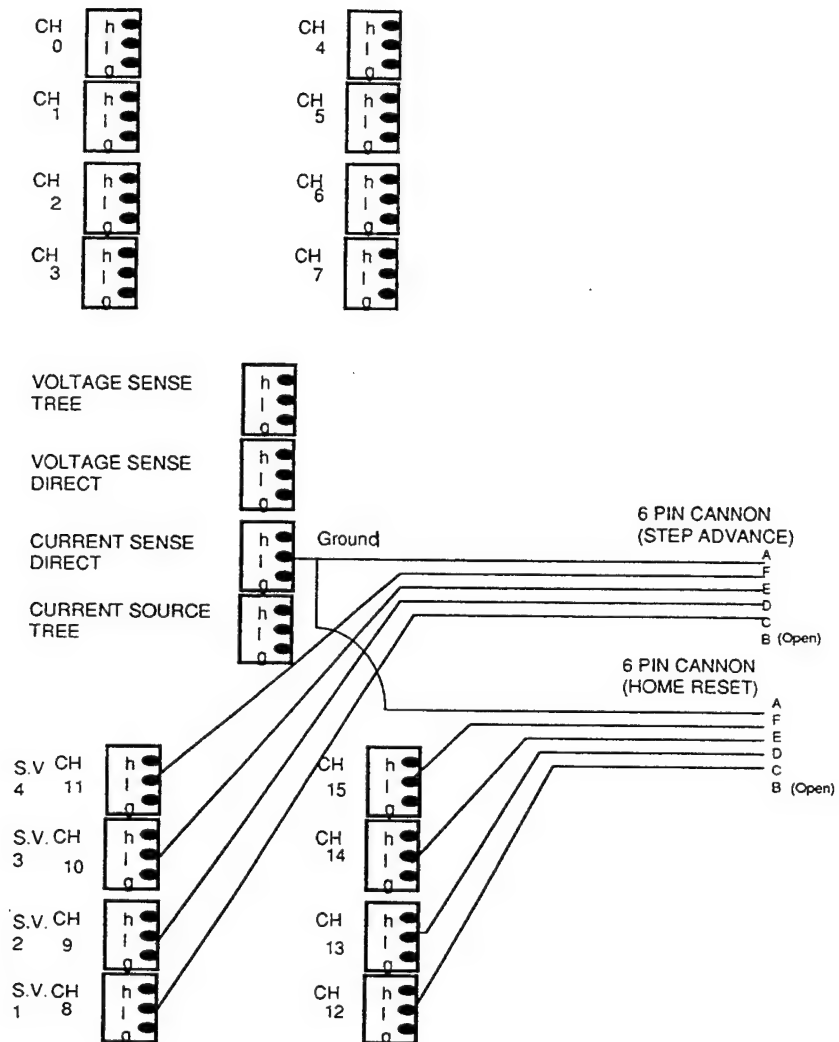


Fig. 7 Schematic of Switchbox Connections to HG-78.

Port #	Scanivalve 1
1	Tare
2	Scale
3	Flow Nozzle P6
4	Flow Nozzle Ps
5	Inlet Ptinfinity 1 Q1 3 O'clock
6	Inlet Ptinfinity 2 Q1 9 O'clock
7	Pnozzle static
8	
9	
10	
11	Kiel Probe
12	Kiel Probe
13	Kiel Probe
14	Kiel Probe
15	Kiel Probe
16	Kiel Probe
17	Kiel Probe
18	Kiel Probe
19	Kiel Probe
20	Kiel Probe
21	Kiel/TC Combination
22	Kiel/TC Combination
23	Kiel/TC Combination
24	Kiel Probe
25	Kiel Probe
26	Kiel Probe
27	Kiel Probe
28	Kiel Probe
29	Kiel Probe
30	Kiel Probe
31	Hub Static Pressures P2 1
32	Hub Static Pressures P2 2
33	Hub Static Pressures P2 3
34	Hub Static Pressures P2 4
35	Hub Static Pressures P3 1
36	Hub Static Pressures P3 2
37	Hub Static Pressures P3 3
38	Hub Static Pressures P3 4
39	Shroud Static Pressures P1 3 O'clock
40	Shroud Static Pressures P1 9 O'clock
41	Shroud Static Pressures P3 3 O'clock
42	Shroud Static Pressures P3 6 O'clock
43	Shroud Static Pressures P3 9 O'clock
44	Shroud Static Pressures Old style 1 P3
45	Shroud Static Pressures Old style 2 P2
46	Shroud Static Pressures Old style 3 P1
47	Shroud Static Pressures Old style 4 P1
48	Shroud Static Pressures Old style 5 Pi
Time References are from turbine out	

Table 3. Scanivalve Port Assignments.

The logic sequence for acquiring data from the 48 ports of the Scanivalve was as follows:

1. Reset to port 1
2. Ensure the Scanivalve was actually at port 1
3. Take the transducer reading using the DVM
4. Step to the next port
5. Ensure the Scanivalve was actually at the next port
6. Take the transducer reading using the DVM
7. Go to step 4 until all 48 ports were read

2. Scanning Digital Voltmeter

Connecting a 16-channel multiplexer to the DVM using the 'Analog Bus' allowed the multiplexer and DVM to operate together as a Scanning Multimeter. ['Scanning Multimeter' implies that one or more multiplexers were used with the multimeter as part of the same instrument using the same HP-IB secondary address]. The power of this configuration was that the multimeter was extended from having one set of terminals to having sixteen for each connected multiplexer. Two types of scanning multiplexer were employed. The first type was a thermocouple relay multiplexer module (HP 1347A). A thermistor was contained inside the terminal module, and its resistance used to determine temperature with which to compensate for temperature measurements made with the thermocouples. The second type was a standard relay multiplexer module (HP 1345A), which allowed the measurement of sixteen different channels using a single multiplexer/DVM

connection. The channel assignment for the two multiplexers is given in Table 4.

Multiplexer Channel	Thermocouples/Mux 100	DVM Scanner/Mux 200
00		Scanivalve 1 Transducer
01	T_t Station Inf @ 3 o'clock	Scanivalve 2 Transducer
02	T_t Station Inf @ 9 o'clock	Scanivalve 3 Transducer
03	T_t Station 3 Probe 21	Scanivalve 4 Transducer
04	T_t Station 3 Probe 22	Torque-Flexure Strain Gauge Array
05	T_t Station 3 Probe 23	
06		
07		
08		
09		
10	ΔT_t - Station Inf @ 3 o'clock and Probe 21	
11	ΔT_t - Station Inf @ 3 o'clock and Probe 23	
12		
13		
14		
15		

Table 4. Scanning Multiplexer Channel Assignments.

Readings from the four controlled Scanivalve transducers and the torque-flexure strain gauges were read directly and controlled by the DVM driver software.

To measure temperature directly, the thermocouple wires were connected directly to the thermocouple terminal module and the voltage measured and converted to degrees Fahrenheit. To measure the instantaneous differential temperature between stations 3 and Inf, a different process

was required. The thermocouples were connected as shown in Fig. 8.

The logic process was as follows:

1. Measure the temperature at station Inf (using the thermocouple multiplexer).

2. Convert the temperature measured in step 1 to volts using the equation relating temperature to voltage for a J type thermocouple.

3. Measured the voltage between the two thermocouples (using the scanning multiplexer).

4. Added the measured voltage of step 3 to the voltage obtained in step 2.

5. Converted the voltage obtained in step 2 to a temperature using the equation relating voltage to temperature for a J type thermocouple.

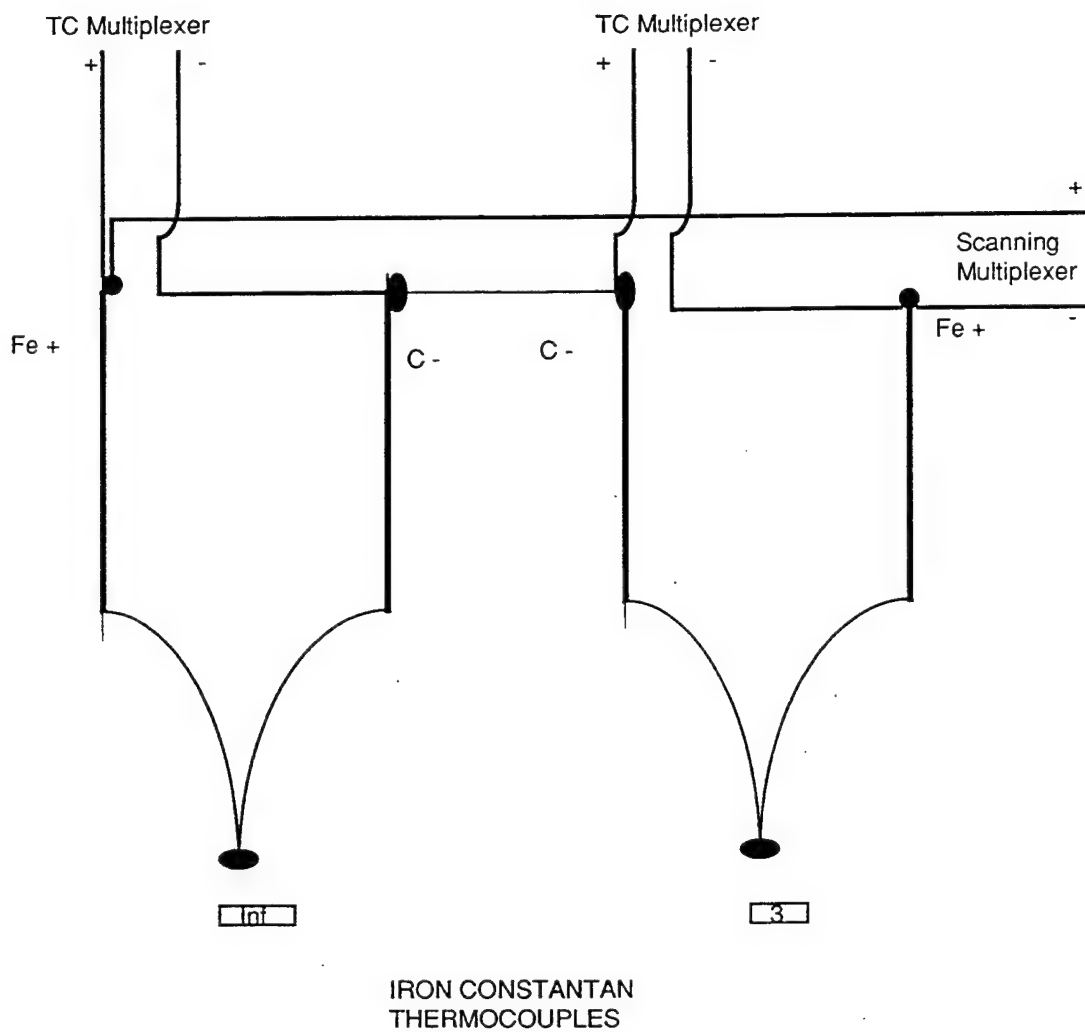


Fig. 8 Schematic of Differential Temperature Measurement.

3. Counter/Totalizer

The Counter/Totalizer was used to measure the frequency produced by the magnetic speed pickup. The pickup produced six pulses per revolution. Therefore, the frequency measured, in Hz, multiplied by 10 produced the RPM of the rotor. The signal produced was extremely noisy near the zero volt level. To reject this noise, the level to trigger the counter was set to +1 volt. The rotational velocity of the rotor was verified using a calibrated strobe light.

C. SOFTWARE

HPVEE was the software used to control the instrumentation. Software drivers were available in HPVEE for all instruments inside the mainframe. The 'panel' driver for the specific instrument served two purposes. First, it allowed the definition of a measurement state, that is the settings of all instrument functions. When the panel driver operated, the corresponding physical instrument was automatically programmed to match the settings defined in the panel driver. Secondly, the panel driver acted as a virtual control panel for interactively controlling the instrument.

In addition to controlling the instruments, HPVEE also allowed immediate reduction of the measured values to

engineering units. This allowed immediate feedback of data and made troubleshooting simpler.

D. DATA REDUCTION

The data were reduced using HPVEE. In the description which follows, the final form of the data reduction program is described. The results presented were calculated with the following methods.

The mass flow rate (in lbm/sec) through the flow nozzle, was given by

$$\dot{m} = 33135 \cdot C \cdot \sqrt{\frac{P_t \cdot \Delta_s}{459.7 + T_{inf}}} \cdot \left(1 - 0.021926 \cdot \frac{\Delta_s}{P_t}\right) \quad (1)$$

where $\Delta_s = (P_t - P_s)$ was in inches of water and the P_t was in inches of mercury. The constant C represented the discharge coefficient and was calibrated to be 1.03.

The first measure of the power absorbed by the compressor was obtained from the measurements of torque, M , and speed, N , as

$$HP_{C1} = 15865 \times 10^{-5} \cdot M \cdot N \quad (2).$$

The second measure of power was obtained from the flow rate and temperature rise across the stage, namely

$$HP_{C2} = 14137 \cdot C_p \cdot \dot{m} \cdot (T_{t3} - T_{t1}) \quad (3).$$

The performance of the compressor was described in terms of referred quantities that retain their original units:

$$\dot{m}_{ref} = \dot{m} \cdot \frac{\sqrt{\theta}}{\delta}$$

$$N_{ref} = \frac{N}{\sqrt{\theta}}$$

$$HP_{ref} = \frac{HP}{\delta \cdot \sqrt{\theta}} \quad (4)$$

$$M_{ref} = \frac{M}{\delta}$$

where $\theta = \frac{T_{tinf}}{T_{REF}}$, and $\delta = \frac{P_{tinf}}{P_{REF}}$, and where $T_{ref} = 518.7^\circ R$ and

$P_{ref} = 29.92$ inches of mercury.

The performance to be evaluated was of the rotor and stator combination. The honeycomb flow straightener in the outlet duct was necessary in order for the torque to be measured, but the losses occurring in this section are not included in appraising the compressor performance. The total-to-total (T-T) pressure ratio and efficiency from station 1 to station 3 were the parameters which gave the performance of the stage.

The total-to-total efficiency was defined as the ratio of the power required in an isentropic compression to the same outlet pressure, to the actual power required. The actual power was given by equation (2), using measurements of torque and speed, or by equation (3), using measurements of mass flow rate and temperature rise. The ideal power was given by

$$IHP_c = 14137 \cdot \dot{m} \cdot C_p \cdot [(T_{t3})_{is} - T_{tinf}] \quad (5)$$

where $(T_{t3})_{is}$ is related isentropically to the pressures by

$$\left(\frac{(T_{t3})_{is}}{T_{tinf}} \right) = \left(\frac{P_{t3}}{P_{tinf}} \right)^{\frac{\gamma-1}{\gamma}} \quad (6)$$

where γ is the ratio of specific heats. Substitution into equation (5), gives

$$IHP_c = 14137 \cdot \dot{m} \cdot C_p \cdot T_{tinf} \cdot \left[\left(\frac{P_{t3}}{P_{tinf}} \right)^{\frac{\gamma-1}{\gamma}} - 1 \right] \quad (7)$$

Three different methods were used to calculate the total-to-total efficiency. Method 1 simply used the temperature rise and total-to-total pressure ratio across the stage

$$\eta_h = \frac{IHP_c}{HP_{C2}} = \frac{T_{tinf}}{T_{t3} - T_{tinf}} \cdot \left[\left(\frac{P_{t3}}{P_{tinf}} \right)^{\frac{\gamma-1}{\gamma}} - 1 \right] \quad (8)$$

The second method used inlet static pressure measurements and mass flow rate to calculate an inlet stagnation pressure. Defining

$$B_{inf} = \left[\left(\frac{\gamma}{\gamma-1} \right) \cdot \frac{P_{inf}}{V_t \cdot \left(\frac{\dot{m}}{Area} \right)} \right] \quad (9)$$

where the area corresponded to where the P_{inf} measurement was taken, it follows that

$$\left(\frac{P_{t3}}{P_{tinf}}\right)^{\frac{\gamma-1}{\gamma}} = \left(\frac{P_{t3}}{P_{tinf}}\right)^{\frac{\gamma-1}{\gamma}} \cdot 2 \cdot B_{inf} \cdot X_{inf} \quad (10)$$

where $X_{inf} = \frac{V_{inf}}{V_{tinf}}$ and $V_{tinf} = \sqrt{2 \cdot C_p \cdot T_{tinf}}$. X_{inf} was given by

$$X_{inf} = \sqrt{B_{inf}^2 + 1} - B_{inf} \quad (11).$$

Thus

$$\eta_2 = \frac{T_{tinf}}{T_{t3} - T_{tinf}} \cdot \left[\left(\frac{P_{t3}}{P_{tinf}}\right)^{\frac{\gamma-1}{\gamma}} \cdot 2 \cdot B_{inf} \cdot X_{inf} - 1 \right] \quad (12)$$

was an efficiency which involved the mass flow rate measurement, whereas η_1 did not.

The final method for calculating efficiency depended on the measurement of torque and mass flow rate but did not depend on the measurement of the temperature rise across the stage, namely

$$\eta_b = \frac{IHP_C}{HP_{C1}} = \eta_h \cdot \frac{HP_{C2}}{HP_{C1}} = 0.89108 \cdot \frac{\dot{m} \cdot C_p \cdot T_{tinf}}{10^{-5} \cdot M \cdot N} \left[\left(\frac{P_{t3}}{P_{tinf}}\right)^{\frac{\gamma-1}{\gamma}} - 1 \right] \quad (13).$$

IV. RESULTS OF THE TEST PROGRAM

A. INTRODUCTION

The performance of the stage was measured at 50%, 60%, 65%, 70%, and 80% of the design speed of 27,085 rpm. The instrumentation remained constant during all runs and no changes to the data acquisition or reduction system were required. Some changes were made in how the reduced data were saved making plots of torque, horsepower and stage temperature rise versus mass flow rate only available for 70% speed and 80% speed. Each set of plotted experimental performance data was fitted with a second order least-squares curve. The exit impact pressure profiles and axial static pressure distributions were also plotted.

B. STAGE PERFORMANCE MAPS

The total-to-total pressure ratio, efficiency calculated by equations (8), (12) and (13), referred torque, referred horsepower and stage temperature rise were plotted versus the referred mass flow rate, for constant speed conditions expressed as a percentage of design speed.

Figure 9 shows the total-to-total pressure ratio vs referred mass flow rate. The plot shows the characteristic increase of pressure ratio and decrease of mass flow rate as the flow was throttled. At all speeds except for 80% speed the stage was throttled to stall. The loss of the stage

occurred before stall was reached at 80% speed. The open-throttle 'choke' condition for the stage could not be reached due to the pressure drop across the honeycomb flow straightener.

Figures 10, 11, and 12 are efficiency plots. The efficiency η_3 was expected to be the most accurate as it used torque and speed measurements which provided an integral measurement of the work to the compressor. The other two efficiency measurements used the temperature rise across the stage. Since the total temperature was not expected to be constant radially at the exit and the measurement was taken at only three points in the center of the passage, the η_1 and η_2 measurements of efficiency were likely to be optimistic. The results show that η_3 varied in the same way as the other two efficiency measurements, but was consistently lower in magnitude. The data for η_3 at 80% speed measured 2.5% lower than the other constant speed lines. This was possibly the result of drift in the strain-gauge bridge output (caused by increased temperature) which was not balanced to zero before the final run was started. The drift was observed after the loss of the stage. The results for η_1 and η_2 support this contention since no appreciable drop was observed in the 80% speed results.

The CFD analysis results shown on the performance maps were obtained for the rotor geometry, and did not include the stator. These results are discussed in the following section.

Figure 13 shows the increased torque required as the compressor was throttled. Figure 14 shows the increase in the stage temperature rise as the compressor was throttled. The stage temperature rise was calculated as the average of the differential temperature of one probe at station Inf with two probes at station 3. Figure 15 shows a comparison of the horsepower required to drive the stage calculated using the mass flow rate and stage temperature rise, (Eq. (3)), with that calculated using the torque and speed measurements (Eq. (2)). The horsepower measured by torque and speed was consistently greater than horsepower deduced from mass flow rate and temperature rise.

C. PRESSURE PROFILES

Figures 16 and 17 show the exit total pressure profiles at 70% speed and 80% speed respectively. (Note that the probes were at different peripheral settings in the radial direction shown in Table 2). The ratio of each measured total pressure at station 3 to the total pressure at station 1 was calculated. Three different throttle settings are shown at each speed. At design conditions, the stage was

designed to have nearly uniform total pressure across the exit [Ref. 1]. The plots show that as the stage was throttled, at an intermediate throttle setting the total pressure was nearly uniform across the annulus, except near the walls. The plots also show that as stall was approached, which corresponded to the lowest mass flow rate curve, a separation had progressed radially outward from the hub.

Figures 18 and 19 are plots of the static pressure measured at different axial stations at the same rotor speeds and throttle settings shown in the data in Figs. 16 and 17 respectively. All pressures are scaled by the pressure at station infinity.

At station 2 a strong static pressure gradient existed from hub-to-tip at all measured states of throttling and wheel speed. This gradient is consistent with the high tangential velocities expected at the rotor exit. The pressure rise through the stator behaved in a consistent way with throttling at each of the speeds measured. First, the pressure rise at the hub was large at all throttle settings. At the tip, the rise improved with closing throttle, until the static pressure difference between hub and tip at station 3 disappeared as the stage approached stall.

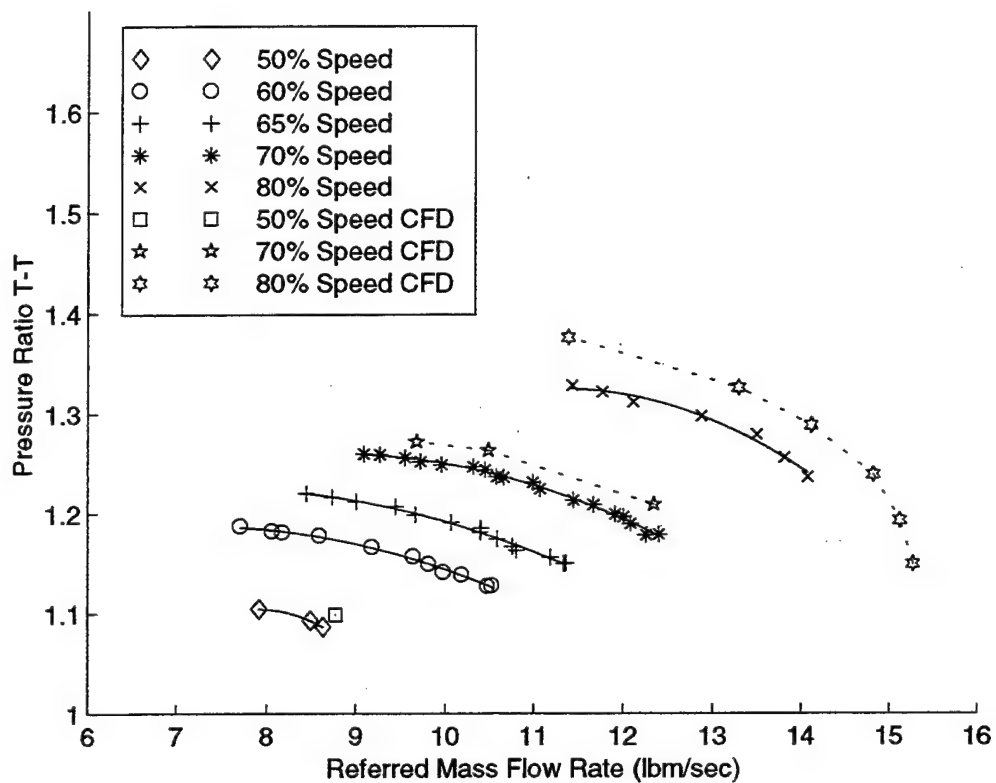


Fig. 9 Pressure Ratio (T-T) vs Referred Mass Flow Rate.

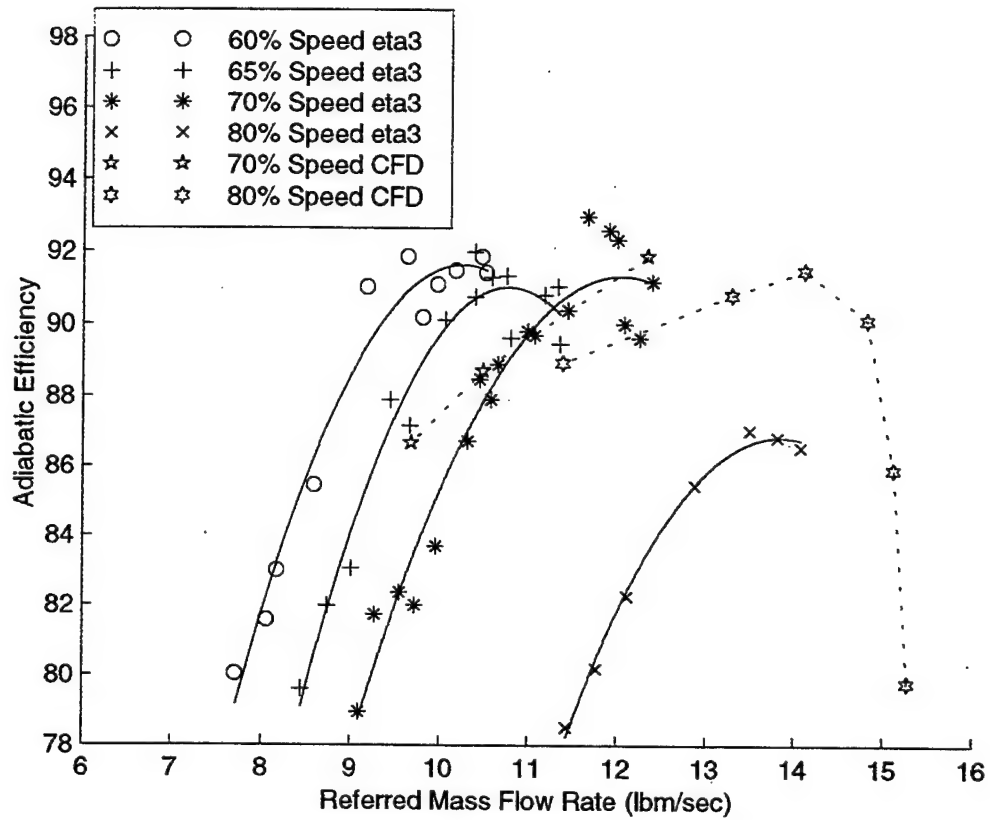


Fig. 10 Adiabatic Efficiency (η_a) vs Referred Mass Flow Rate.

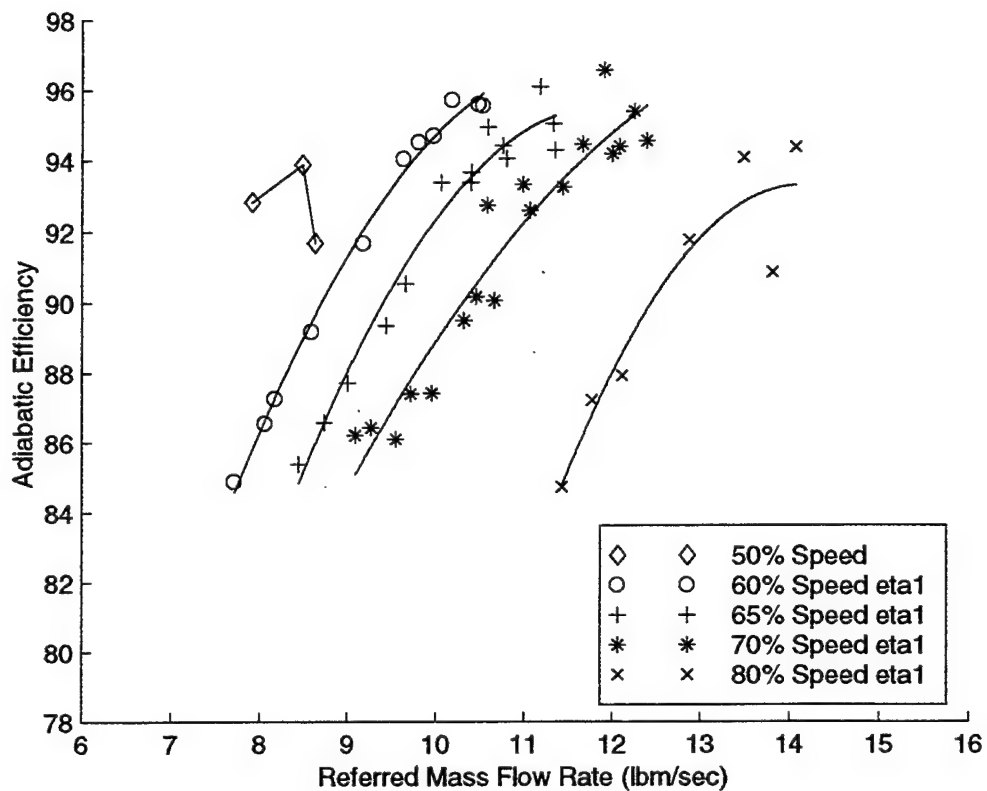


Fig. 11 Adiabatic Efficiency (η_1) vs Referred Mass Flow Rate.

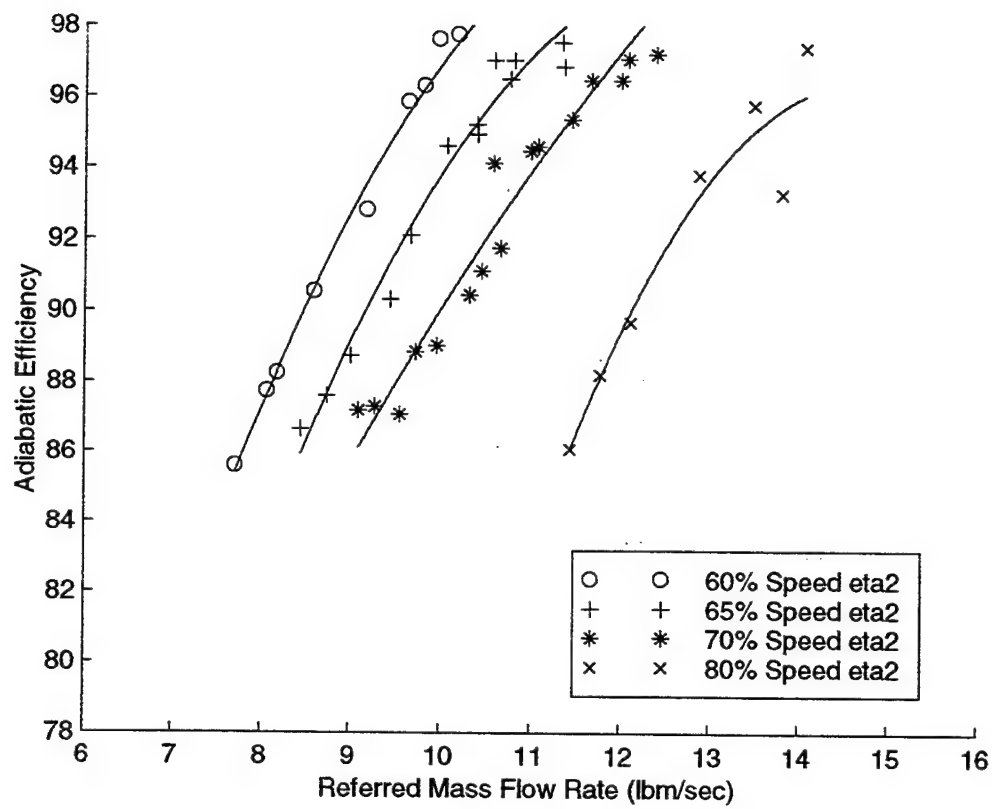


Fig. 12 Adiabatic Efficiency (η_2) vs Referred Mass Flow Rate.

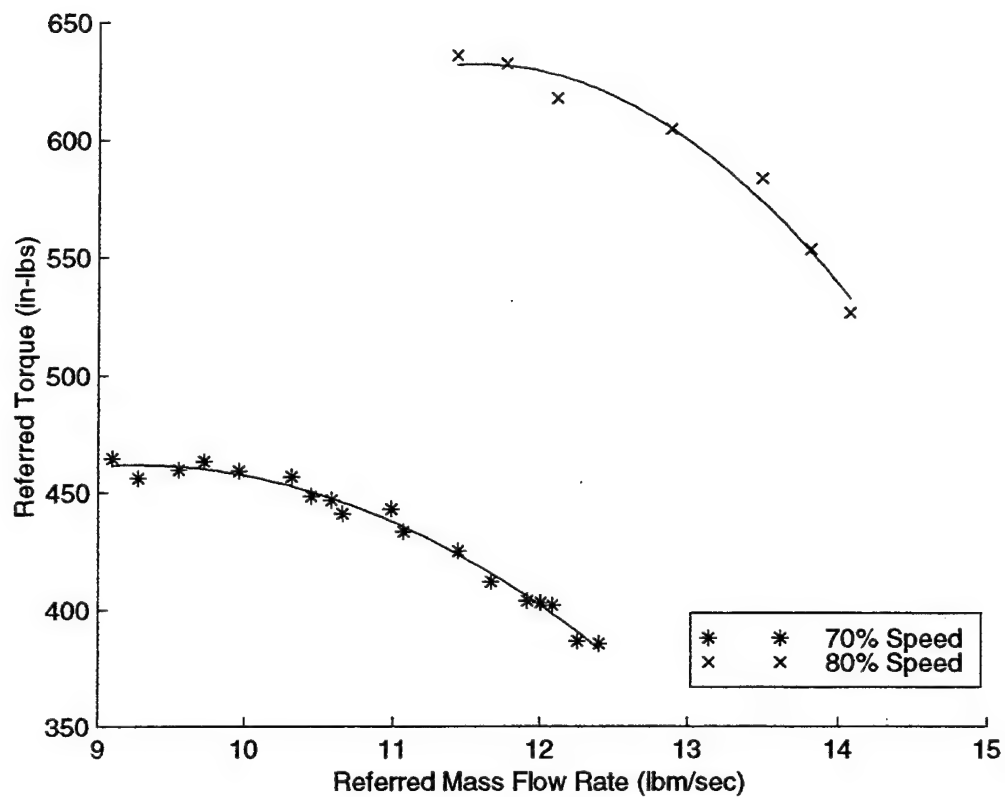


Fig. 13 Referred Torque vs Referred Mass Flow Rate.

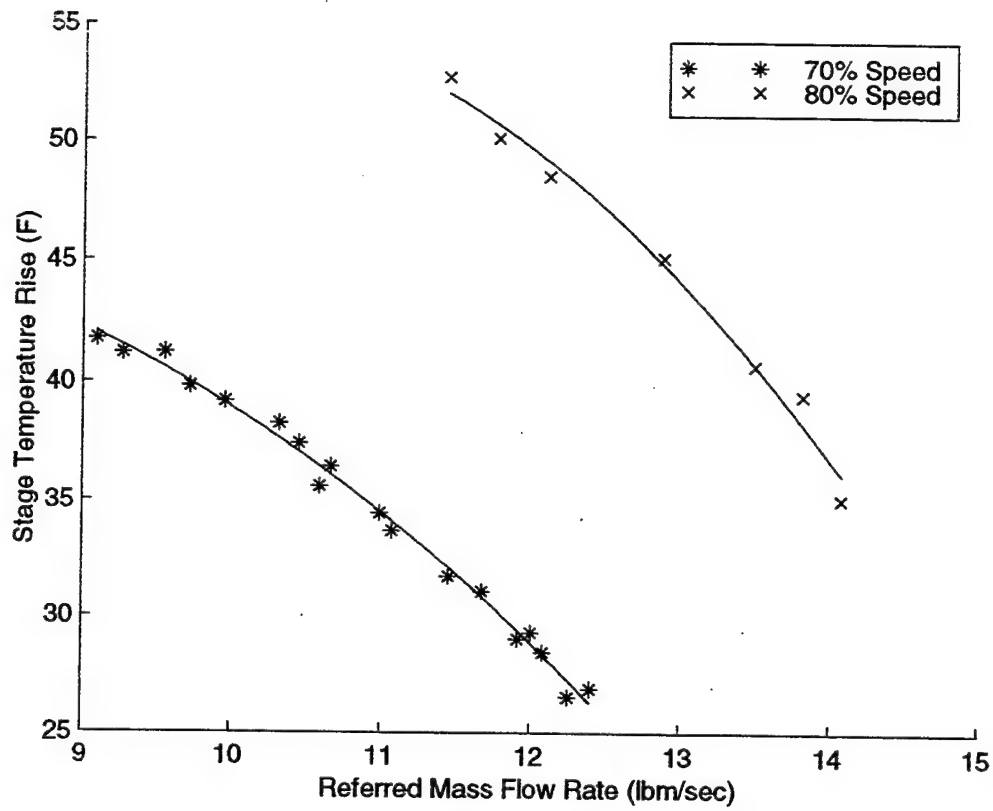


Fig. 14 Stage Temperature Rise vs Referred Mass Flow Rate.

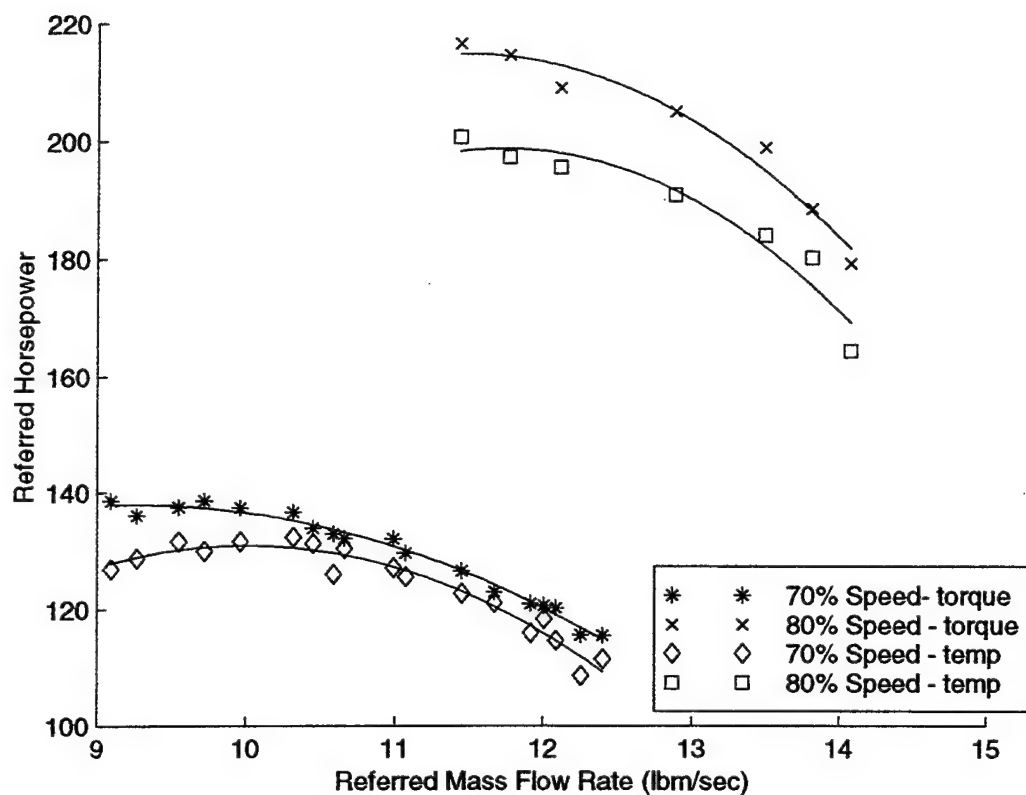


Fig. 15 Referred Horsepower vs Referred Mass Flow Rate.

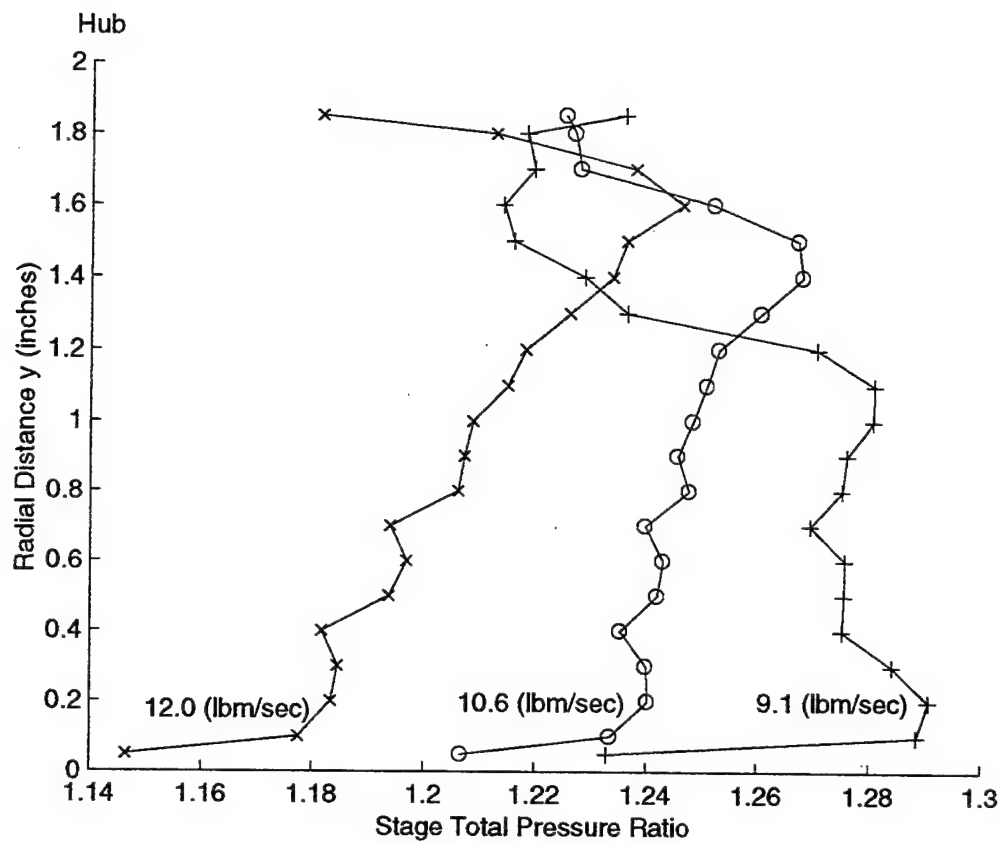


Fig. 16 Exit Pressure Distribution at 70% Speed.

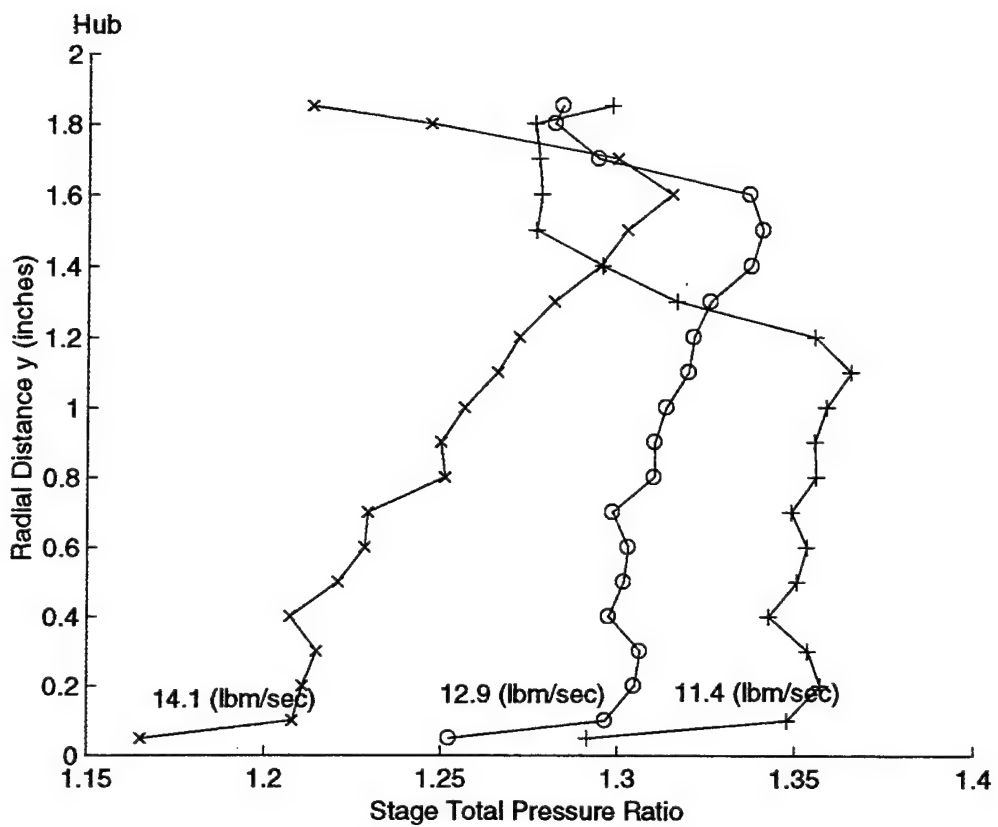


Fig. 17 Exit Pressure Distribution at 80% Speed.

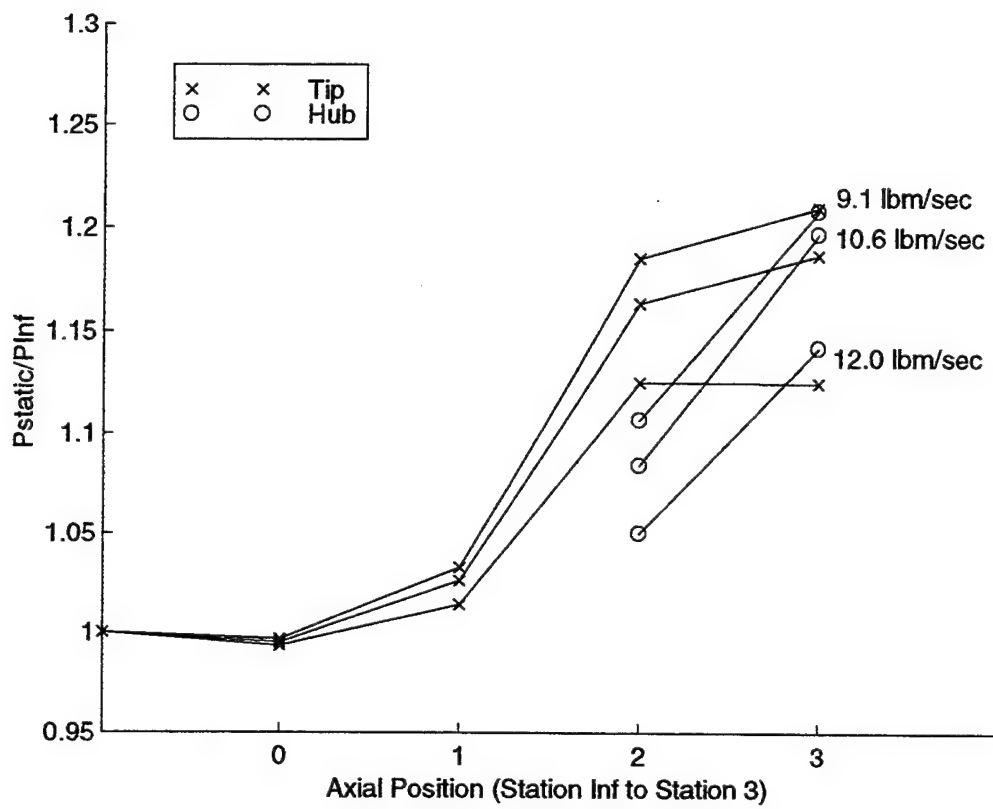


Fig. 18 Axial Static Pressure Distribution at 70% Speed.

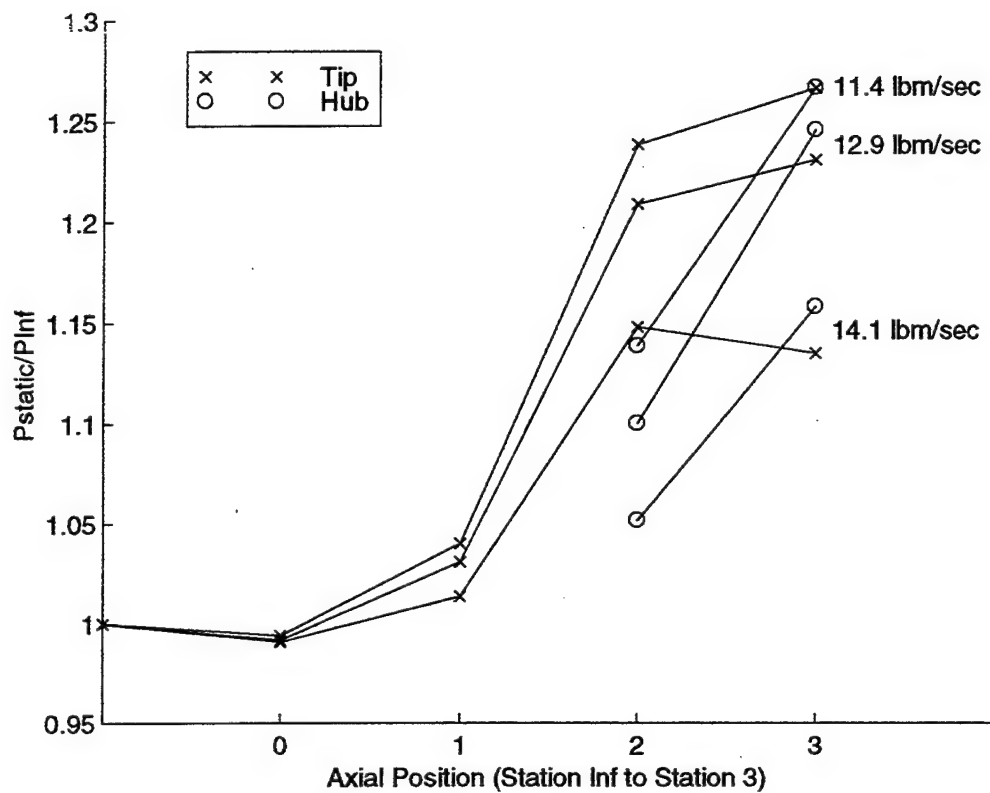


Fig. 19 Axial Static Pressure Distribution at 80% Speed.

V. RESULTS OF CFD ANALYSIS

A. INTRODUCTION

Before starting the experimental work, the flow through the rotor was analyzed and the rotor performance was predicted using CFD. Specifically, Rotor Viscous Code 3-D (RVC3D), a computer code for analysis of three-dimensional viscous flows in turbomachinery [Ref. 3], was used to compute performance maps of the rotor from 50% to 100% of the design speed. Additionally, using the graphics package FAST from NASA Ames, a number of parameters were calculated and graphically displayed for 100% speed. The predicted results for the rotor were compared to the experimentally-obtained maps for the stage and they were observed to be numerically consistent with each other.

B. GRID GENERATION

The geometry data for the hub, tip and blade for the stage were provided electronically by NASA Lewis. The data were in MERIDL (z, r, theta, dtheta) format.

The geometry file was entered into Turbomachinery C GRID (TCGRID) which generated a three-dimensional C type grid compatible with the Rotor Viscous Code 3-D (RVC3D) [Ref. 7]. The grid which was 185X40X49 (in i, j, and k) is shown in Fig.20. The output grid was stored in plot3d multiple grid format. A FORTRAN program was used to rotate

the grid one grid width to form the multi-block grid that was an input to FAST.

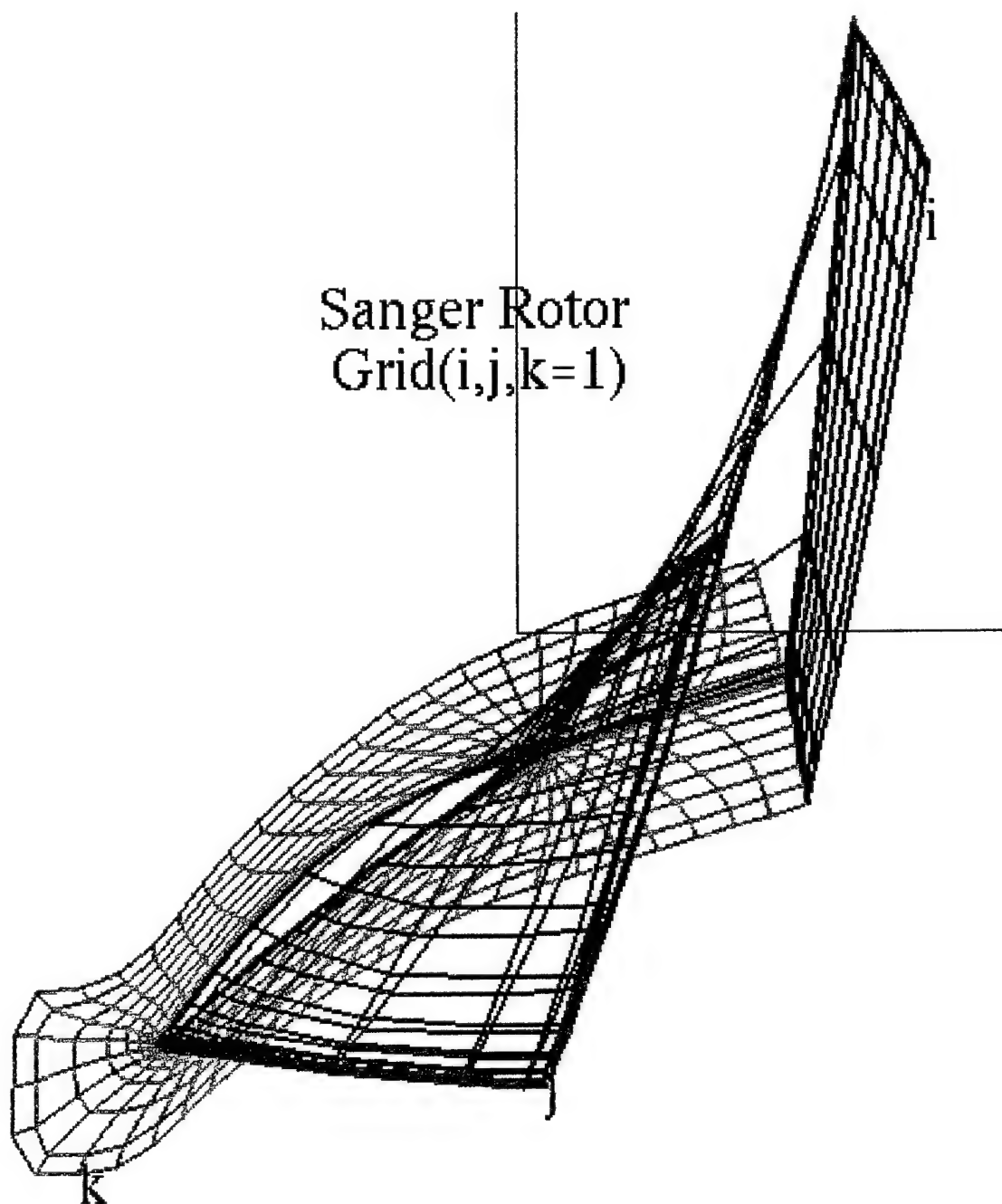


Fig. 20 Computational Grid for RVC3D Calculations

C. COMPUTATION

The code solved the thin-layer Navier-Stokes equations with an explicit four stage Runge-Kutta scheme. The number of stages was optional; however, four was recommended by the author. A spatially-varying time step (Δt) was used to accelerate the convergence of the code. Δt was updated every fifty iterations.

Since the flow was supersonic, a second-difference artificial viscosity term was used. The value was set to 1.0 in order to produce a well defined shock with little smearing or waviness. No first-order artificial viscosity term was required.

RVC3D used an implicit residual smoothing routine which allows the multistage scheme to run at a high, unstable Courant number, but stability was maintained by smoothing the residual using an implicit filter. The initial Courant number chosen was 5.0.

The code ran completely non-dimensionally, with variables referenced to speed of sound, reference temperature and reference pressure. The input parameters that controlled the flow were the normalized blade row rotational speed per unit length and the ratio of the hub exit static pressure to the reference total pressure.

D. RESULTS

Version 208 of the code was run on three different machines, a Silicon Graphics Indigo2 workstation, the NPS Cray, and NASA Ames Cray. On the NASA Ames Cray, each iteration took 2.3 seconds of CPU time and required 9Mw of storage. The code was compiled using FORTRAN 90 and O2 optimization that gave good scalar and vector optimization and performed autotasking. Six processors were normally used. In order for the grid, solution, and restart files to be compatible with each machine, IEEE format was selected for the data input and output.

To compute the operating lines at a constant rotational speed, from the choke region to the stall region, the ratio of the hub exit static pressure to the reference total pressure (p_{rat}) was increased in steps. For each p_{rat} at which a solution converged, the mass flow rate, the mass-averaged inlet and exit total pressures, and the adiabatic efficiency were recorded from the output file for plotting. When a converged solution could not be obtained (near stall), the rotational speed was changed and a new range of values of p_{rat} was selected and entered. The operating speeds computed in this manner were 70%, 80%, 90% and 100% of design speed. Additionally, one point was computed at 50% of design speed. The results are shown plotted in Figs. 21 and 22. The results were observed to be extremely close to the results Sanger obtained using an Euler solver with boundary layer

modeling (Denton's Code [Ref. 1]). At design mass flow rate of 17.1 lbm/sec Sanger obtained a total pressure ratio of 1.61, and using RVC3D a total pressure ratio of 1.601 was found.

The predicted results for the rotor at 70% and 80% speed are shown plotted with the experimental data for the stage in Figs 9 and 10. A direct numerical comparison is not meaningful since the predicted results were only for the rotor. However, the computed results are qualitatively consistent with what was measured for the stage behavior. The pressure ratio computed for the rotor was consistently higher than was measured for the stage, and the range of mass flow rate predicted at each rotor speed was consistent with the stage measurements. At 80% speed, solutions were obtained closer to choke (more open throttle) than could be achieved in the test program for the stage.

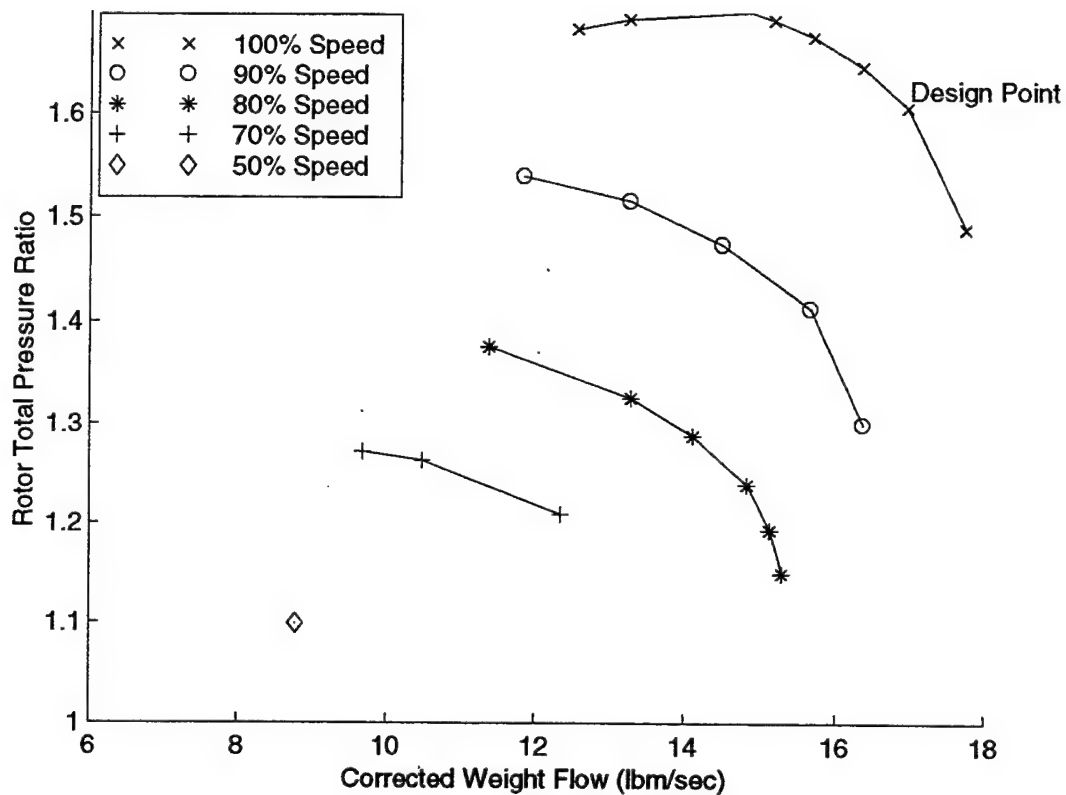


Fig. 21 Rotor Total Pressure Ratio vs Corrected (Referred) Mass Flow Rate Computed Using RVC3D

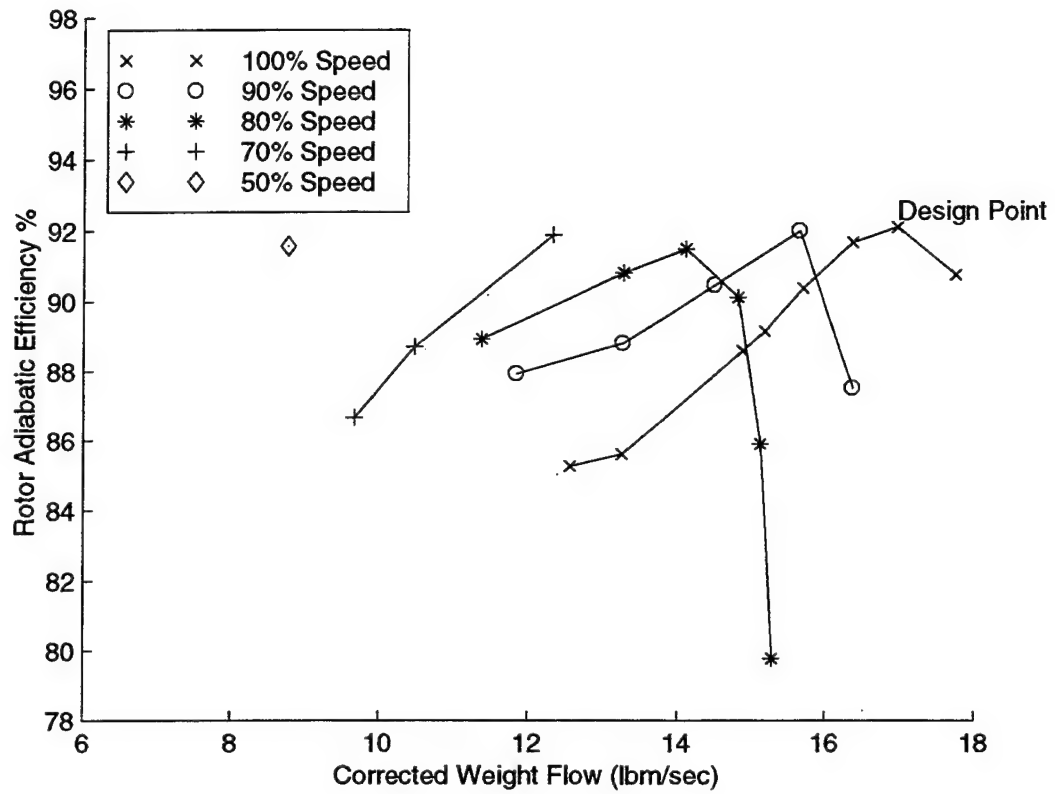


Fig. 22 Rotor Adiabatic Efficiency vs Corrected (Referred) Mass Flow Rate Computed Using RVC3D

VI. CONCLUSIONS AND RECOMMENDATIONS

A test program was conducted to 80% of design speed to evaluate the performance of a new transonic axial compressor stage. Tests to 100% speed were prevented by the failure of the spinner retaining bolt which led to the loss of the stage. The cause of the failure was shown by analysis and tests will resume when replacement parts are delivered.

A new data acquisition system, using PC-based control of VXI-bus instrumentation, was programmed and used successfully in the tests. HPVEE software was used with the VXI-bus hardware for Scanivalve control, acquisition of pressures, temperatures, strains and frequencies, and for the reduction of data. The system was found to be extremely flexible and well-suited to the researcher in the laboratory environment.

The flow through the rotor alone was computed using the RVC3D code. The test results obtained agreed qualitatively with the predicted rotor performance and were also numerically consistent with them. This was a first step in the code validation process. The next step will be to measure the flow profile at the exit of the rotor and compare what is measured to the predicted flow field. The final step will be to measure the flow between the rotor blades and pressure distribution on the blade surfaces and compare these to predicted results.

With the experience obtained from the present study the following specific recommendations are made:

- With the inlet temperature fluctuations caused by the coastal location of the laboratory, increased use of averaging is required. First, a scan of temperatures and wheel speed should be conducted, then a pressure scan, then a second scan of temperatures and wheel speed should be taken and averaged with the first one to define one data point. Three data points should then be taken and averaged to produce an averaged data point to plot on the performance maps.
- The torque-flexure strain gauge bridge output should be readjusted to zero between each constant speed run. (The output should be zero with no torque applied. However, the zero tended to drift with increased operating temperatures and therefore needed to be adjusted).
- Install a strain gauge multiplexer for strain measurements. Software procedures would then make the previous recommendation unnecessary and would be the preferred solution.
- In rebuilding the stage, use only a solid steel spinner retaining bolt, use a transparent case wall, and re-use the video-monitoring and recording system demonstrated in the present study.

LIST OF REFERENCES

1. Sanger, N. L., Design of a Low Aspect Ratio Transonic Compressor Stage Using CFD Techniques, ASME Paper No. 94-GT-236, Presented at the International Gas Turbine and Aeroengine Congress and Exposition, The Hague, The Netherlands, June 13-16, 1994.
2. Reid, William D., Transonic Axial Compressor Design Case Study and Preparations for Testing, Master's Thesis, Naval Postgraduate School, Monterey, California, September 1995.
3. Chima, Roderick V., "RVC3D - Rotor Viscous Code 3-D User's Manual and Documentation", NASA Lewis Research Center, March, 1992.
4. United Sensor Corporation, "List Price Schedules", 3 Northern Boulevard, Amherst, NH 03031-2329, April 04, 1994.
5. Shreeve, R. P., Report on the Testing of a Hybrid (Radial-To-Axial) Compressor, Technical Report NPS-57Sf73112A, Naval Postgraduate School, Monterey, California, November 1973.
6. Geopfarth, Robert N., Development of a Device for the Incorporation of Multiple Scanivalves into a Computer-Controlled Data System, Master's Thesis NPS67-79-002, Naval Postgraduate School, Monterey, California, March 1979.
7. Chima, Roderick V., "TCGRID - Turbomachinery C-grid User's Manual", NASA Lewis Research Center, November 1990.

APPENDIX A ANALYSIS OF THE SPINNER BOLT FAILURE

A. OVERVIEW

While operating at 80% speed, with the inlet throttled to produce near stall conditions, the bolt attaching the spinner to the rotor failed. The spinner detached and contacted the rotor, causing complete loss of the stage and casing. Photos of the failed bolt, the destroyed stage, and the damaged Lucite casing are shown in Figs. A1, A2, and A3 respectively. While running the compressor, a video camera was being used to monitor and film the operation. Using the video film (at 30 frames/sec) and pressure readings measured immediately before the event, an analysis was conducted of the failure.

B. CONSTRUCTION

The spinner used with the stage had been modified from the design used on the Vavra stage. The retaining bolt was required to be two inches longer; namely, 3.09 inches versus 1.09 inches for the Vavra spinner retaining bolt. The bolt was a Socket Head Cap Screw #8-32, which was not manufactured (standard) with the new required length. In order to increase the length of the bolt, a 1-1/8 inches bolt was cut in half. A metal sleeve with 5/32 inches o.d. and 1/8 inches i.d. was placed over the two halves that had been turned down to 1/8 inches o.d. The metal sleeve was

then silver brazed at 1050° F to form the extension. After spin balancing the rotor and drive shaft, the spinner was attached using the bolt and the assembly rebalanced. This required removing material from the inner edge of the spinner. When balance was finally achieved, the bolt attaching the spinner was 'lightly torqued'. Only after the event was it found that the metal was cut from copper tubing.

C. ANALYSIS

In order to estimate the aerodynamic load on the spinner the pressure measurements recorded just before the failure occurred were used. The throttle had been closed a small fraction more when the failure occurred; therefore, the previously scanned pressure values are considered to be very close to those that were present. For a worst-case analysis, the pressure inside the spinner was assumed to be the stagnation pressure at the nose of the spinner. (This assumption is reasonable since the hole that the bolt passed through was not sealed and leakage in would have occurred. The shoulder at the rim of the spinner was also not sealed and the pressure behind the spinner would leak out and be less than this 'worst case' assumption). The pressure on the outer wall was taken to be the average of the static pressures taken at station one, another static pressure reading taken mid-length of the spinner, and the static

pressure at the nose of the spinner. All the static pressure measurements were taken at the casing wall. With this pressure distribution an axial force of 11.0 lbf was calculated. This axial force would have caused a tensile stress of 1.6 ksi in the copper sleeve of the bolt. The stress in the copper sleeve due to the torque used to attach the bolt to the rotor was estimated to have been 10.3 ksi. The maximum steady total tensile stress in the copper sleeve was therefore 11.9 ksi.

From the videotape of the event, it was observed that the spinner went upstream and disappeared from view within 2 video frames, came back and 'flew' stably for several seconds, moving around the annulus, and then fell into the blading. Since the frame speed was known to have been 30 frames/sec, an estimate of the acceleration of the spinner as it left the rotor was made by comparing the relative positions of the spinner over two frames. The estimated average acceleration was 225 ft/sec^2 . The drag force on the spinner (downstream) was calculated to have been 2.52 lbf. The net force required to accelerate the spinner upstream was calculated to have been 2.33 lbf. The initial force on the spinner necessary to explain the video images was therefore 4.85 lbf. This compares to the estimate made using pressure measurements that calculated a force of 11.0 lbf. The image on the first frame following detachment was blurred as the spinner moved rapidly upstream, making an

accurate estimation of the instantaneous acceleration at the time of detachment impossible. Therefore, although the calculations do not agree closely, they do demonstrate that the forces calculated to be present were of the order of magnitude necessary to explain the observed behavior of the spinner if the copper sleeve failed in tension.

The tensile strength of annealed copper is 32 ksi and the yield strength is 5 ksi. Copper has the property of strain hardening. Therefore, each time the sleeve was stressed into plastic deformation the tensile strength would have decreased. With a stress twice the yield strength present, failure of the bolt occurred when the tensile force exceeded the reduced tensile strength.

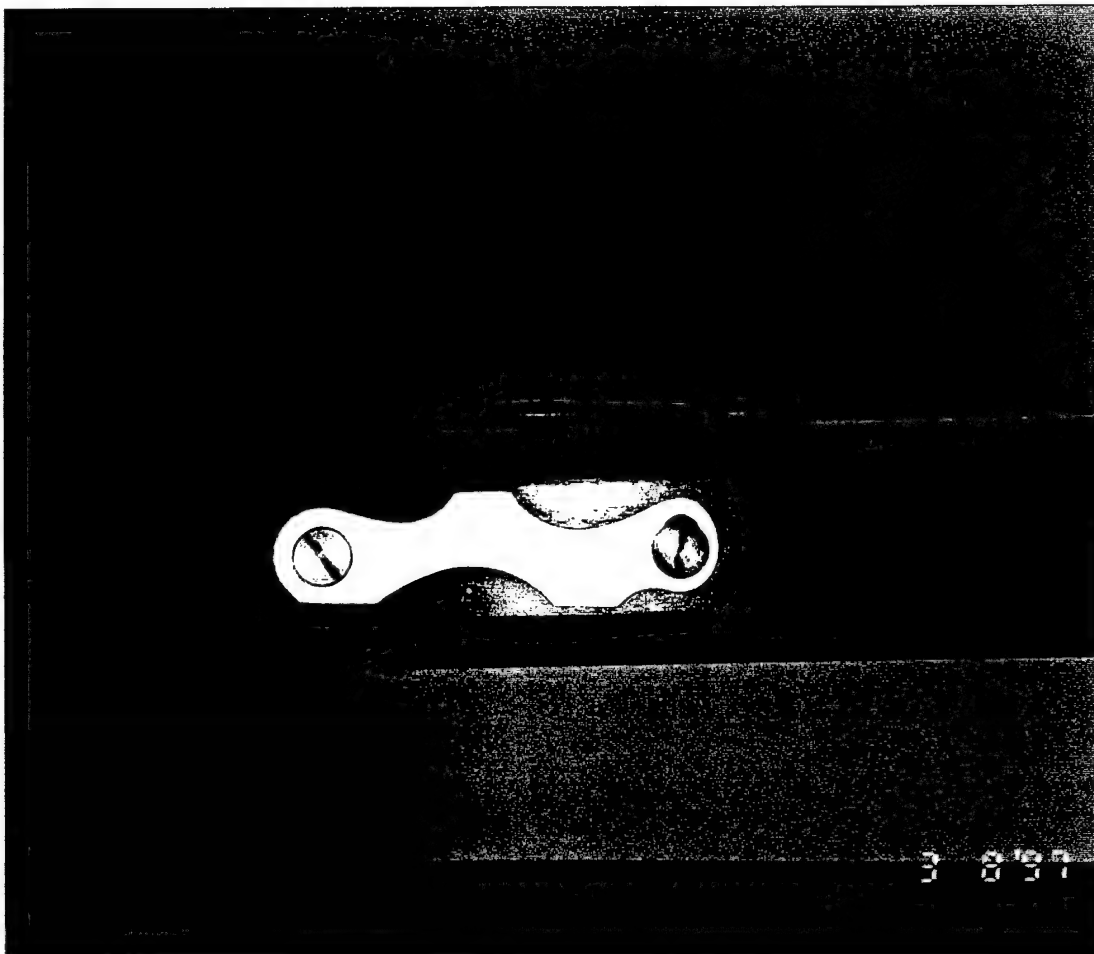


Fig. A1 View of the Failed Spinner
Retaining Bolt

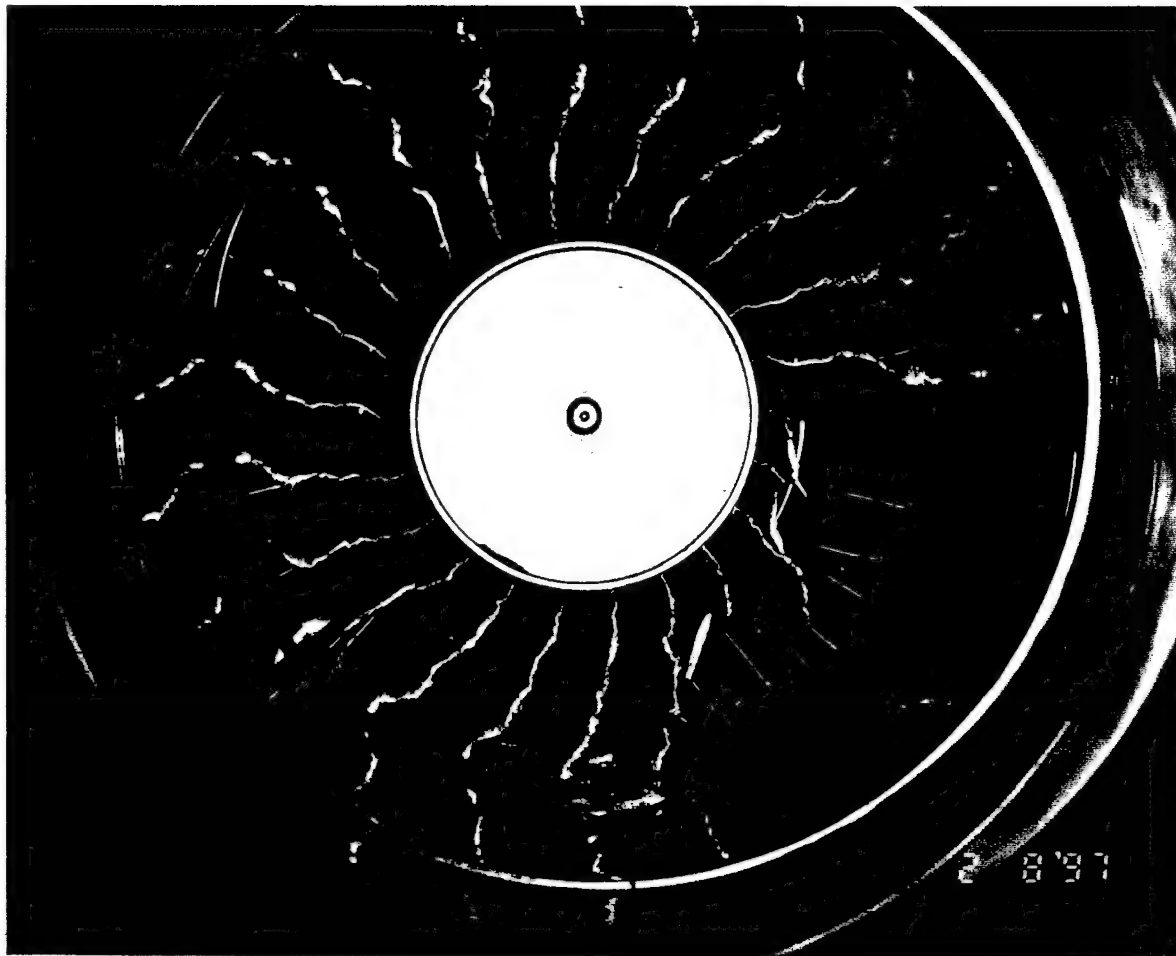


Fig. A2 View of Stage After Failure

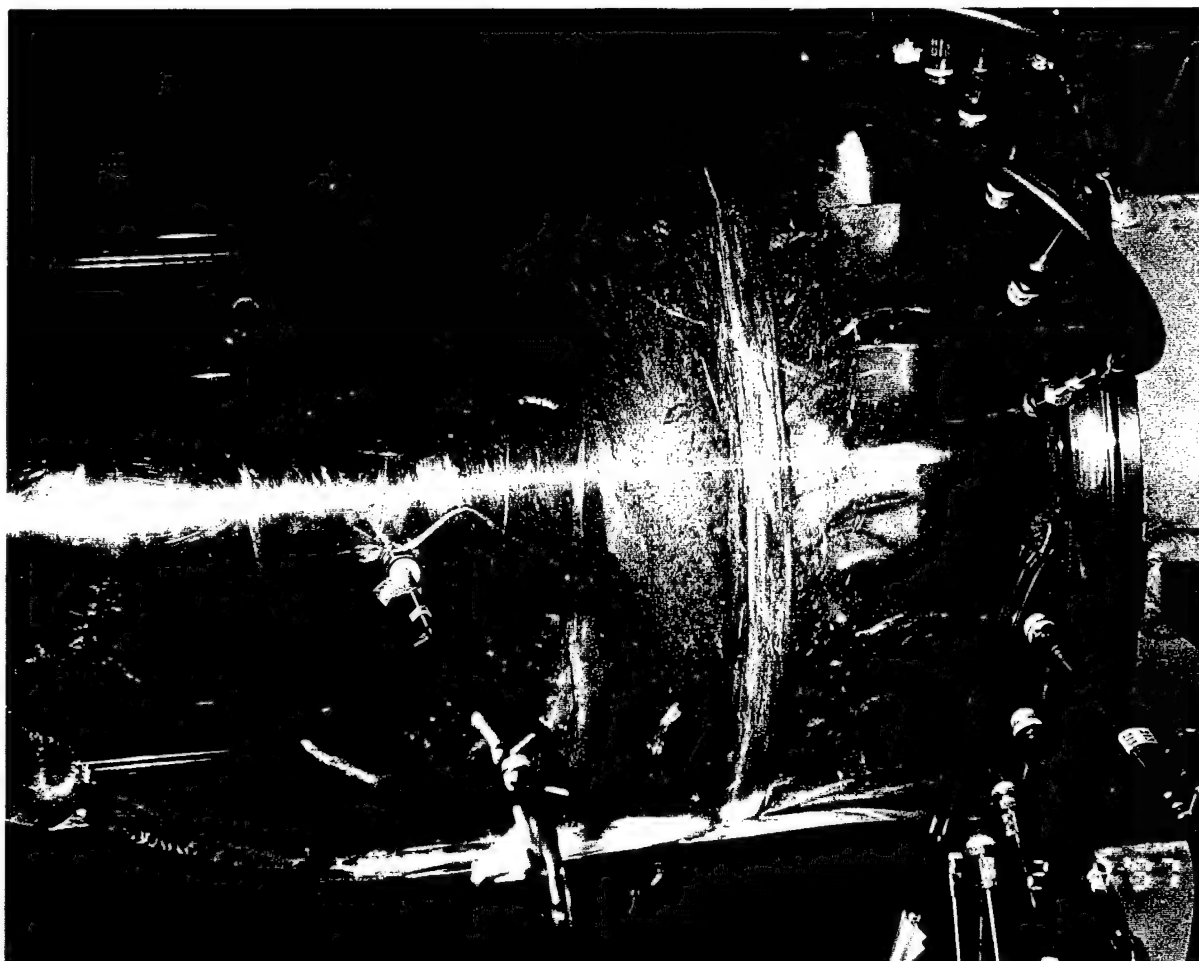


Fig. A3 View of Lucite Casing After Failure

APPENDIX B RESULTS

The reduced results of all test runs are presented below. Data points with no values present for horsepower were caused by problems with the data acquisition system. The point at the same state was re-measured until a complete data scan was obtained. The corresponding raw data file raw_tcr.dat is not printed but is held on a 3.5 inch floppy disk by Dr. Shreeve.

Data Point	Time Stamp	Mass Flow	Referred Mass Flow	HP - Torque	HP - Referred Torque	HP - Temp	HP - Referred - Temp	RPM	Torque Referred	Pressure Ratio	η_1	η_2	η_3	Percent of Design Speed
1	Not Taken	8.18	8.49	31.67	32.43	40.11	41.07	13472.40	151.71	1.09	0.94	0.94	1.19	49.74
2	Not Taken	7.46	7.91	31.60	32.98	41.49	43.30	13398.67	155.16	1.10	0.93	0.94	1.22	49.47
3	Not Taken	8.37	8.63	32.62	32.94	39.51	39.90	13468.54	154.16	1.09	0.92	0.93	1.11	49.73
4	63005621999	6.53	6.62	17.07	17.20	16.27	16.40	10149.44	106.82	1.05	0.97	0.99	0.93	37.47
5	63005623141	10.17	10.47	135.98	139.12	65.36	66.87	32216.44	272.18	1.13	0.95	0.98	0.46	118.95
6	63005623483	10.19	10.48	68.06	69.67	65.40	66.95	16119.58	272.44	1.13	0.96	0.98	0.92	59.51
7	63005624182	9.42	9.98	71.00	73.94	68.30	71.13	16164.54	288.32	1.14	0.95	0.98	0.91	59.68
8	63005625126	8.95	9.69	73.02	78.26	71.72	76.87	16183.05	304.83	1.16	0.94	0.96	0.92	59.75
9	63005625211	8.90	9.62	73.30	78.52	72.36	77.51	16223.12	305.09	1.16	0.92	0.95	0.91	59.80
10	63005625290	8.85	9.62	73.19	78.10	70.56	75.30	16162.88	304.56	1.16	0.95	0.97	0.92	59.67
11	63005625558	8.85	9.66	74.89	79.68	72.59	77.23	16255.67	308.97	1.16	0.94	0.96	0.91	60.02
12	63005626919	8.89	9.65	72.63	77.67	71.28	76.23	16127.75	303.57	1.16	0.94	0.96	0.93	59.54
13	63005628177	8.32	9.19	73.45	79.97	72.92	79.40	16150.72	312.09	1.17	0.92	0.93	0.91	59.63
14	63005628631	7.21	8.18	75.61	84.48	71.92	80.35	16114.79	330.43	1.18	0.87	0.88	0.83	59.50
15	63005629011	6.77	7.73	76.02	85.75	71.56	80.72	16162.88	334.42	1.19	0.85	0.86	0.80	59.67
16	63005629209	6.74	7.71	75.69	85.16	71.46	80.40	16123.32	332.91	1.19	0.85	0.86	0.80	59.53
17	63005629276	6.77	7.72	75.51	85.06	71.18	80.17	16117.25	332.65	1.19	0.85	0.86	0.80	59.51
18	63005629470	7.12	8.07	76.04	85.26	71.56	80.24	16139.16	332.99	1.18	0.87	0.88	0.82	59.59
19	63005629652	7.13	8.06	76.05	85.34	71.81	80.58	16152.61	333.03	1.18	0.86	0.88	0.81	59.64
20	63005629960	7.67	8.59	76.21	84.66	73.03	81.13	16179.08	329.83	1.18	0.89	0.91	0.85	59.73
21	63005630540	9.13	9.82	73.50	77.74	70.14	74.18	16161.29	303.20	1.15	0.94	0.96	0.90	59.67
22	63005630792	9.60	10.19	71.49	73.90	68.33	70.63	16069.02	289.86	1.14	0.96	0.98	0.91	59.33
23	63005631022	10.20	10.54	69.32	70.87	66.33	67.81	16127.90	276.99	1.13	0.96	0.98	0.91	59.55
24	63005634452	10.85	11.33	90.64	92.39	84.77	86.41	17475.01	333.25	1.15	0.94	0.97	0.88	64.52
25	63005635258	10.83	11.38	89.12	90.28	85.78	86.90	17402.68	327.00	1.15	0.94	0.96	0.91	64.25
26	63005635569	10.04	10.81	89.95	93.59	85.72	89.19	17278.97	341.42	1.16	0.94	0.97	0.90	63.80
27	63005635762	9.67	10.59	90.66	95.98	87.17	92.29	17303.58	349.64	1.17	0.95	0.97	0.91	63.89
28	63005635964	9.35	10.41	92.97	100.57	90.07	97.44	17327.43	365.86	1.19	0.94	0.95	0.91	63.97
29	63005636115	8.48	9.66	93.89	103.72	90.41	99.88	17320.89	377.45	1.20	0.91	0.92	0.87	63.95
30	63005636295	7.74	9.01	95.72	108.02	90.65	102.30	17392.84	391.48	1.21	0.88	0.89	0.83	64.22
31	63005636491	7.21	8.45	95.58	109.41	89.10	101.99	17474.72	394.64	1.22	0.85	0.87	0.80	64.52
32	63005636725	7.49	8.74	94.98	108.05	89.94	102.32	17418.48	390.98	1.22	0.87	0.88	0.82	64.31
33	63005636956	8.21	9.44	93.29	104.40	91.76	102.69	17367.27	378.89	1.21	0.89	0.90	0.88	64.12

Data Point	Time Stamp	Mass Flow	Referred Mass Flow	HP - Torque	Referred HP Torque	HP - Temp	Referred HP Temp	RPM	Torque Referred	Pressure Ratio	η_1	η_2	η_3	Percent of Design Speed
34	63005637203	8.99	10.06	92.17	100.67	88.95	97.16	17346.79	365.81	1.19	0.93	0.95	0.90	64.05
35	63005637464	9.37	10.40	90.95	97.34	89.59	95.89	17364.77	353.33	1.18	0.93	0.95	0.92	64.11
36	63005637691	9.96	10.76	89.15	93.44	86.24	90.39	17281.95	340.80	1.17	0.94	0.96	0.91	63.81
37	63005637849	10.54	11.18	89.10	91.66	84.20	86.62	17366.01	332.69	1.16	0.96	0.99	0.91	64.12
38	63005638107	10.82	11.33	87.62	89.01	83.93	85.27	17353.50	323.29	1.15	0.95	0.98	0.91	64.07
39	63005639663	11.53	12.16	109.53	111.55	102.82	104.71	16545.68	379.11	1.17	0.95	0.98	0.90	68.47
40	63006223815	6.59	6.68	18.93	18.95	17.59	17.61	10437.60	114.43	1.05	0.96	0.99	0.90	38.54
41	63006224987	11.93	12.40	112.90	115.55	108.87	111.43	18890.51	385.55	1.18-	0.95	0.97	0.91	69.75
42	63006225294	11.22	12.00	113.76	120.64	111.55	118.30	18870.96	402.95	1.20	0.94	0.96	0.92	69.67
43	63006225501	10.40	11.44	115.49	126.55	111.98	122.69	18769.16	424.98	1.21	0.93	0.95	0.90	69.30
44	63006225735	9.68	10.99	117.68	132.04	113.24	127.06	18796.73	442.76	1.23	0.93	0.94	0.90	69.40
45	63006225927	9.21	10.59	117.49	132.85	111.38	125.95	18749.53	446.61	1.24	0.93	0.94	0.88	69.22
46	63006226126	8.86	10.32	118.81	136.58	115.14	132.36	18859.52	456.47	1.25	0.89	0.90	0.87	69.63
47	63006226271	8.27	9.72	119.25	138.51	111.90	129.97	18859.64	462.92	1.25	0.87	0.89	0.82	69.63
48	63006226511	7.83	9.27	115.84	136.09	109.54	128.68	18810.97	456.00	1.26	0.86	0.87	0.82	69.45
49	63006226714	7.64	9.09	118.25	138.49	108.30	126.84	18795.14	464.45	1.26	0.86	0.87	0.79	69.39
50	63006226955	8.07	9.55	118.01	137.48	112.89	131.51	18857.41	459.55	1.26	0.86	0.87	0.82	69.62
51	63006227121	8.54	9.96	118.63	137.37	113.59	131.54	18870.00	458.85	1.25	0.87	0.89	0.84	69.67
52	63006227315	9.03	10.45	117.01	133.80	114.80	131.27	18811.82	448.30	1.24	0.90	0.91	0.88	69.45
53	63006227500	9.32	10.66	116.88	132.08	115.37	130.37	18884.24	440.85	1.24	0.90	0.92	0.89	69.72
54	63006227736	9.88	11.07	116.71	129.62	113.07	125.58	18852.17	433.38	1.22	0.93	0.95	0.90	69.60
55	63006228032	10.59	11.54	114.10	122.98	112.33	121.06	18821.40	411.84	1.21	0.94	0.96	0.93	69.49
56	63006228131	10.65	11.67	114.00	120.96	109.31	115.98	18886.22	403.70	1.20	0.97	0.99	0.93	69.73
57	63006228466	11.09	11.91	114.00	120.96	110.01	114.68	18854.21	401.99	1.19	0.94	0.97	0.90	69.61
58	63006228631	11.40	12.09	115.35	120.25	110.01	114.68	18854.21	401.99	1.19	0.94	0.97	0.90	69.62
59	63006228832	11.79	12.26	113.01	115.61	106.21	108.64	18855.27	386.46	1.18	0.95	0.99	0.90	69.62
60	63006231282	13.39	14.07	113.01	115.61	157.58	162.94	21389.09	525.53	1.24	0.95	0.98	0.00	78.97
61	63006231467	13.38	14.11	173.36	178.54	158.80	163.54	21413.47	525.53	1.24	0.95	0.97	0.87	79.06
62	63006232069	13.48	14.17	#####	#####	#####	#####	21553.24	#####	1.24	0.00	0.00	0.00	79.58

Data Point	Time Stamp	Mass Flow	Referred Mass Flow	HP - Torque	HP Referred Torque	HP - Temp	HP Referred - Temp	RPM referred	Torque Referred	Pressure Ratio	η_1	η_2	η_3	Percent of Design Speed
63	63006232177	13.36	14.09	#####	#####	161.01	165.68	21488.24	#####	1.24	0.94	0.97	0.00	79.34
64	63006232257	13.39	14.08	175.68	181.57	157.49	162.77	21461.78	533.26	1.24	0.95	0.99	0.86	79.24
65	63006232594	13.48	14.16	#####	#####	#####	#####	21469.83	#####	1.24	0.00	0.00	0.00	79.27
66	63006232723	13.37	14.05	171.78	177.43	161.46	166.77	21512.54	519.88	1.24	0.93	0.96	0.87	79.43
67	63006233100	12.63	13.69	#####	#####	#####	#####	21483.63	#####	1.26	0.00	0.00	0.00	79.32
68	63006233265	12.69	13.76	#####	#####	#####	#####	21521.46	#####	1.26	0.00	0.00	0.00	79.46
69	63006233425	12.59	13.71	#####	#####	#####	#####	21488.31	#####	1.25	0.00	0.00	0.00	79.34
70	63006233590	12.63	13.81	176.99	188.44	169.18	180.13	21475.86	553.08	1.26	0.91	0.93	0.87	79.29
71	63006233932	11.86	13.40	#####	#####	#####	#####	21447.61	#####	1.28	0.00	0.00	0.00	79.19
72	63006234059	11.89	13.45	#####	#####	166.84	184.26	21447.38	#####	1.28	0.93	0.95	0.00	79.19
73	63006234162	11.87	13.47	#####	#####	167.12	184.00	21424.62	#####	1.28	0.94	0.96	0.00	79.10
74	63006234256	11.83	13.36	#####	#####	163.88	181.46	21404.63	#####	1.28	0.94	0.96	0.00	79.03
75	63006234409	11.91	13.50	#####	#####	167.02	184.44	21467.18	#####	1.28	0.94	0.95	0.00	79.26
76	63006234557	11.98	13.50	178.87	198.79	165.51	183.95	21479.08	583.37	1.28	0.94	0.96	0.87	79.30
77	63006234874	11.07	12.90	#####	#####	167.03	191.60	21457.71	#####	1.30	0.92	0.94	0.00	79.22
78	63006234991	10.95	12.88	180.14	204.91	167.77	190.85	21373.05	604.32	1.30	0.92	0.94	0.85	78.91
79	63006235177	10.31	12.30	#####	#####	167.98	197.78	21435.33	#####	1.31	0.88	0.91	0.00	79.14
80	63006235296	10.08	12.11	177.42	208.98	166.04	195.57	21330.57	617.52	1.31	0.88	0.90	0.82	78.75
81	63006235595	9.70	11.84	#####	#####	#####	#####	21420.98	#####	1.32	0.00	0.00	0.00	78.09
82	63006235718	9.68	11.77	179.11	214.59	164.69	197.32	21389.43	632.37	1.32	0.87	0.88	0.80	78.97
83	63006235895	9.25	11.38	#####	#####	#####	#####	21391.61	#####	1.33	0.00	0.00	0.00	78.98
84	63006236086	9.30	11.43	179.75	216.52	166.57	200.65	21463.61	635.85	1.33	0.85	0.86	0.79	79.25

APPENDIX C SOFTWARE USER'S GUIDE

A. HPVEE

The procedure for operating the HPVEE data acquisition routine was as follows:

1. The input array for the Scanivalve Control user's object was initialized. The 0th element was the Scanivalve Position (1 through 4) and the next 48 elements of the array indicated whether the corresponding port should be measured (0 - no skip, 1 - yes measure)
2. When the rig was stable and at the desired condition for measurement the START button was depressed. Desired quantities were input as prompted.
3. When the data acquisition process was finished the data were automatically written to the hard disk.
4. The operating condition was changed and the process repeated from step 1.

All programs used were saved on a 3.5 inch floppy and are in the possession of Dr. Shreeve. A graphical listing of the program, with redundant portions for scanivalve positions 2 through 4 removed, follows:

Save File Name: C:\BART\lcr_reduction_print.vee

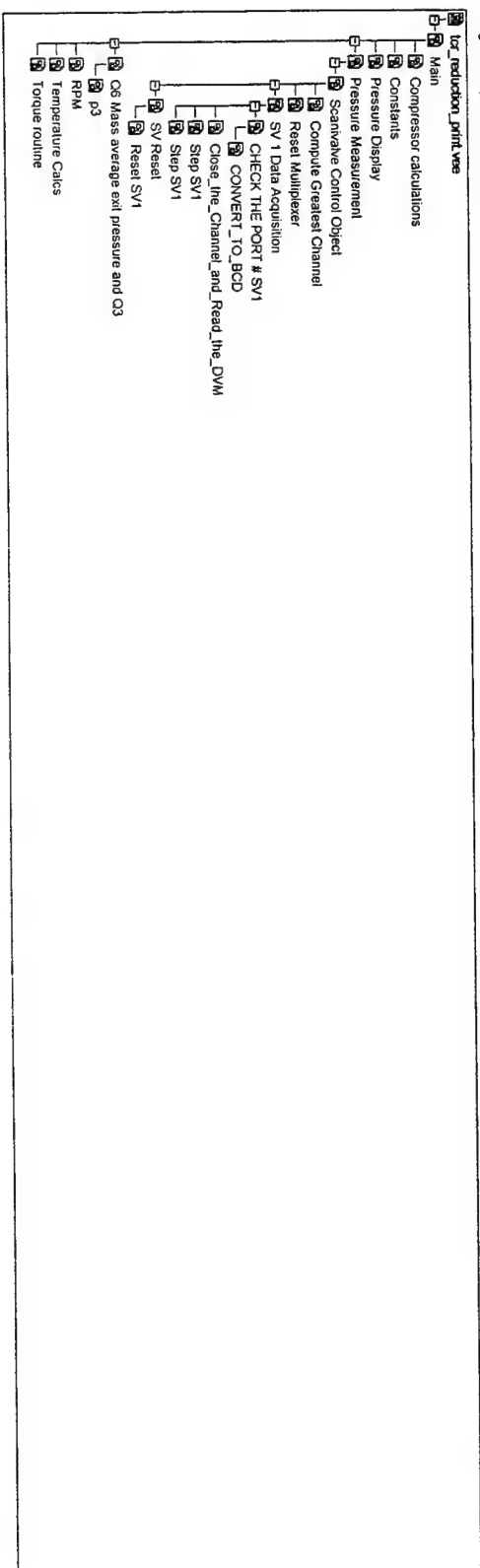
Save File Last Revised: Sat Sep 20 11:50:38 1997

Save File Format: 2.3

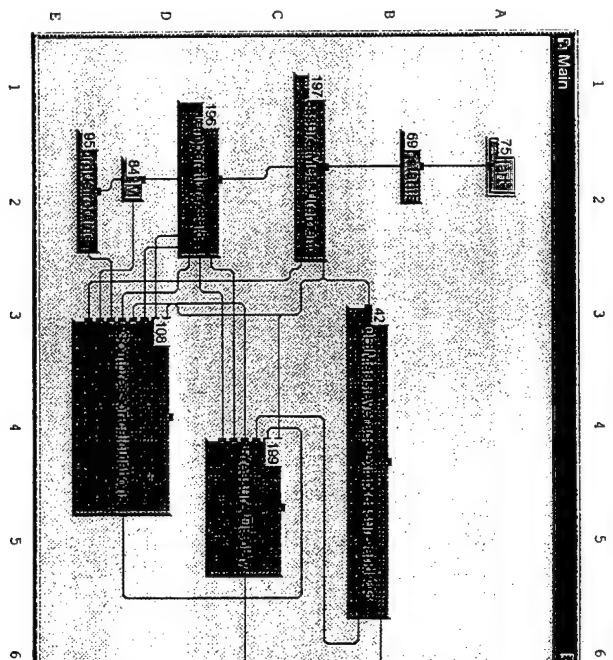
HP VEE Revision: 4.01

Execution mode: VEE 3 Compatibility

Program Explorer Overview



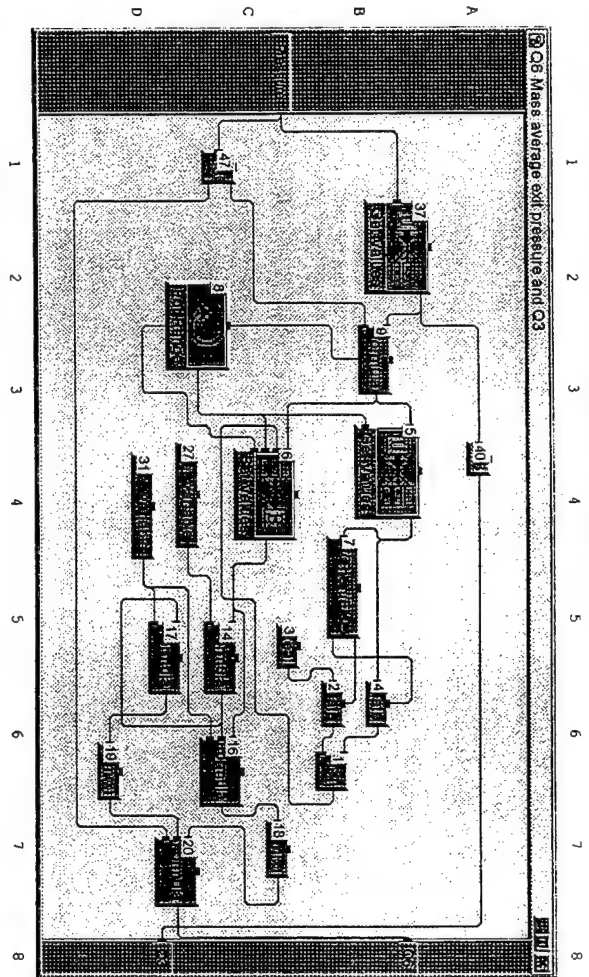
Main (M): Detail View, Total Objects: 9



Main "Main"

- 42 at: B4 UserObject "C6 Mass average exit pressure and Q3"
- 69 at: B2 UserObject "Constants"
- 75 at: A2 Start "Start"
- 84 at: D2 UserObject "RPM"
- 95 at: E2 UserObject "Torque routine"
- 108 at: D4 UserObject "Compressor calculations"
- 196 at: D2 UserObject "Temperature Calcs"
- 197 at: C2 UserObject "Pressure Measurement"
- 199 at: C5 UserObject "Pressure Display"

Main: Q6 Mass average exit pressure and Q3 (M.42): Detail View, Total Objects: 20



UserObject "Q6 Mass average e..."

- 1 at: B6 Junction "JCT"
- 2 at: B6 Gate "Gate"
- 3 at: C5 Constant "Real"
- 4 at: B6 Gate "Gate"
- 5 at: B4 Get Values "Get Values"
- 6 at: C4 Set Values "Set Values"
- 7 at: B5 If/Then/Else "If/Then/Else"
- 8 at: C2 For Range "For Range"
- From Value: 0
- Thru Value: 19
- Step Value: 1
- 9 at: B3 Formula "Formula"
- Formula: A/B
- 14 at: C5 Formula "Formula"
- Formula: ((1/A)^(1/Gamma))*sqrt(1-(1/A)^(1/Gamma))*A
- 16 at: C6 Formula "Formula"
- Formula: A*B*C
- 17 at: D5 Formula "Formula"
- Formula: A*B

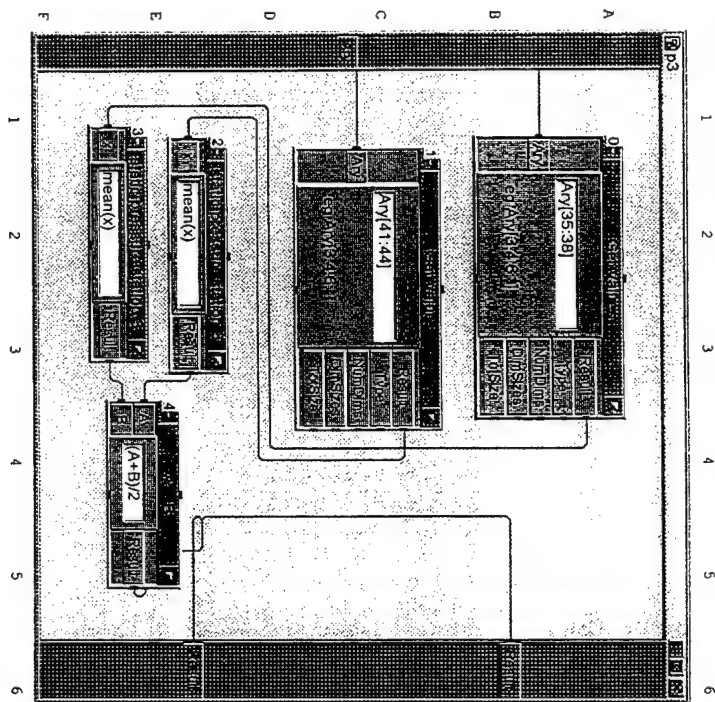
Sat 20/Sep/1997 12:23:32

C:\BARTVcr_reduction_print.vae

4

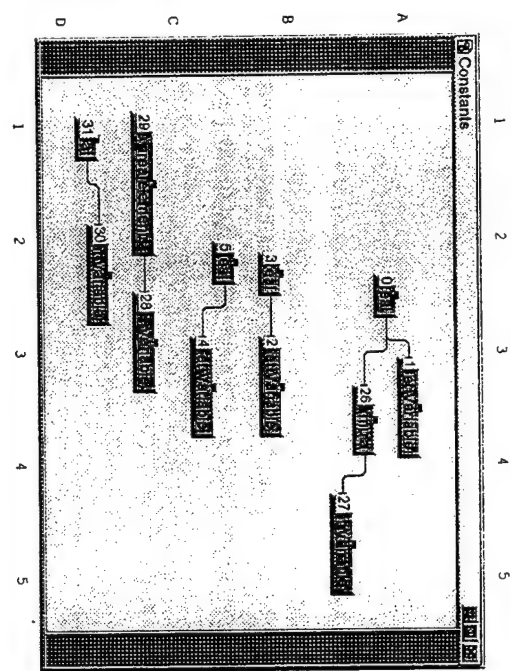
```
- 18 at: C7 Formula "sum(x)"
  L Formula: sum(x)
- 19 at: D6 Formula "sum(x)"
  L Formula: sum(x)
- 20 at: D7 Formula "Formula"
  L Formula: A/B*C
- 27 at: D4 Get Variable "Get Variable"
  L Variable Name: "gamma"
- 31 at: D4 Get Variable "Get Variable"
  L Variable Name: "H_fractional areas"
- 37 at: B2 Get Values "Get Values"
  L Formula: Ary[11:30]
- 40 at: A4 Formula "Q3"
  L Formula: mean(x)
- 47 at: C1 UserObject "p3"
```

Main: Q6 Mass average exit pressure and Q3: p3 (M:42.47): Detail View, Total Objects: 5



```
UserObject "p3"
-0 at: A2 Get Values "Get Values"
  Formula: Ary(35:38)
-1 at: C2 Get Values "Get Values"
  Formula: Ary(41:44)
-2 at: E2 Formula "static pressure station 3"
  Formula: mean(x)
-3 at: F2 Formula "static pressure station 3"
  Formula: mean(x)
-4 at: E4 Formula "A + B"
  Formula: (A+B)/2
```

Main: Constants (M.69): Detail View, Total Objects: 12

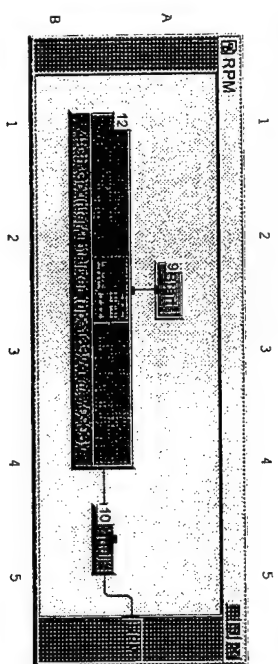


```

UserObject      "Constants"
- 0 at: A2      Constant "Real"
- 1 at: A3      Set Variable "Set Variable"
  Variable Name: "qgamma"
- 2 at: B3      Set Variable "Set Variable"
  Variable Name: "AQ0"
- 3 at: B2      Constant "Real"
- 4 at: C3      Set Variable "Set Variable"
  Variable Name: "CQ0"
- 5 at: C2      Constant "Real"
- 26 at: A4      Formula "Formula"
  Formula: (G-1)/G
- 27 at: B5      Set Variable "Set Variable"
  Variable Name: "qgamma1"
- 28 at: C3      Set Variable "Set Variable"
  Variable Name: "H fractional areas"
- 29 at: C1      Constant "20 area elements"
- Constant size fixed: true
- 30 at: D2      Set Variable "Set Variable"
  Variable Name: "Torque coefficients"
- 31 at: D1      Constant "Real"
- Constant size fixed: true

```

Main: RPM (M.84): Detail View, Total Objects: 3

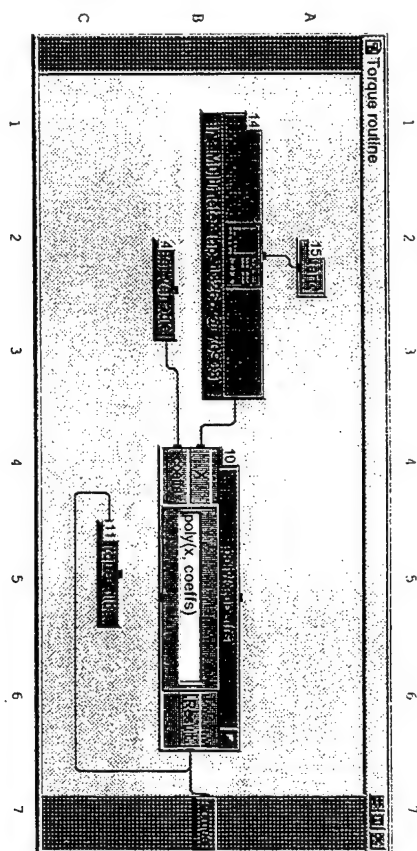


```

UserObject "RPM"
- 9 at: A2 Start "Start"
- 10 at: B5 Formula "Formula"
  Formula: A*10
- 12 at: B2 State Driver "4-Ch Counter/Totalizer (Imp1332a @ 70906)"

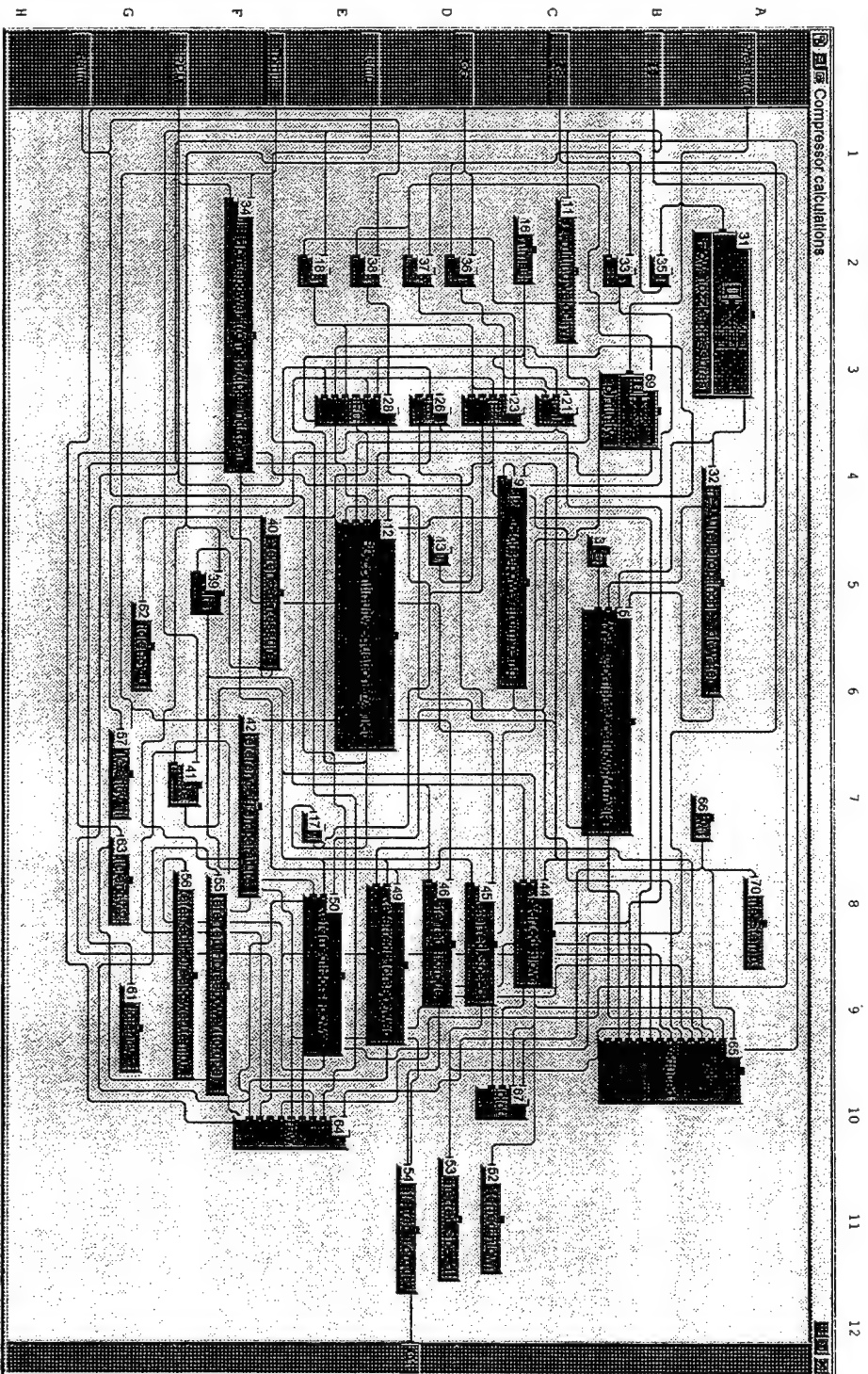
```

Main: Torque routine (M.95): Detail View, Total Objects: 5



UserObject "Torque routine"
 - 4 at: B2 Get Variable "get Variable"
 - Variable Name: "Torque_coefficients"
 - 10 at: B5 Formula "poly(x, coeffs)"
 - Formula: poly(x, coeffs)
 - 11 at: C5 AlphaNumeric "Torque inlbs"
 - 14 at: B2 State Driver "Int_Multimeter (hpel326b @ 70903)"
 - 15 at: A2 Start "Start"

Main: Compressor calculations (M.109): Detail View, Total Objects: 45



UserObject "Compressor calcul..."
 -3 at: C5 Get Variable "Cov"
 L Variable Name: "Cov"
 -5 at: B6 Formula "W2 - Compressor flow formula"
 L Formula: 16.5424*(1-(0.039346*A)/B(10))*Cov*sqrt(B(10)*A/(C-459.671))
 -9 at: C5 Formula "W2 - Horsepower from temp"
 L Formula: 0.33957*W*D

```

- 11 at: C2 Formula "V0 limiting velocity"
  L Formula: 109.62*sqrt(T1+459.67)
- 12 at: E5 Formula " B0 continuity equation @ inlet"
  L Formula: (32.172*pinf*A)/(G1*W2*V0*2.036)
- 13 at: D5 Get Variable "A0"
  L Variable Name: "A0"
- 16 at: C2 Get Variable "gamma1"
  L Variable Name: "gamma1"
- 17 at: E7 Formula "X0"
  L Formula: sqrt(B*2+1)-B
- 18 at: E2 Formula "S3"
  L Formula: (T+459.67)/D
- 21 at: C3 Formula "E1"
  L Formula: (Y^G-1)*S
- 23 at: D3 Formula "E2"
  L Formula: (Y^G+2*B*X-1)*S
- 26 at: D3 Formula "E3"
  L Formula: E*U2/U1
- 28 at: E3 Formula "E0"
  L Formula: S*(2*B*X+Y^G1-1)*U2/U1
- 31 at: A2 Get Values "Flow nozzle pressures"
  L Formula: ArY[3:4]
- 32 at: A5 Formula "Pressure Drop inches of water"
  L Formula: (A(0)-A(1))*13.6
- 33 at: B2 Formula "D2"
  L Formula: A-B
- 34 at: F3 Formula "W1 Horsepower from torque and rpm"
  L Formula: .000015865*torque*RPM
- 35 at: B2 Formula "Q1"
  L Formula: (A(5)+A(6))/2
- 36 at: D2 Formula "Y1"
  L Formula: Q6/Q1
- 37 at: D2 Formula "Y2"
  L Formula: Q6/pinf
- 38 at: E2 Formula "Y3"
  L Formula: Patm/pinf
- 39 at: F5 Formula "delta"
  L Formula: Q1/Pref
- 40 at: F5 Constant "Reference Pressure"
- 41 at: F7 Formula "theta"
  L Formula: (T1+459.67)/Tref
- 42 at: F7 Constant "Reference Temperature"
- 44 at: C8 Formula "Referred Flow"
  L Formula: W2*sqrt(t)/d
- 45 at: D8 Formula "Referred Speed"
  L Formula: N/sqrt(t)
- 46 at: D8 Formula "Referred Torque"
  L Formula: M/d
- 49 at: E9 Formula "Referred Horsepower"
  L Formula: U1/(sqrt(t)*d)

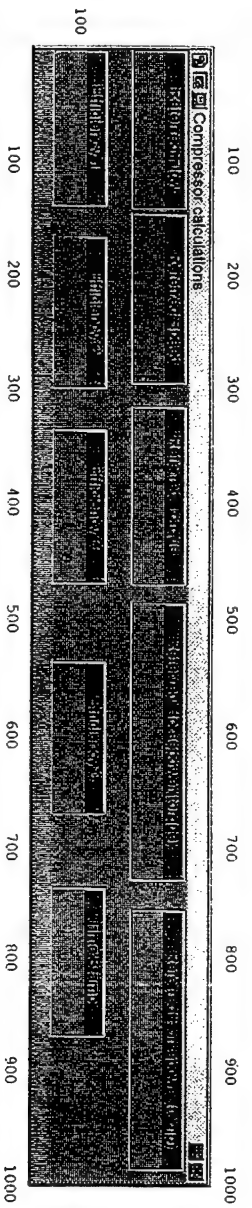
```

```

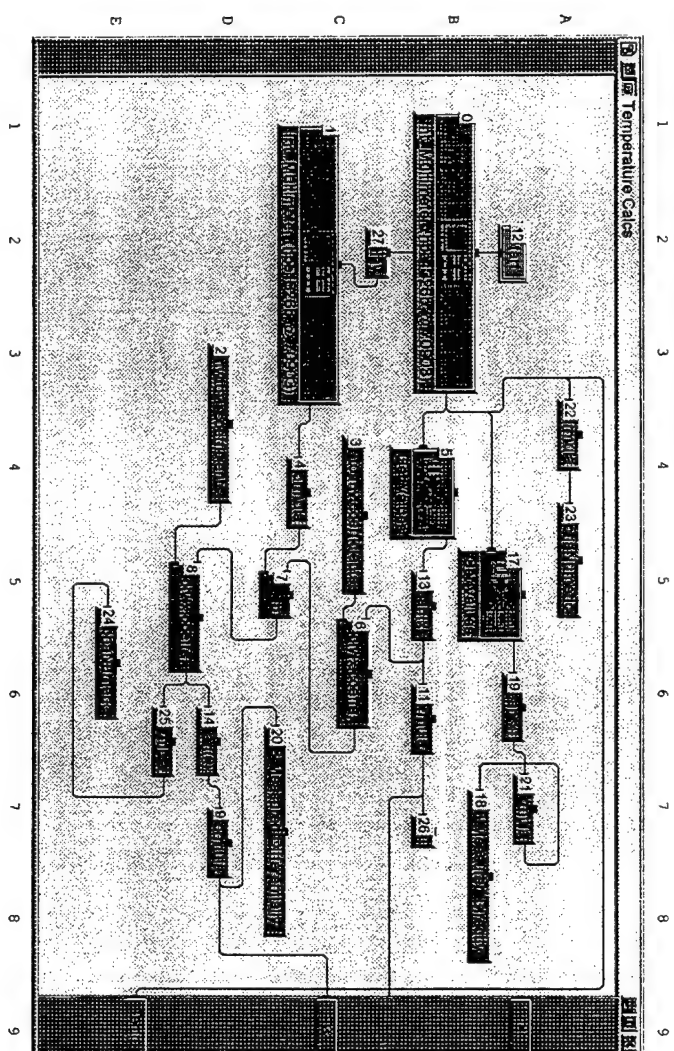
- 50 at: E9 Formula "Referred Horsepower"
  - Formula:  $U2/\sqrt{(t)*d}$ 
- 52 at: D11 AlphaNumeric "Referred Flow" is added to panel
- 53 at: D11 AlphaNumeric "Referred Speed" is added to panel
- 54 at: D11 AlphaNumeric "Referred Torque" is added to panel
- 55 at: F9 AlphaNumeric "Referred Horsepower(torque)" is added to panel
- 56 at: F9 AlphaNumeric "Referred Horsepower(temp)" is added to panel
- 57 at: G7 AlphaNumeric "Efficiency 1" is added to panel
- 61 at: G9 AlphaNumeric "Efficiency 3" is added to panel
- 62 at: G6 AlphaNumeric "Efficiency 0" is added to panel
- 63 at: G8 AlphaNumeric "Efficiency 2" is added to panel
- 64 at: E10 To File "raw"
  - Transactions: 4 lines.
    - WRITE TEXT t EOL
    - WRITE TEXT Pressure EOL
    - WRITE TEXT temp EOL
    - WRITE TEXT T1, " ", T3, " ", Q1, " ", Q6, " ", N, " ", RPM, " ", Patm EOL
- 65 at: B10 To File "reduced"
  - Transactions: 2 lines.
    - /NOP/ WRITE TEXT t EOL
    - WRITE TEXT t, " ", W, " ", Wf, " ", U1, " ", U1f, " ", U2, " ", U2f, " ", RPMf, " ", Nf, " ", E0, " ", E1, " ", E2, " ", E3, " " EOL
- 66 at: B7 Formula "now()"
  - Formula: now()
- 67 at: C10 To File "plot"
  - Transactions: WRITE TEXT t, " ", Wf, " ", E1, " ", Y1 EOL
- 69 at: B3 Get Values "pinfinity"
  - Formula: Aty(48)
- 70 at: A8 AlphaNumeric "Time Stamp" is added to panel

```

Main: Compressor calculations: Panel View



```
PanelView "Compressor calcul..." (w=993, h=134)
-52: AlphaNumeric "Referred Flow" (x=0, y=0) (w=137, h=50)
-53: AlphaNumeric "Referred Speed" (x=140, y=0) (w=151, h=50)
-54: AlphaNumeric "Referred Torque" (x=310, y=0) (w=156, h=50)
-55: AlphaNumeric "Referred Horsepower" (x=480, y=0) (w=244, h=50)
-56: AlphaNumeric "Referred Efficiency" (x=750, y=0) (w=233, h=50)
-57: AlphaNumeric "Efficiency 1" (x=0, y=70) (w=135, h=50)
-63: AlphaNumeric "Efficiency 2" (x=160, y=70) (w=135, h=50)
-61: AlphaNumeric "Efficiency 3" (x=330, y=70) (w=135, h=50)
-62: AlphaNumeric "Efficiency 0" (x=530, y=70) (w=135, h=50)
-70: AlphaNumeric "Time Stamp" (x=730, y=70) (w=135, h=50)
```



```

userobject "temperature Cals"
- 0 at: B2 State Driver "Int_Multimeter (hpel326b @ 70903)"
- 1 at: C2 State Driver "Int_Multimeter (hpel326b @ 70903)"
- 2 at: D4 Constant "nm to T coefficients"
- 3 at: C4 Constant "true"
- 4 at: C4 Constant "nm to T coefficients"
- 5 at: B4 Get Values "Get Values"
- 6 at: C6 Formula "poly(x, coeffs)"
- 7 at: D5 Formula "a + b"
- 8 at: D5 Formula "poly(x, coeffs)"
- 9 at: D7 Formula "Formula"
- Formula: A*B
- Formula: A^9/5+32

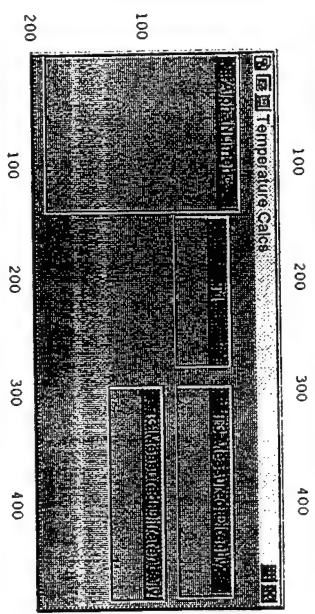
```

Sat 20/Sep/1997 12:23:32

C:\BARTVC_reduction_print.vee

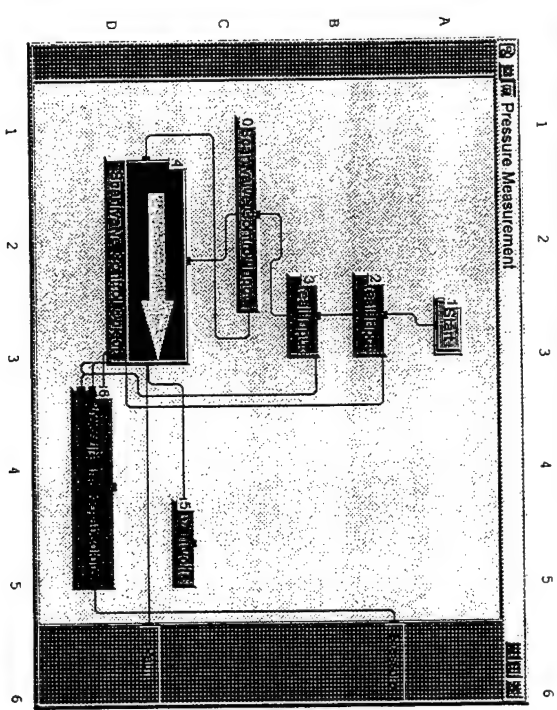
13

```
- 11 at: B6 Formula "Formula"
  L Formula: A*9/5+32
- 12 at: A2 Stat "Start"
- 13 at: B5 Formula "mean(x)"
  L Formula: mean(x)
- 14 at: D6 Formula "mean(x)"
  L Formula: mean(x)
- 17 at: B5 Get Values "Get Values"
  L Formula: Aty[2:4]
- 18 at: B8 AlphaNumeric "T3 Measured Directly" is added to panel
- 19 at: A6 Formula "mean(x)"
  L Formula: mean(x)
- 20 at: D7 AlphaNumeric "T3 Measured Differentially" is added to panel
- 21 at: A7 Formula "Formula"
  L Formula: A*9/5+32
- 22 at: A4 Formula "Formula"
  L Formula: A*9/5+32
- 23 at: A5 AlphaNumeric "AlphaNumeric" is added to panel
- 24 at: E6 AlphaNumeric "AlphaNumeric"
- 25 at: E6 Formula "Formula"
  L Formula: A*9/5+32
- 26 at: B7 AlphaNumeric "T1" is added to panel
- 27 at: C2 Delay "Delay"
  L Delay: 0.2
```



PanelView "Temperature Calcs" (w=484, h=192)

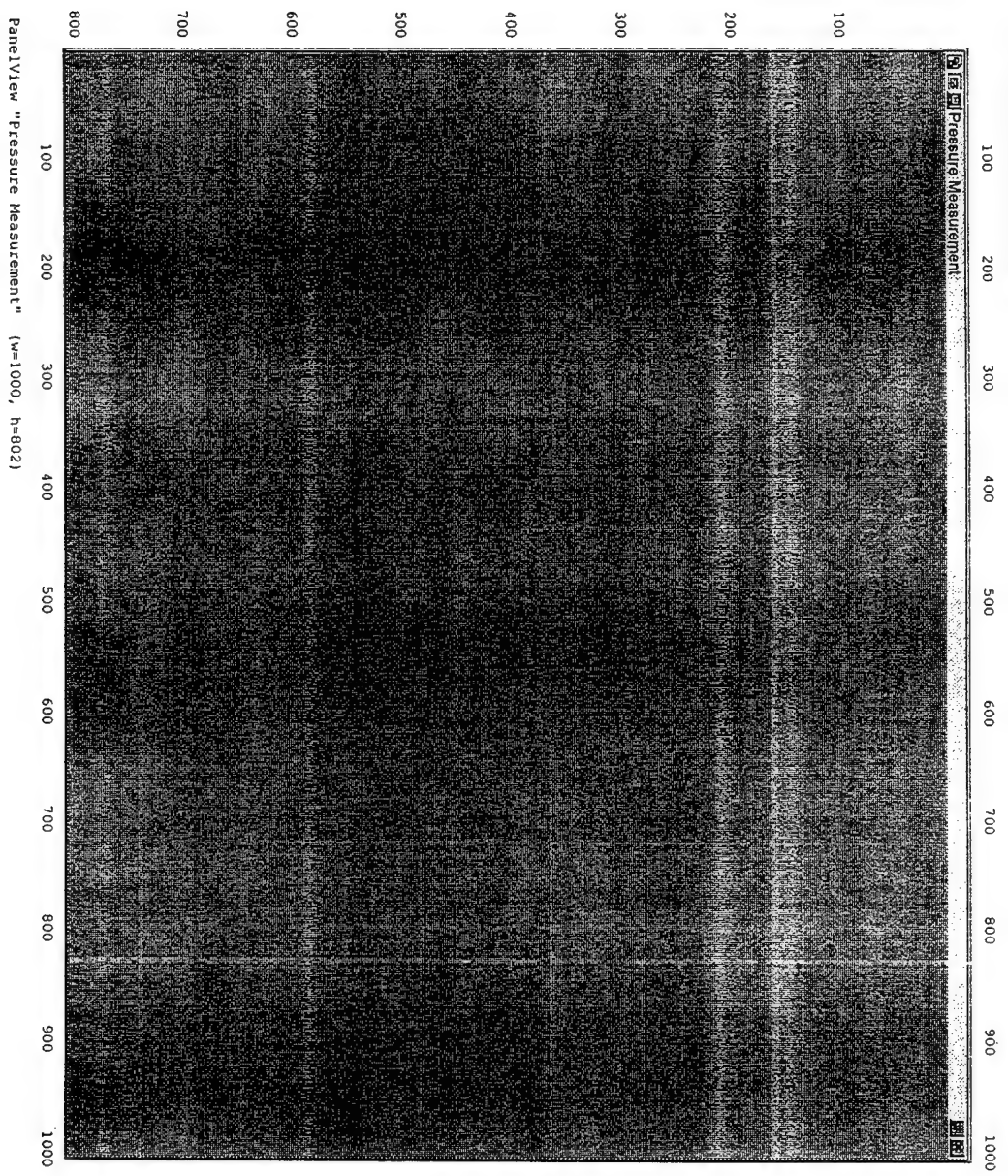
- 26: AlphaNumeric "T1" (x=140, y=20) (w=135, h=50)
- 23: AlphaNumeric "AlphaNumeric" (x=0, y=10) (w=138, h=175)
- 18: AlphaNumeric "T3 Measured Directly" (x=290, y=20) (w=188, h=50)
- 20: AlphaNumeric "T3 Measured Differentially" (x=290, y=80) (w=190, h=50)



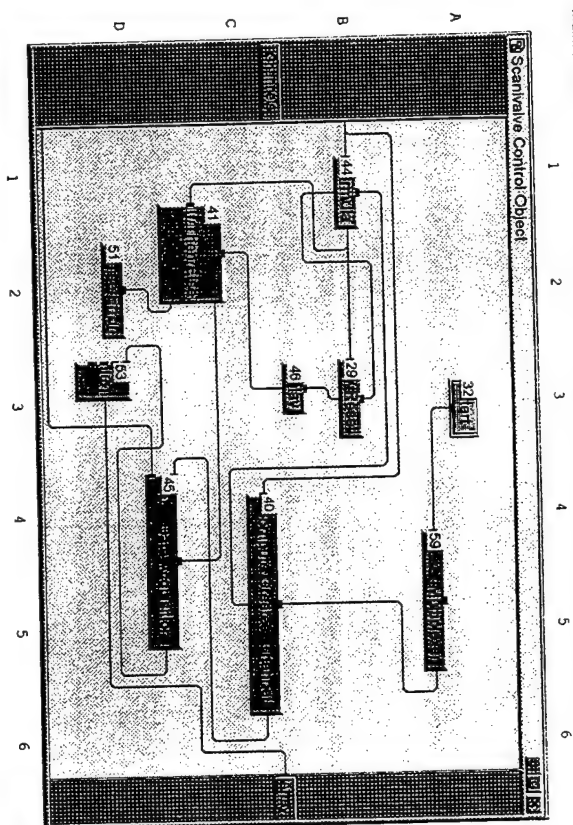
UserObject "Pressure Measurement"

- 0 at: C2 Constant "Scanivalve Control Input"
- Description: 3 lines.
- Element zero is scanivalve desired.
- Elements one through 48 contain a one if desire that channel to be scanned a zero if that channel should be skipped.
- Constant size fixed: true
- 1 at: A3 Start "Start"
- 2 at: B3 Real Input "Real Input"
- Dialog Popup Title: "Text Input"
- Dialog Popup Position: 276, 347
- Prompt/Label: "Enter Cal Pressure in ins Hg gage"
- Default Value: "10"
- Value Constraint: "0<=value AND value<=10"
- Error Message: "You must enter a real number between 0 and 10."
- 3 at: B3 Real Input "Real Input"
- Dialog Popup Title: "Text Input"
- Dialog Popup Position: 252, 368
- Prompt/Label: "Enter Ambient Pressure in ins Hg absolute"
- Default Value: "30.01"
- Value Constraint: "25<=value AND value<=35"
- Error Message: "Remember: inches of mercury or a hurricane is in Monterey."
- 4 at: D2 UserObject "Scanivalve Control Object"
- 5 at: C5 AlphaNumeric "SV in volts"
- 6 at: D4 Formula "Pressure ins Hg absolute"
- Formula: (A-A[1])*(B/(A[2]-A[1]))*C

Main: Pressure Measurement: Panel View

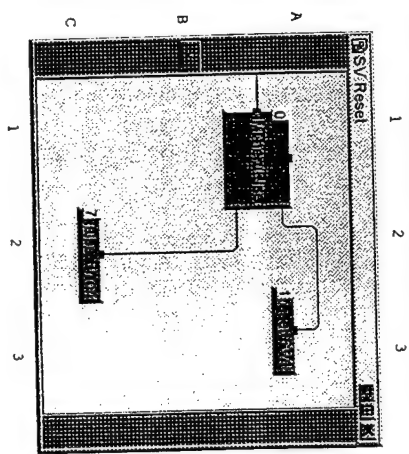


Main: Pressure Measurement: Scanvalve Control Object (M.197.4). Detail View, Total Objects: 10



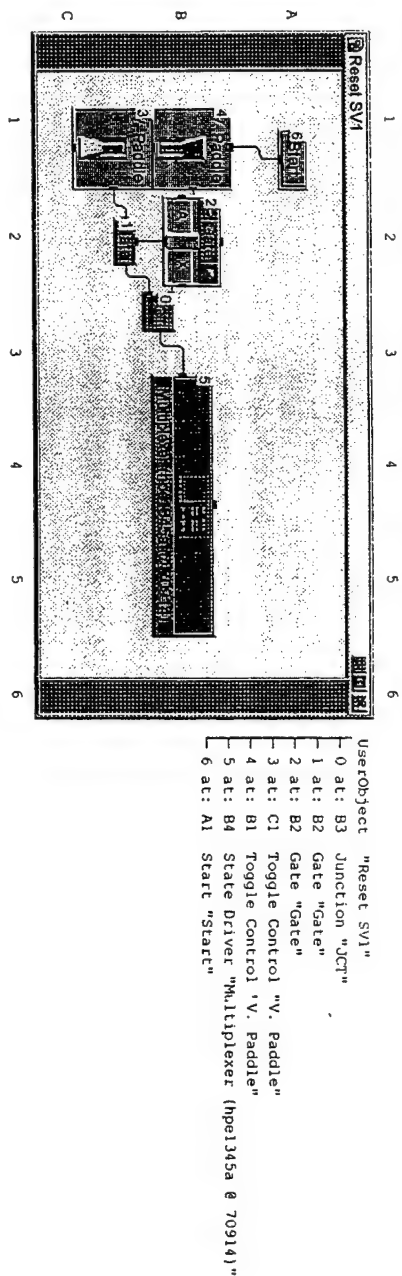
UserObject "Scanvalve Contro..."
 -29 at: B3 UserObject "SV Reset"
 -32 at: A3 Start "Start"
 -40 at: C5 UserObject "Compute Greatest Channel"
 -41 at: C2 If/Then/Else "If/Then/Else"
 - If/Else cases: 4 lines.
 - V==1
 - V==2
 - V==3
 - V==4
 -44 at: B1 Formula "Formula"
 -45 at: D4 UserObject "SV 1 Data Acquisition"
 -46 at: B3 Delay "Delay"
 - Delay: 0.1
 -51 at: D2 Raise Error "Raise Error"
 - Error code: 1
 - Message: "Error Improper Scanvalve Chosen"
 -53 at: D3 Junction "JCT"
 -59 at: A5 UserObject "Reset Multiplexer"

Main: Pressure Measurement: Scanvalve Control Object: SV Reset (M.197.4.29). Detail View, Total Objects: 3

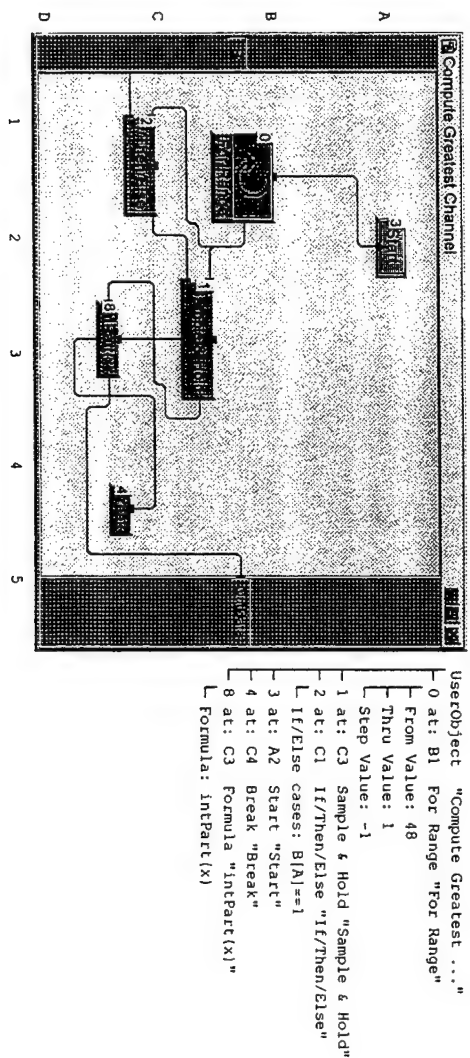


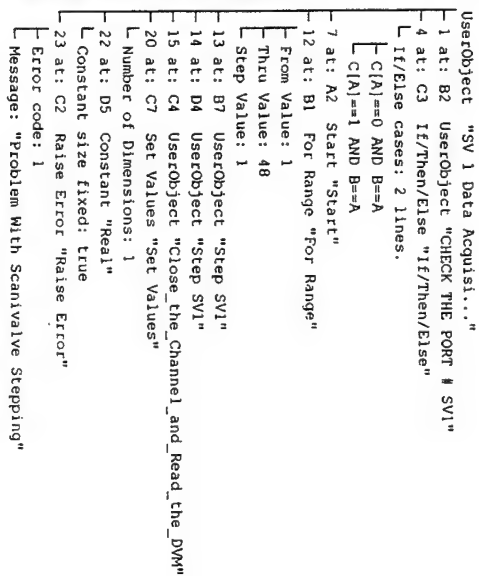
UserObject "SV Reset"
 -0 at: A1 If/Then/Else "If/Then/Else"
 - If/Else cases: 4 lines.
 - V==1
 - V==2
 - V==3
 - V==4
 -1 at: A3 UserObject "Reset SV1"
 -7 at: C2 Raise Error "Raise Error"
 - Error code: 1
 - Message: "Error Improper Scanvalve Chosen"

Main: Pressure Measurement; Scanivalve Control Object: SV Reset: Reset SV1 (M.197.4.29.1): Detail View, Total Objects: 7

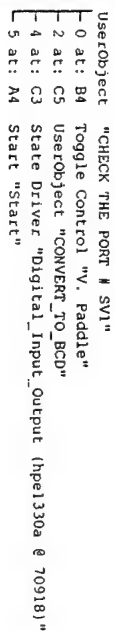


Main: Pressure Measurement; **Scanivalve Control Object:** Compute Greatest Channel (M.197.4.40); **Detail View, Total Objects:** 6

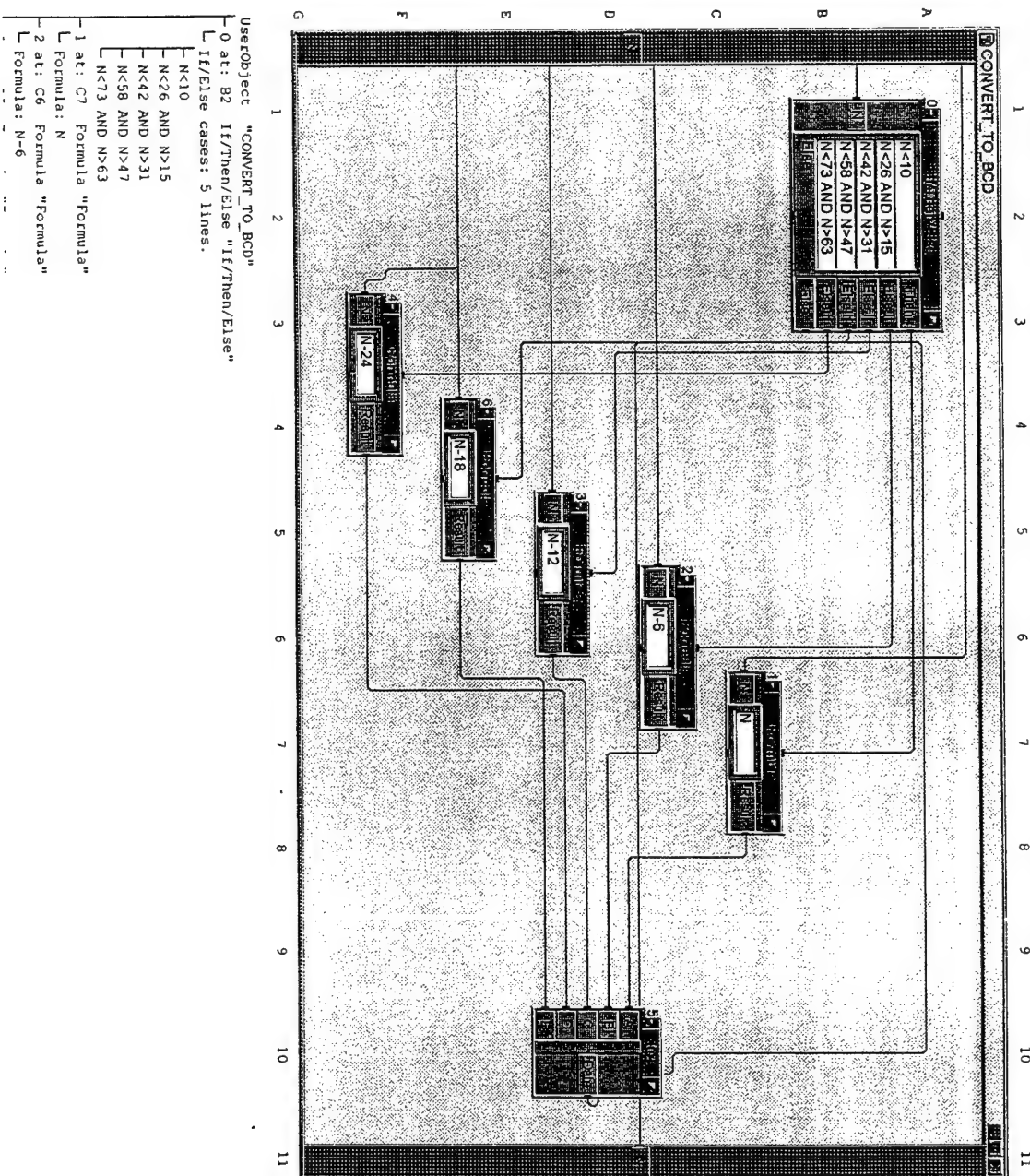




Main: Pressure Measurement: Scanivalve Control Object: SV 1 Data Acquisition: CHECK THE PORT # SV1 (M.197.4.45.1): Detail View, Total Objects: 4



Main: Pressure Measurement: Scanvalve Control Object: SV 1 Data Acquisition: CHECK THE PORT # SV1: CONVERT_TO_BCD (M.197.4.45.1.2): Detail View, Total Objects: 7



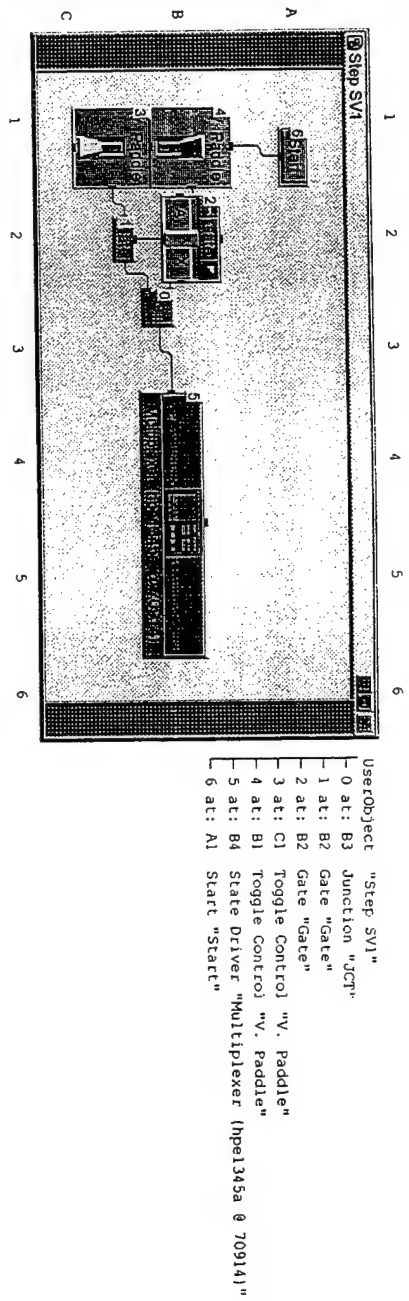
Sat 20/Sep/1997 12:23:32

C:\BART\or_reduction_print.vae

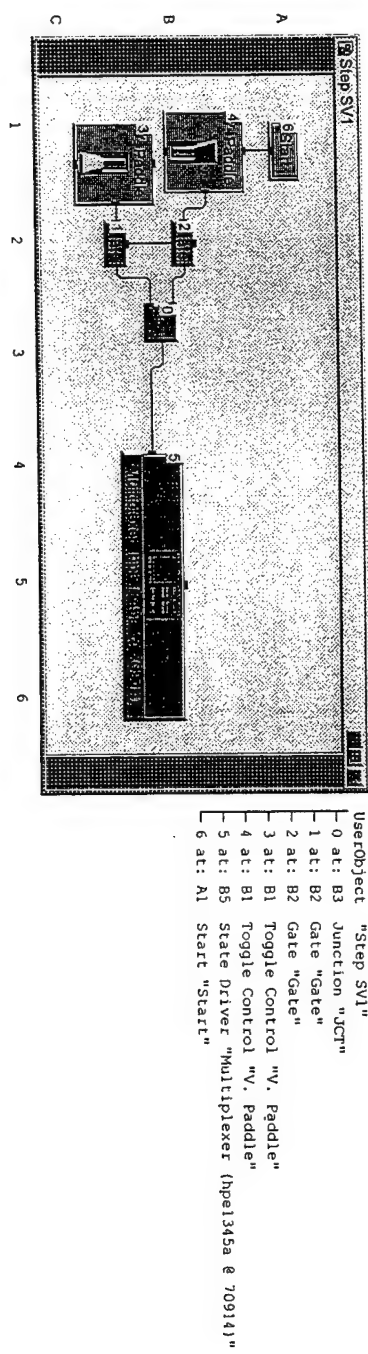
20

```
3 at: D5 Formula "Formula"
└ Formula: N-12
4 at: F3 Formula "Formula"
└ Formula: N-24
5 at: D10 Junction "JCT"
└ at: E4 Formula "Formula"
└ Formula: N-18
```

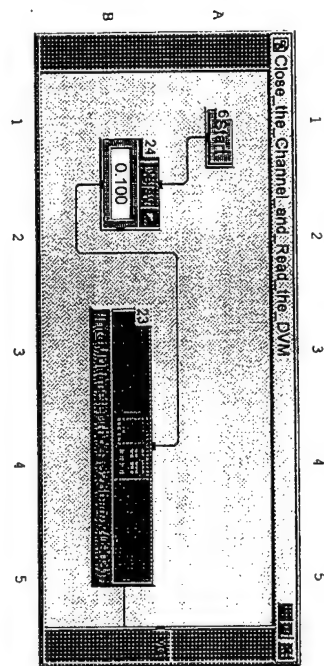
Main: Pressure Measurement: Scanvalve Control Object: SV 1 Data Acquisition: Step SV1 (M.197.4.45.13): Detail View, Total Objects: 7



Main: Pressure Measurement: Scanvalve Control Object: SV 1 Data Acquisition: Step SV1 (M.197.4.45.14): Detail View, Total Objects: 7

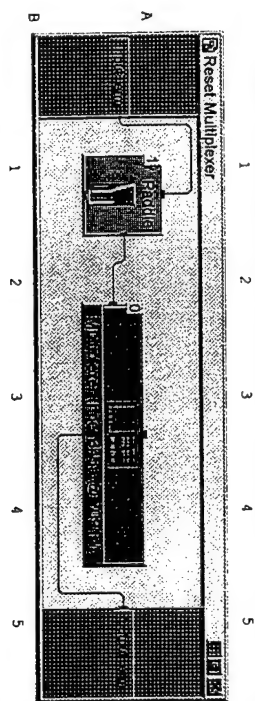


Main: Pressure Measurement: Scanvalve Control Object: SV 1 Data Acquisition: Close_the_Channel_and_Read_the_DVM (M:197.4.45.15): Detail View, Total Objects: 3



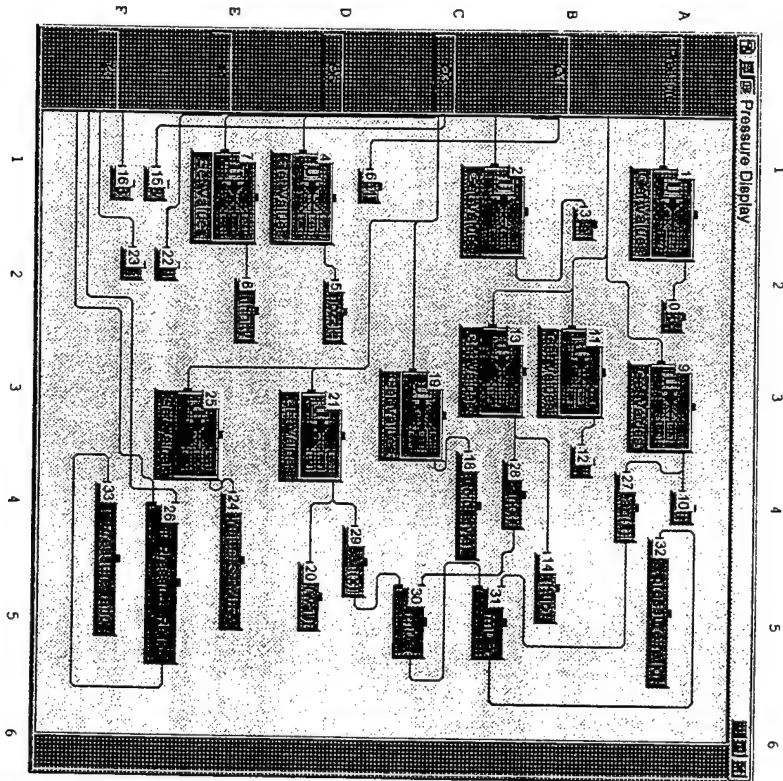
UserObject "Close_the_Channel..."
 - 6 at: A1 Start "Start"
 - 23 at: B4 State Driver "Inc_Multimeter (hpel326b @ 70903)"
 - 24 at: B1 Delay "Delay"
 Delay: 0.1

Main: Pressure Measurement: Scanvalve Control Object: Reset Multiplexer (M:197.4.59): Detail View, Total Objects: 2



UserObject "Reset Multiplexer"
 - 0 at: A3 State Driver "Multiplexer (hpel345a @ 70914)"
 - 1 at: A1 Toggle Control "V. Paddle"

Main: Pressure Display (M.199): Detail View, Total Objects: 33



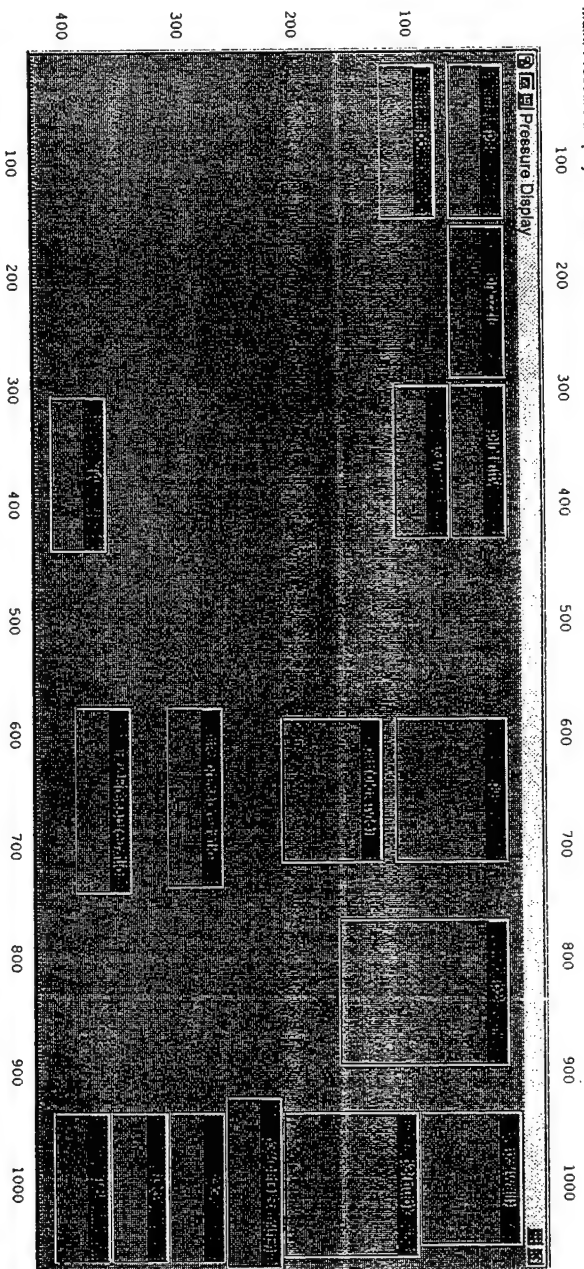
```

UserObject "Pressure Display"
- 0 at: A2 AlphaNumeric "p6" is added to panel
- 1 at: A1 Get Values "Get Values"
  L Formula: Ary(3)
- 2 at: C1 Get Values "Get Values"
  L Formula: Ary(4)
- 3 at: B1 AlphaNumeric "ps" is added to panel
- 4 at: D1 Get Values "Get Values"
  L Formula: Ary(7)
- 5 at: D2 AlphaNumeric "pnozzle" is added to panel
- 6 at: D1 AlphaNumeric "q1" is added to panel
- 7 at: E1 Get Values "Get Values"
  L Formula: Ary(48)
- 8 at: E2 AlphaNumeric "pinfinity" is added to panel
- 9 at: A3 Get Values "Get Values"
  L Formula: Ary(39:40)
- 10 at: A4 AlphaNumeric "p1" is added to panel
- 11 at: B3 Get Values "Get Values"
  L Formula: Ary(31:34)
- 12 at: B4 AlphaNumeric "p2" is added to panel
- 13 at: C3 Get Values "Get Values"
  L Formula: Ary(35:38)
- 14 at: B5 AlphaNumeric "p3(hub)" is added to panel
- 15 at: F1 AlphaNumeric "q3" is added to panel
- 16 at: F1 AlphaNumeric "q6" is added to panel
- 18 at: C4 AlphaNumeric "p1 (old style)" is added to panel
- 19 at: C3 Get Values "Get Values"
  L Formula: Ary(46:47)
- 20 at: D5 AlphaNumeric "p3(wall)" is added to panel
- 21 at: D3 Get Values "Get Values"
  L Formula: Ary(41:43)
- 22 at: F2 AlphaNumeric "T1" is added to panel
- 23 at: F2 AlphaNumeric "T3" is added to panel
- 24 at: E4 AlphaNumeric "p3(OLD STYLE)" is added to panel
- 25 at: E3 Get Values "Get Values"
  L Formula: Ary(44)
- 26 at: F5 Formula "T-T Pressure Ratio"
  L Formula: A/B
- 27 at: A4 Formula "mean(x)"
  L Formula: mean(x)
- 28 at: B4 Formula "mean(x)"
  L Formula: mean(x)
- 29 at: D4 Formula "mean(x)"
  L Formula: mean(x)
- 30 at: C5 Formula "Formula"
  L Formula: (A+B)/2
- 31 at: C5 Formula "Formula"
  L Formula: B/A

```


[32 at: A5 AlphaNumeric "s-s pressure ratio" is added to panel
33 at: f4 AlphaNumeric "T-T Pressure ratio" is added to panel

Main: Pressure Display: Panel View



```

PanelView "Pressure Display" (w=1070, h=423)
- 3: AlphaNumeric "ps" (x=10, y=10) (w=135, h=50)
- 0: AlphaNumeric "p6" (x=10, y=70) (w=135, h=50)
- 22: AlphaNumeric "p1" (x=300, y=360) (w=135, h=50)
- 32: AlphaNumeric "s-s pressure ratio" (x=570, y=260) (w=162, h=50)
- 33: AlphaNumeric "t-t pressure ratio" (x=570, y=340) (w=167, h=50)
- 10: AlphaNumeric "p1" (x=580, y=10) (w=130, h=100)
- 12: AlphaNumeric "p2" (x=760, y=10) (w=130, h=150)
- 16: AlphaNumeric "Q6" (x=930, y=310) (w=135, h=50)
- 15: AlphaNumeric "Q3" (x=930, y=260) (w=135, h=50)
- 24: AlphaNumeric "p3(OLD STYLE)" (x=917, y=210) (w=153, h=50)
- 18: AlphaNumeric "p1 (old style)" (x=580, y=120) (w=130, h=90)
- 23: AlphaNumeric "p3" (x=930, y=360) (w=135, h=50)
- 20: AlphaNumeric "p3(wall)" (x=930, y=0) (w=120, h=90)
- 14: AlphaNumeric "p3(hub)" (x=930, y=90) (w=130, h=120)
- 6: AlphaNumeric "Q1" (x=290, y=60) (w=135, h=50)
- 8: AlphaNumeric "pinfinity" (x=290, y=10) (w=135, h=50)
- 5: AlphaNumeric "pnozzle" (x=150, y=10) (w=135, h=50)

```

Index Page

Program Explorer Overview.	1
Main (M): Detail View, Total Objects: 9.	2
Q6 Mass average exit pressure and Q3 (M.421): Detail View, Total Objects: 20.	3
P3 (M.42.47): Detail View, Total Objects: 5.	5
Constants (M.69): Detail View, Total Objects: 12.	6
RPM (M.84): Detail View, Total Objects: 3.	6
Torque routine (M.95): Detail View, Total Objects: 5.	7
Compressor calculations (M.108): Detail View, Total Objects: 45.	8
Panel View.	11
Temperature Calcs (M.196): Detail View, Total Objects: 25.	12
Panel View.	14
Pressure Measurement (M.197): Detail View, Total Objects: 7.	14
Panel View.	15
Scanivalve Control Object (M.197.4): Detail View, Total Objects: 10.	16
SV Reset (M.197.4.29): Detail View, Total Objects: 3.	16
Reset SV1 (M.197.4.29.1): Detail View, Total Objects: 7.	17
Compute Greatest Channel (M.197.4.40): Detail View, Total Objects: 6.	17
SV 1 Data Acquisition (M.197.4.45): Detail View, Total Objects: 10.	18
CHECK THE PORT # SV1 (M.197.4.45.1): Detail View, Total Objects: 4.	18
CONVERT_TO_BCD (M.197.4.45.1.2): Detail View, Total Objects: 7.	19
Step SV1 (M.197.4.45.13): Detail View, Total Objects: 7.	21
Step SV1 (M.197.4.45.14): Detail View, Total Objects: 7.	21
Close_the_Channel_and_Read_the_DVM (M.197.4.45.15): Detail View, Total Objects: 3.	22
Reset Multiplexer (M.197.4.59): Detail View, Total Objects: 2.	22
Pressure Display (M.199): Detail View, Total Objects: 33.	23
Panel View.	25

B. RVC3D

All software used and results obtained using RVC3D and associated programs are stored in a directory /jedi/d3/blgrossm on the NPS Cray. Dr. G. V. Hobson has access to the files. The procedure for operating RVC3D was as follows:

1. Input the geometry provided as geometry.dat into TCGRID to obtain the grid file fort.1. geometry.out was produced and examined to ensure the grid was properly produced. The command used was "tcgrid.exec <geometry.dat >geometry.out".
2. Modified rvc.in to reflect the desired initial conditions to be analyzed [Ref. 3].
3. Submitted the job to the queue using rvc3d.nqs.
4. After completion, a solution file q.sol and a result file rvc.out were output.
5. If further iterations were desired, modified rvc.in such that iresti=1 and renamed q.sol to q.res.
6. Resubmitted the job to the queue.

Ample assistance was available from computer center personnel. Examples of geometry.dat, rvc.in and rvc3d.nqs are included in the following pages.

Listing of rvc3d.ngs:

```
#QSUB -q reg -lT 15280 -lt 15280 -lM 9Mw -me

set RUN = grid
  assign -F f77 -N ieee -a ${RUN}.ieee u:1

set RUN = q
  assign -F f77 -N ieee -a ${RUN}.sol u:3
  assign -F f77 -N ieee -a ${RUN}.res u:2

cd /d3/blgrossm/termproj
rvc3d <rvc.in >rvc.out
```

Listing of rvc.in:

```
'sanger rotor'
&n11 im=185 jm=40 km=49 itl=20 iil=85 &end
&n12 nstg=4 cfl=5 avisc1=0 avisc2=1.0 avisc4=.5 irs=1 epi=0.60 epj=0.70
epk=0.70 ivdt=1 itmax=5100 &end
&n13 ibcin=1 ibcex=3 ires=10 icrnt=50 iresti=1 &end
&n14 om=-2.54 prat=1.1905 emxx=.46 alex=52 igeom=1 &end
&n15 ilt=2 iltin=2 renr=6.651e6 tw=0 vispwr=.6667 cmutm=14 jedge=25
kedge=18 srtip=0 xrle=-.2 xrte=0.3 dblh=0.001 dblt=0.02 &end
&n16 &end
```

Listing of geometry.dat:

```
&nam1 merid=3 im=185 jm=40 km=49 itl=20 icap=16 k2d=11 &end
&nam2 nle=15 nte=10 dsle=3.5e-4 dste=2.5e-4 dshub=1.5e-5 dstip=1.5e-5
dswte=3.5e-4 dswex=.010 dsthre=.39 dsmin=1.2e-5 dsmax=.002
dsin=.010 clear=.00000 rcorn=.008 &end
&nam3 iterm=100 idbg=0 0 0 0 0 0 0 0 aabb=.6 ccdd=.2 &end
&nam4 zbc=-0.100 -0.040 0.2000 -0.1000 -0.0400 0.2000
rbc= 0.220 0.220 0.2800 0.4560 0.4560 0.4560 &end
```

'NPGS TRANSONIC DESIGN -GENER. FROM V8FBND13INCDP-BASE=DEC13 INNER'

```
32 14
-.833 -.667 -.5833 -.50 -.4583 -.425 -.40833 -.3917
-.3333 -.25 -.16666 -.0833 0. .0833 .1 .1167
.125 .133 .14167 .15 .1583 .16666 .175 .183
.19166 .208 .25 .3333 .41666 .5 .667 .8333

.00083 .00083 .00083 .00083 .001667 .00625 .01083 .01667
.04467 .08937 .13405 .17873 .2234 .2681 .277 .286
.2904 .29333 .295583 .297667 .29933 .30033 .30166 .3025
.303333 .304166 .306083 .306083 .306083 .306083 .306083 .306083

-.8333 -.7637 -.666666 -.5 -.33333 -.2083 -.1239 -.04167
```

.0529 .2167 .3083 .5 .66666 .83333

.4583 .4583 .4583 .4583 .4583 .4583 .4583 .4583

.4583 .4583 .4583 .4583 .4583 .4583

11 23 22

0.000000 0.000514 0.002301 0.005027 0.008746 0.013525 0.019448
0.025568
0.031878 0.038395 0.045135 0.052088 0.059237 0.066568 0.074067
0.081719
0.089506 0.097415 0.104086 0.109470 0.113531 0.116248 0.116636
0.001360 0.001751 0.003532 0.006238 0.009908 0.014595 0.020362
0.026281
0.032350 0.038563 0.044956 0.051567 0.058387 0.065405 0.072609
0.079987
0.087529 0.095222 0.101740 0.107019 0.111013 0.113692 0.114041
0.002013 0.002353 0.004135 0.006837 0.010492 0.015144 0.020848
0.026682
0.032644 0.038731 0.044945 0.051351 0.057968 0.064787 0.071798
0.078992
0.086358 0.093887 0.100278 0.105463 0.109392 0.112029 0.112356
0.002617 0.002913 0.004692 0.007384 0.011017 0.015627 0.021259
0.027000
0.032848 0.038800 0.044857 0.051036 0.057417 0.064001 0.070780
0.077748
0.084894 0.092212 0.098434 0.103490 0.107325 0.109902 0.110207
0.003875 0.004123 0.005878 0.008529 0.012096 0.016608 0.022099
0.027672
0.033327 0.039064 0.044881 0.050778 0.056765 0.062939 0.069314
0.075885
0.082643 0.089584 0.095503 0.100323 0.103986 0.106450 0.106724
0.007383 0.007577 0.009239 0.011743 0.015099 0.019322 0.024430
0.029584
0.034782 0.040025 0.045312 0.050643 0.056018 0.061437 0.066995
0.072754
0.078711 0.084862 0.090132 0.094442 0.097727 0.099942 0.100171
0.010925 0.011094 0.012640 0.014965 0.018075 0.021980 0.026692
0.031430
0.036196 0.040990 0.045811 0.050659 0.055534 0.060436 0.065366
0.070365
0.075575 0.081001 0.085687 0.089541 0.092492 0.094488 0.094690
0.012591 0.012749 0.014226 0.016447 0.019417 0.023145 0.027641
0.032161
0.036707 0.041277 0.045871 0.050490 0.055133 0.059800 0.064492
0.069210
0.074074 0.079161 0.083566 0.087197 0.089983 0.091869 0.092059
0.014092 0.014243 0.015665 0.017803 0.020663 0.024255 0.028587
0.032945
0.037327 0.041734 0.046166 0.050623 0.055105 0.059611 0.064143
0.068699
0.073344 0.078207 0.082428 0.085913 0.088589 0.090402 0.090584
0.014068 0.014213 0.015624 0.017747 0.020588 0.024157 0.028465
0.032800
0.037163 0.041553 0.045971 0.050417 0.054890 0.059390 0.063918
0.068472
0.073071 0.077861 0.082024 0.085465 0.088111 0.089904 0.090081

0.014718	0.014854	0.016226	0.018291	0.021057	0.024535	0.028737
0.032972						
0.037239	0.041537	0.045868	0.050230	0.054624	0.059050	0.063508
0.067997						
0.072518	0.077153	0.081192	0.084538	0.087114	0.088863	0.089032
0.222890	0.223164	0.224119	0.225574	0.227560	0.230111	0.233273
0.236541						
0.239910	0.243389	0.246988	0.250699	0.254516	0.258430	0.262434
0.266519						
0.270677	0.274899	0.278461	0.281335	0.283503	0.284954	0.285162
0.251549	0.251717	0.252483	0.253645	0.255222	0.257236	0.259714
0.262257						
0.264864	0.267534	0.270281	0.273121	0.276052	0.279067	0.282162
0.285332						
0.288573	0.291878	0.294678	0.296946	0.298663	0.299814	0.299964
0.267527	0.267655	0.268328	0.269348	0.270728	0.272485	0.274639
0.276842						
0.279093	0.281391	0.283738	0.286156	0.288655	0.291230	0.293877
0.296593						
0.299375	0.302218	0.304631	0.306589	0.308072	0.309068	0.309192
0.284586	0.284683	0.285263	0.286140	0.287324	0.288826	0.290661
0.292532						
0.294438	0.296378	0.298351	0.300365	0.302444	0.304590	0.306799
0.309070						
0.311399	0.313784	0.315811	0.317459	0.318709	0.319549	0.319648
0.309498	0.309561	0.310012	0.310694	0.311611	0.312770	0.314181
0.315614						
0.317067	0.318542	0.320037	0.321552	0.323091	0.324678	0.326317
0.328005						
0.329743	0.331527	0.333048	0.334287	0.335228	0.335861	0.335932
0.357485	0.357513	0.357749	0.358105	0.358582	0.359182	0.359909
0.360641						
0.361380	0.362126	0.362877	0.363635	0.364399	0.365170	0.365960
0.366779						
0.367626	0.368500	0.369249	0.369862	0.370329	0.370644	0.370677
0.398682	0.398694	0.398800	0.398959	0.399173	0.399441	0.399764
0.400090						
0.400417	0.400746	0.401077	0.401410	0.401744	0.402081	0.402419
0.402763						
0.403120	0.403493	0.403815	0.404079	0.404282	0.404419	0.404433
0.418757	0.418763	0.418826	0.418920	0.419046	0.419204	0.419394
0.419585						
0.419778	0.419971	0.420166	0.420362	0.420558	0.420756	0.420955
0.421154						
0.421360	0.421576	0.421762	0.421916	0.422034	0.422114	0.422122
0.428363	0.428368	0.428414	0.428484	0.428578	0.428696	0.428837
0.428980						
0.429124	0.429268	0.429413	0.429559	0.429706	0.429853	0.430002
0.430151						
0.430303	0.430462	0.430600	0.430714	0.430802	0.430861	0.430867
0.441651	0.441654	0.441683	0.441726	0.441784	0.441857	0.441945
0.442033						
0.442122	0.442211	0.442301	0.442392	0.442483	0.442575	0.442667
0.442760						
0.442854	0.442951	0.443036	0.443106	0.443160	0.443197	0.443201

0.455686 0.455687 0.455696 0.455711 0.455730 0.455754 0.455783
 0.455812
 0.455841 0.455871 0.455901 0.455931 0.455961 0.455992 0.456023
 0.456054
 0.456085 0.456117 0.456145 0.456168 0.456186 0.456198 0.456199

 0.000000 0.003130 0.013824 0.029582 0.050062 0.074802 0.103219
 0.130240
 0.155860 0.179937 0.202284 0.222896 0.241772 0.258919 0.274350
 0.288078
 0.300126 0.310517 0.317930 0.323057 0.326440 0.328478 0.328755
 0.003128 0.005248 0.014776 0.028894 0.047394 0.069991 0.096331
 0.121816
 0.146442 0.170204 0.192927 0.214376 0.234537 0.253398 0.270953
 0.287196
 0.302128 0.315751 0.326106 0.333741 0.339090 0.342478 0.342908
 0.006040 0.007780 0.016799 0.030195 0.047807 0.069419 0.094760
 0.119448
 0.143479 0.166850 0.189543 0.211273 0.231916 0.251457 0.269884
 0.287186
 0.303358 0.318393 0.330054 0.338813 0.345050 0.349050 0.349537
 0.007812 0.009253 0.017833 0.030604 0.047445 0.068195 0.092652
 0.116621
 0.140101 0.163087 0.185579 0.207502 0.228555 0.248690 0.267892
 0.286148
 0.303448 0.319781 0.332650 0.342455 0.349523 0.354099 0.354630
 0.009343 0.010493 0.018600 0.030696 0.046703 0.066514 0.089999
 0.113166
 0.136014 0.158540 0.180744 0.202624 0.224143 0.245014 0.265160
 0.284567
 0.303219 0.321104 0.335414 0.346469 0.354528 0.359790 0.360368
 0.012457 0.013335 0.020849 0.032095 0.047041 0.065645 0.087855
 0.109937
 0.131892 0.153720 0.175419 0.196989 0.218430 0.239739 0.260729
 0.281254
 0.301299 0.320851 0.336758 0.349226 0.358424 0.364482 0.365102
 0.015765 0.016553 0.023727 0.034476 0.048786 0.066639 0.088013
 0.109331
 0.130593 0.151800 0.172950 0.194043 0.215080 0.236060 0.256983
 0.277785
 0.298246 0.318337 0.334786 0.347746 0.357349 0.363693 0.364329
 0.017368 0.018125 0.025166 0.035718 0.049774 0.067318 0.088335
 0.109313
 0.130251 0.151148 0.172006 0.192823 0.213600 0.234336 0.255031
 0.275683
 0.296131 0.316262 0.332787 0.345836 0.355522 0.361930 0.362568
 0.017681 0.018424 0.025428 0.035926 0.049911 0.067370 0.088289
 0.109172
 0.130021 0.150833 0.171610 0.192351 0.213056 0.233725 0.254357
 0.274953
 0.295433 0.315629 0.332229 0.345354 0.355104 0.361559 0.362199
 0.020481 0.021191 0.028075 0.038395 0.052140 0.069302 0.089865
 0.110394
 0.130889 0.151350 0.171776 0.192168 0.212524 0.232846 0.253132
 0.273383
 0.293579 0.313542 0.329959 0.342944 0.352593 0.358983 0.359607

0.022265 0.022938 0.029745 0.039948 0.053539 0.070507 0.090839
 0.111137
 0.131402 0.151632 0.171829 0.191991 0.212119 0.232212 0.252270
 0.272292
 0.292279 0.312138 0.328482 0.341417 0.351034 0.357405 0.358014

 0.012140 0.013271 0.015723 0.020605 0.026613 0.033270 0.040423
 0.046930
 0.052625 0.056725 0.058821 0.058171 0.055174 0.050923 0.045640
 0.039421
 0.032344 0.024471 0.017334 0.011261 0.006500 0.003227 0.002754
 0.008415 0.009086 0.011001 0.015115 0.020300 0.026140 0.032514
 0.038449
 0.043927 0.048565 0.051401 0.052210 0.050709 0.047455 0.043005
 0.037468
 0.030935 0.023484 0.016620 0.010724 0.006074 0.002868 0.002444
 0.006996 0.007507 0.009179 0.012944 0.017738 0.023178 0.029159
 0.034788
 0.040080 0.044786 0.048184 0.049451 0.048574 0.045817 0.041758
 0.036547
 0.030278 0.023035 0.016306 0.010494 0.005897 0.002722 0.002323
 0.005881 0.006264 0.007690 0.011089 0.015470 0.020478 0.026017
 0.031279
 0.036310 0.040932 0.044751 0.046737 0.046556 0.044468 0.040876
 0.036021
 0.030002 0.022910 0.016238 0.010429 0.005811 0.002612 0.002229
 0.004812 0.005074 0.006210 0.009149 0.013000 0.017449 0.022407
 0.027160
 0.031787 0.036186 0.040080 0.043052 0.044156 0.043004 0.040114
 0.035758
 0.030056 0.023107 0.016429 0.010538 0.005816 0.002528 0.002158
 0.003883 0.004038 0.004859 0.007093 0.010122 0.013734 0.017867
 0.021901
 0.025897 0.029809 0.033485 0.036674 0.039040 0.039943 0.038515
 0.035235
 0.030241 0.023646 0.016996 0.010959 0.006030 0.002559 0.002193
 0.003711 0.003821 0.004584 0.006259 0.008616 0.011596 0.015185
 0.018781
 0.022355 0.025837 0.029117 0.032043 0.034427 0.036053 0.036581
 0.034767
 0.030549 0.024341 0.017731 0.011542 0.006395 0.002729 0.002349
 0.003711 0.003803 0.004605 0.006016 0.008040 0.010721 0.014083
 0.017523
 0.020946 0.024251 0.027322 0.030037 0.032265 0.033869 0.034707
 0.033940
 0.030501 0.024674 0.018166 0.011918 0.006638 0.002844 0.002453
 0.003764 0.003847 0.004695 0.006003 0.007894 0.010468 0.013774
 0.017194
 0.020602 0.023871 0.026880 0.029512 0.031656 0.033208 0.034068
 0.033707
 0.030752 0.025080 0.018572 0.012234 0.006836 0.002934 0.002534
 0.003647 0.003714 0.004599 0.005710 0.007335 0.009645 0.012724
 0.015971
 0.019214 0.022300 0.025098 0.027502 0.029426 0.030807 0.031601
 0.031609
 0.029519 0.024393 0.018209 0.012062 0.006763 0.002905 0.002513

0.003567 0.003619 0.004576 0.005519 0.006910 0.009001 0.011916
0.015057
0.018207 0.021177 0.023823 0.026041 0.027763 0.028960 0.029632
0.029767
0.028414 0.024014 0.018085 0.012047 0.006772 0.002905 0.002519

INITIAL DISTRIBUTION LIST

1. Defense Technical Information Center.....2
 8725 John J. Kingman RD, STE 0944
 Ft. Belvoir, Virginia 22060-6218

2. Dudley Knox Library.....2
 Naval Postgraduate School
 411 Dyer RD
 Monterey, California 93943-5101

3. Department of Aeronautics & Astronautics
 Naval Postgraduate School
 699 Dyer RD - Room 137
 Monterey, California 93943-5106
 ATTN:Chairman, Code AA.....1
 Professor R. P. Shreeve CodeAA/SF.....5
 Assoc. Professor G.V. Hobson, Code AA/HG.....1

4. Naval Air Warfare Center - Aircraft Division
 Propulsion and Power Engineering
 22195 Elmer RD, Unit 4
 Patuxent River, Maryland 20670-1534
 ATTN:J. Zidzik, Code 4.4.7.1, BLDG 106.....1
 S. MacAdams, Code 4.4.7.1, BLDG 106.....1
 C. Gorton, Code 4.4T, BLDG 106.....1

5. Mr. Nelson Sanger.....1
 752 Elmwood RD
 Rocky River, Ohio 44116

6. NASA Lewis Research Center
 21000 Brookpark RD
 Cleveland, Ohio 44135
 ATTN:R. V. Chima, MS 77-6.....1
 Chunill Hah, MS 5-11.....1

7. E. R. Grossman.....1
 5911 Gabor DR
 San Antonio, TX 78240